Analysis of the Functional Interaction of Neurotrypsin and Agrin in the Murine Central Nervous System

Dissertation

zur

Erlangung der naturwissenschaftlichen Doktorwürde
(Dr. sc. nat.)

vorgelegt der
Mathematisch-naturwissenschaftlichen Fakultät

der

Universität Zürich
von

Alexander Stephan

aus

Deutschland

Promotionskomitee

Prof. Dr. Peter Sonderegger (Vorsitz; Leitung der Dissertation)
PD Dr. Jack Rohrer
Prof. Dr. Jean-Marc Fritschy

Zürich, 2008

DISCLAIMER

This thesis is partially based upon and partly adapted from the following publication:

Alexander Stephan, José María Mateos, Serguei V. Kozlov, Paolo Cinelli, Andreas David Kistler, Stefan Hettwer, Thomas Rülicke, Peter Streit, Beat Kunz and Peter Sonderegger, 2008, Neurotrypsin cleaves agrin locally at the synapse, FASEB J, in press, Jan. 29, 2008 [Epub ahead of print]

Table of Contents

Zusammenfassung

Der synaptischen Serinprotease Neurotrypsin wird eine essentielle Rolle in kognitiven Prozessen des Gehirns zugeschrieben, da das Fehlen von funktionellem Neurotrypsin im Menschen zu schwerer geistiger Behinderung führt. Neurotrypsin schneidet das Proteoglykan Agrin an zwei homologen Stellen und setzt dabei ein intermediäres 90-kDa und ein C-terminales 22-kDa Fragment von der N-terminalen Hälfte Agrin's frei. Agrin spielt eine essentielle Rolle bei der Reifung der neuromuskulären Synapse und ist essentiell für deren Stabilität. Neuere Erkenntnisse weisen zudem darauf hin, das Agrin auch eine wichtige Rolle in der Formation, der Stabilität und der Funktion von Synapsen im Zentralen Nervensystem (ZNS) ausübt. Anhand der morphologischen Analyse von ZNS Gewebe konnte gezeigt werden, dass Neurotrypsin in der Präsynapse lokalisiert. Zudem löst synaptische Aktivität die synaptische Sekretion von Neurotrypsin aus. Agrin dagegen ist hauptsächlich im extrazellulären Raum direkt an oder in der Nähe der Synapse zu finden.

Um die Interaktion von Neurotrypsin und Agrin im ZNS zu erforschen, habe ich eine detaillierte biochemische Analyse dieser Interaktion im Gehirn der Maus durchgeführt. Mit der Analyse von Maushirnhomogenaten konnte ich zeigen, dass ausschliesslich jene Agrin-Isoformen von Neurotrypsin im ZNS geschnitten werden, die Glykosaminoglykan-Seitenketten tragen. Weiterführende Studien mit isolierten Synaptosomen, die durch subzelluläre Fraktionierung aus wildtype- und Neurotrypsin überexprimierenden Tieren angereichert wurden, zeigten, dass diese Isoformen den Grossteil von synaptischem Agrin repräsentieren und dass Neurotrypsin hauptsächlich synaptisches Agrin schneidet.

Die funktionelle Rolle dieser Interaktion habe ich *in vitro* mit zellbiologischen Analysen untersucht, hauptsächlich in hippocampalen Neuronenkulturen, um die Systemkomplexität zu reduzieren. Neurotrypsin und Agrin werden in den Zellen dieser Kulturen gebildet, jedoch war die Analyse einer Interaktion der endogen gebildeten Proteine aufgrund des Fehlens von geeigneten Antikörpern und auch wegen der Vielfalt an gebildeten Agrin-Isoformen nicht möglich. Aus diesem Grunde habe ich einen alternativen Ansatz etabliert, um die Interaktion von Neurotrypsin und Agrin und ihre funktionellen Auswirkungen zu untersuchen. In unserem Labor waren bereits Adenoviren kreiert worden, die eine effiziente Expression von Neurotrypsin in neuronalen Kulturen ermöglichen. Zur Vervollständigung des Virusrepertoires für finale Analysen habe ich eine Reihe an weiteren Viren kreiert, die verschiedene Agrin-Varianten exprimieren. Ich konnte zeigen, dass diese Viren eine effiziente und vor allem funktionelle Expression von Agrin in kultivierten Nervenzellen ermöglichen. Desweiteren besteht eine funktionelle Interaktion zwischen Virus-abhängig exprimierten Agrin und Neurotrypsin-Varianten in kultivierten Nervenzellen. Zudem konnte ich bereits publizierte Effekte von Agrin bestätigen, nämlich dass die Überexpression von Agrin zur vermehrten Ausbildung von Filopodien auf sowohl Axonen als auch Dendriten von kultivierten Nervenzellen führt. Ich habe deshalb analysiert, ob Neurotrypsin diese Funktion von Agrin beeinflusst. Die Ausbildung von Filopodien wird in Nervenzellen als auch in cos7 Zellen ausschliesslich von transmembranem Agrin beeinflusst. Mit der Analyse von transient transfizierten cos7 Zellen habe ich ermittelt, dass Neurotrypsin diese Funktion von Agrin inhibiert. Dies geschieht jedoch unabhängig von der katalytischen Aktivität Neurotrypsin's.

Agrin spielt eine zentrale Rolle bei der Formation, der Erhaltung und der Funktion von ZNS Synapsen. Die lokale synaptische Spaltung durch Neurotrypsin könnte darauf hindeuten, dass das Agrin/Neurotrypsin System eine wichtige Funktion in der Regulierung adaptiver Reorganisationen der synaptischen Kreisläufe ausführt. Die Identifikation der funktionellen Auswirkungen dieser Interaktion könnte dazu beitragen, die Rolle von Neurotrypsin im Kontext kognitiver Gehirnfunktionen zu verstehen.

Summary

The synaptic serine protease neurotrypsin is considered to be essential for the establishment and maintenance of cognitive brain functions because humans lacking functional neurotrypsin suffer from severe mental retardation. Neurotrypsin cleaves the proteoglycan agrin at two homologous sites, releasing an intermediate 90-kDa and a C-terminal 22-kDa fragment from the N-terminal moiety of agrin. Agrin is essential for neuromuscular junction maturation and maintenance and it has also recently been shown to play an important role in the formation, maintenance and function of CNS synapses. Morphological analyses of CNS tissue indicate that neurotrypsin is contained in presynaptic terminals and is externalised in association with synaptic activity, while agrin is localised to the extracellular space at or in the vicinity of the synapse.

To elucidate the parameters of a potential neurotrypsin-dependent cleavage of agrin in the CNS *in vivo*, I performed a detailed biochemical analysis of the interaction of neurotrypsin and agrin in the murine brain. In brain homogenates I found that neurotrypsin exclusively cleaves glycanated variants of agrin. Studies with isolated synaptosomes obtained by subcellular fractionation from brains of wildtype and neurotrypsin-overexpressing mice revealed that neurotrypsin-dependent cleavage of agrin was concentrated at synapses, where the most heavily glycanated variants of agrin predominate.

To determine the functional implications of this interaction, I performed cell biological *in vitro* analyses, mainly with dissociated hippocampal neuron cultures, employed to reduce system complexity. Both neurotrypsin and agrin are endogenously expressed in neuronal cultures but because of the lack of suitable antibodies and the presence of a variety of agrin isoforms, I established an alternative approach to analyse the interaction of both proteins in neuronal cultures. Neurotrypsin-expressing recombinant adenoviruses were produced in our lab to achieve efficient ectopic expression of neurotrypsin in cultured neurons. To complete the set of viruses for agrin and neurotrypsin co-expression analyses, I created several recombinant adenoviruses expressing different agrin variants. I established the functional and efficient virus-mediated expression of agrin variants in cultured neurons and also showed the functional interaction of ectopically expressed neurotrypsin and agrin variants in this neuronal culture system. In addition, I confirmed the recently published observation that the overexpression of transmembrane agrin variants causes the additional appearance of filopodia-like protrusions on dendrites as well as axons of cultured neurons. I therefore analysed if neurotrypsin interferes with this function of agrin. In both neurons and cos7 cells, the induction of filopodia-like protrusions is mediated exclusively by the transmembrane variant of agrin. The co-expression of agrin and neurotrypsin in transiently transfected cos7 cells led to the inhibition of agrin's function, however, independent of the catalytic activity of neurotrypsin.

Because agrin has been shown to play an important role in the formation, maintenance and function of CNS synapses, its local cleavage at the synapse implicates the neurotrypsin/agrin system in the regulation of adaptive reorganisations of the synaptic circuitry. Determining the functional implications of this local interaction may be key to understanding neurotrypsin's role in the context of cognitive functions, such as learning and memory.

Abbreviations

The abbreviations used are:

AChR,	acetylcholine receptor
ADP,	adenovirus death protein
AMPA,	α-amino-3-hydroxy-5-methly-4-isoxazole propionic acid
AMPAR,	AMPA-type glutamate receptor
AV,	adenovirus
bp,	base pairs
BRF,	branched retraction fibres
CA^{2+},	calcium-ion
CA1-3,	Cornus Ammonis 1-3
CAM,	cell adhesion molecule
CaMKII,	α-calcium-calmodulin-dependent protein kinase II
cAMP,	cyclic adenosine monophosphate
cDNA,	complementary DNA
CSF,	cerebrospinal fluid
CNS,	central nervous system
DIV,	day in vitro
DMEM,	Dulbecco's Modified Eagle Medium
DNA,	deoxyribonucleic acid
eCFP,	enhanced cyan fluorescent protein
ECM,	extracellular matrix
eGFP,	enhanced green fluorescent protein
ERK1/2,	extracellular signal-regulated kinase 1/2
Ex,	embryonic day x
FCS,	fetal calf serum
FGF-2,	fibroblast growth factor 2
FMR1,	fragile X mental retardation 1 gene
FMRP,	FMR1 protein
GABA,	γ-aminobutyric acid
$GABA_A$,	ionotropic GABA receptor
$GABA_B$,	metabotropic GABA receptor
HBSS,	Hank's Balanced Salt Solution
HEK293,	human embryonic kidney cells, line 293
IQ,	intelligence quotient
K^+,	potassium-ion
kb,	kilo-base pairs
kDa,	kilodalton
L1CAM,	cell-adhesion molecule L1
Lamp-1,	lysosomal-associated membrane protein 1
LB,	lysogeny broth (Luria-Bertani broth)
LDLR,	low-density lipoprotein receptor
LG,	laminin-globular domain
LG-3,	laminin-globular domain 3 of agrin

LN-agrin,	secreted agrin-x12, y4, z8
LRP-1,	low-density lipoprotein receptor-related protein 1
LTD,	long-term depression
LTP,	long-term potentiation
MAP,	mitogen-activated protein kinase
MAP-2,	microtubule-associated protein 2
MARCKS,	myristoylated alanine-rich C-kinase substrate protein
mNT,	mouse neurotrypsin
MOI,	multiplicity of infection
Mr,	molecular mass
MR,	mental retardation
mRFP,	monomeric red fluorescent protein
mRNA,	messenger RNA
MuSK,	‘muscle-specific’ kinase
Na^+,	sodium-ion
NMDA,	N-methyl-D-aspartate
NMDAR,	NMDA-type glutamate receptor
NMJ,	neuromuscular junction
NSMR,	nonsyndromic MR
NtA,	N-terminal domain of secreted agrin
NT-inact,	inactive mouse neurotrypsin
Ntd,	neurotrypsin-deficient mice
Nto-act,	mice overexpressing active human neurotrypsin
Nto-inact,	mice overexpressing inactive mouse neurotrypsin
pAd,	final recombinant E1, E3-deficient adenovirus vector
PAI-1,	plasminogen activator inhibitor-1
PB,	phosphate buffer
PBS,	phosphate-buffered saline
PKA,	protein kinase A
Px,	postnatal day x
PCR,	polymerase chain reaction
RNA,	ribonucleic acid
RT-PCR,	reverse transcriptase PCR
SDS-PAGE,	sodium dodecyl sulfate polyacrylamide gel electrophoresis
S.E.M.,	standard error of the mean
SN-agrin,	transmembrane agrin-x12, y4, z8
SN-agrin-mutant,	not cleavable variant of transmembrane agrin-x12, y4, z8 carrying point-mutations in the P1 positions (mutated to alanine, respectively) of the neurotrypsin cleavage sites
SRCR,	scavenger receptor cysteine-rich
STP,	short-term potentiation
TBS,	Tris-buffered saline
TBST,	TBS with Tween-20
tPA,	tissue-type plasminogen activator
uPA,	urokinase-type plasminogen activator
wt,	wild-type
XLMR,	X-chromosome-linked MR

1. Introduction

1.1 The brain and behaviour

The ability to perceive, to orientate within and to create our environment depends on a complex and refined machinery of sensory receptors connected to a highly flexible neuronal system, known as the central nervous system (CNS), that is able to discriminate and process the enormous range of information presented. The brain, a part of the CNS, is able to organise the continuous stream of sensory information and to integrate this information for appropriate behavioural responses. Furthermore, its ability to store information and to recall these memories enables the further refinement of future actions. The brain is composed of a variety of cell-types and the nerve cell or neuron constitutes the major information processing unit. The human brain consists of around 10^{11} neurons that can be classified into a multitude of different types (Kandel, 2000). However, all neurons share the same basic architecture (Fig. 1). The complexity of neuronal functions depend less on the specialisation of these neurons and more on their ability to form a specific and refined network of anatomic circuits. Hence, neurons with basically similar properties can produce a variety of potentially different actions depending on the way they are connected with each other or with sensory receptors or with the final output units, the muscles. The communication interface between neurons or between neurons and their alternative target cells is called the synapse, a highly specialised cell-cell contact site (section 1.1.3). Each CNS neuron forms, on average, tens of thousands of synapses, establishing the complex communication pattern found within the CNS.

Thus, the 10^{11} neurons in the human brain, forming 10^{15} synapses, generate a complex and organised but plastic network of anatomically defined circuits that have the capacity to translate experiences into a vast number of memories and actions (Chklovskii et al., 2004).

1.1.1 Neural plasticity

The nervous system has the ability to adapt to environmental stimuli and to alter and improve its performance over time, regulated by experience. This general capacity to functionally adapt, by undergoing molecular and structural changes, is termed neural plasticity. The fact that neural changes induced by experience can persist for a very long time, virtually for the whole life of the individual, suggests that neural plasticity represents the basis of the higher brain functions such as learning and memory (Benfenati, 2007).

A highly diverse array of neuron intrinsic mechanisms, influenced and controlled by its complex environment, are responsible for the positioning and maturation of neurons and their functional integration during development (Lagercrantz and Ringstedt, 2001; Dickson, 2002; Du and Dreyfus, 2002; Garner et al., 2002; Shen, 2004; Liu et al., 2006; McAllister, 2007). Neurons are highly polarised cells and are composed of distinct functional compartments, accounting for their specialised roles in communication and information

processing (Fig. 1). These distinct functional compartments enable the receipt of information (dendrites and cell body), the integration of all received information in time and space (initial

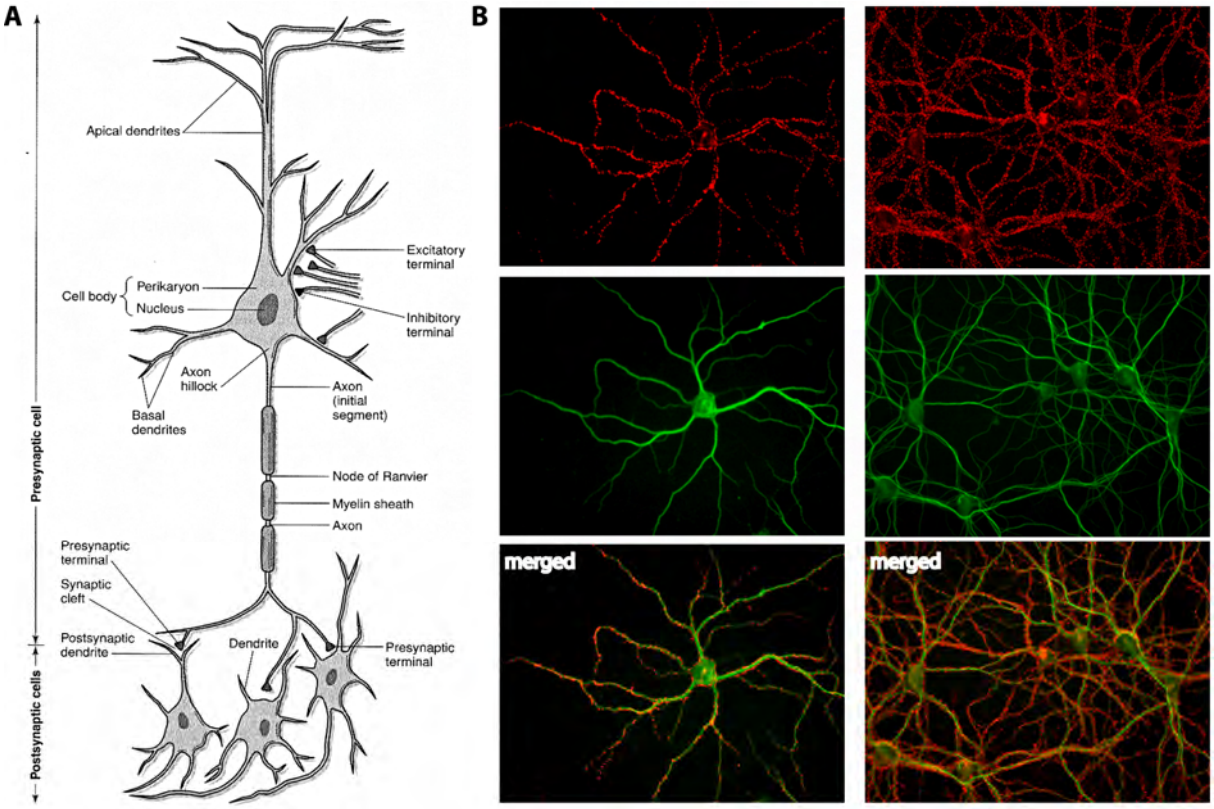

Figure 1. Structure of neurons. ***A,*** Schematic drawing of connected neurons. Most neurons in the vertebrate nervous system have several main features in common. The cell body contains the nucleus and gives rise to two types of cell processes, axons and dendrites. Axons, the transmitting elements of neurons, can vary greatly in length; some can extend more than 3 m within the body. Most axons in the CNS are very thin (between 0.2 and 20 μm in diameter) compared with the diameter of the cell body (50 μm or more). Many axons are insulated by a fatty sheath of myelin that is interrupted at regular intervals by the nodes of Ranvier. The action potential, the cell's conducting signal, is initiated either at the axon hillock, the initial segment of the axon, or in some cases slightly farther down the axon at the first node of Ranvier. Branches of the axon of one neuron (the presynaptic neuron) transmit signals to another neuron (the postsynaptic cell) at a site called synapse. The branches of a single axon may form synapses with as many as 1000 other neurons. Whereas the axon is the output element of the neuron, the dendrites (apical and basal) are input elements of the neuron. Together with the cell body, they receive synaptic contacts from other neurons. Figure and text taken and modified from (Kandel, 2000). ***B,*** Examples of cultured dissociated hippocampal neurons grown for 14 days *in vitro* to visualise the complexity of synaptic connections between neurons. Immunofluorescence analyses, widefield microscopy. Dendritic processes of cultured neurons were visualised with antibodies against the dendritic marker microtubule-associated protein 2 (MAP-2; green). Individual synapses along the dendrites, formed with axons of contacting neurons (not seen), were visualised using an antibody against the synaptic marker synaptophysin (red).

segment of the axon), the rapid transfer of nerve impulses (axon) and the transmission of signals (synapses) to the respective target cells (Kandel, 2000). The establishment of functional neuronal circuits during development requires the refinement or remodelling of neuronal connections by various forms of neuronal activity (Lagercrantz and Ringstedt, 2001; Juttner and Rathjen, 2005). However, the complex and functional neuronal network

established in the adult CNS does not remain static but continuously undergoes changes to meet the demands of learning and memory processes (Duffau, 2006). These changes include the remodelling of specific functional circuits (De Paola et al., 2006) as well as the generation and integration of new neurons into the neuronal circuitry (Ming and Song, 2005; Kitabatake et al., 2007; Toni et al., 2007). These changes occur as modifications of neuronal circuits, most likely at the level of synaptic connections, including both changes in the efficacy of existing synapses and the addition or subtraction of synapses (Chklovskii et al., 2004).

1.1.2 Synapses and dendritic spines

Synapses are a form of cell-cell contact sites specialised to transmit information between neurons or neurons and other targets, e.g., the muscle. The predominant type within the CNS is the chemical synapse, employing small molecules (neurotransmitters) to stimulate a response in the postsynaptic cell. In contrast, electrical synapses, which involve a direct electrical coupling between cells, are far less frequent (Garner et al., 2006). Chemical synapses are asymmetric structures, composed of elements originating from both cells. The presynaptic bouton and postsynaptic reception apparatus are separated by a small gap called the synaptic cleft. An electrical signal generated by the source neuron, propagated as an action potential, triggers the presynaptic release of neurotransmitters into the synaptic cleft to stimulate postsynaptic receptors that translate this chemical signal back into electric information within the target cell (Benfenati, 2007). Basically, depending on the type of neurotransmitter employed and on postsynaptic receptor function, transmitted signals elicit excitatory, inhibitory or modulatory functions on the postsynaptic cell. However, these basic functional properties are determined and modified by a variety of physiological parameters depending on complex mechanisms of regulation, in turn influenced and triggered by synaptic activity (section 1.1.3).

Synapse formation is a multi-step process formed in most cases at contact sites between an axon and a dendrite or between an axon and the cell body. However, also axo-axonic as well as dendro-dendritic synapses exist (Garner et al., 2002; Garner et al., 2006). Several steps of maturation involve the assembly of cell-adhesion molecules (CAM) at contact sites, CAM-dependent or other receptor-ligand-dependent signalling and the subsequent assembly of sophisticated macromolecular protein complexes at pre- and postsynaptic specialisations (Garner et al., 2006; McAllister, 2007). Many steps of synapse formation rely directly on processes initiated and executed by neurons. However, recent findings confirm the important roles of astrocytes in synapse formation, maturation and function by both secretion of soluble factors and contact mediated processes (Oliet et al., 2004; Allen and Barres, 2005; Nadkarni and Jung, 2007; Witcher et al., 2007).

Astrocytes are a branched and star-shaped type of CNS glial cell and extend their processes in an area of around 100 μm. Processes of a single astrocyte contact neuronal membranes as well as the vasculature. By forming endfeet around the endothelia and smooth muscle cells and, on the neuronal side, by contacting synapses in several regions of the brain,

astrocytes play a key function in metabolic support of neurons. The observation that astrocytic processes contact both presynaptic and postsynaptic elements has led to the formulation of the concept of the three-sided or tripartite synapse (Fig. 2). By tightly enclosing the synapse, astrocyte processes provide a physical barrier to inhibit the diffusion of molecules, i.e., the spillover of neurotransmitters and other neuroactive substances outside the synaptic cleft. The synaptic functions of astrocytes are diverse and include the uptake, and therefore, clearance of synaptic transmitters released from the presynapse and the recycling of glutamate. Astrocytes also respond to synaptic activity by the release of gliotransmitters that can further influence synaptic activity (Fig. 2B). One astrocyte interacts with around 100.000 synapses and up to 60 percent of all synapses are enwrapped by astrocytic processes. It is speculated that synaptic strength and the degree of substances that leave the synaptic proximity determines if an astrocytic process ensheaths or retracts from synapses (Oliet et al., 2004; Bains and Oliet, 2007; Halassa et al., 2007; Witcher et al., 2007).

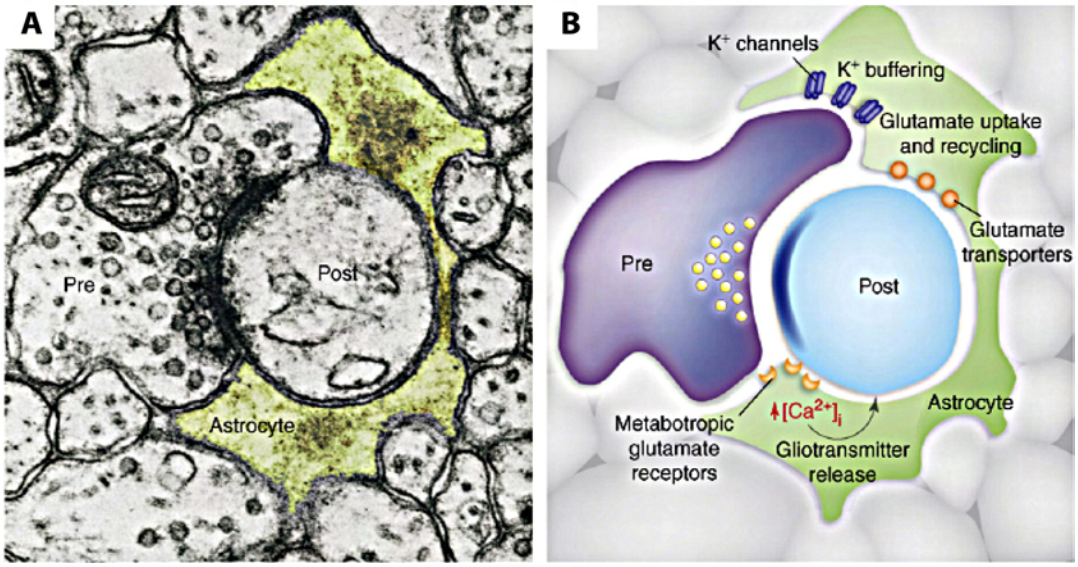

Figure 2. The astrocytic process is the third active element forming the tripartite synapse. ***A,*** Electron micrograph showing a presynaptic (Pre) and postsynaptic (Post) terminal enwrapped by the astrocytic process (green) forming the tripartite synapse. ***B,*** The close association of the astrocytic process with the presynaptic and postsynaptic terminals exerts crucial roles in clearing K+ ions that accumulate following neuronal activity, and in the uptake of the synaptic transmitter glutamate by the activity of plasma-membrane glutamate transporters. Additionally, neurotransmitter release from presynaptic terminals can activate astrocytic metabotropic receptors, which induce the inositol (1,4,5)-trisphosphate (Ins(1,4,5)P3)-dependent release of Ca^{2+} from internal stores, which in turn triggers the release of several neuroactive compounds (gliotransmitters) from these cells. Locations of astrocytic transporters and receptors in this figure do not necessarily represent their exact spatial distribution. Figure and text taken and modified from (Halassa et al., 2007).

The mature presynaptic terminal contains up to thousands of neurotransmitter-filled vesicles and a specialised molecular machinery mediating the docking and fusion of vesicles to release their contents at a specific region of the plasma membrane, called the active zone. Opposite the active zone, at the postsynaptic plasma membrane, a network of structural and scaffolding proteins is assembled, enabling the clustering of neurotransmitter receptors and

their associated signalling machinery. Both presynaptic and postsynaptic membranes are connected via a complex network of CAM and extracellular matrix (ECM) molecules that shape, stabilise and functionally modulate the synaptic structure (Yamaguchi, 2002; Dityatev and Schachner, 2003; Garner et al., 2006).

In terms of synaptic diversity, the main types of chemical synapses, i.e., inhibitory and excitatory synapses, differ in their molecular composition and structural features (Triller and Choquet, 2003). γ-aminobutyric acid (GABA) is the main inhibitory neurotransmitter in the vertebrate CNS with a modulatory role in practically every aspect of brain function. Signalling of GABA occurs via ionotropic ($GABA_A$) or metabotropic ($GABA_B$) receptors expressed at the postsynaptic membrane of potentially every CNS neuron (Fritschy and Brunig, 2003). Most excitatory neurotransmission in the CNS is mediated by glutamate, which act on a variety of ionotropic or metabotropic receptors. Three subclasses of ionotropic glutamate receptors exist, named after their selective agonists. The ligand-gated ionotropic α-amino-3-hydroxy-5-methly-4-isoxazole propionic acid-(AMPA)-type glutamate receptors (AMPAR) are the main mediators of excitatory neurotransmission but also kainate receptors contribute to postsynaptic responses. The voltage and ligand-gated N-methyl-D-aspartate (NMDA) receptors (NMDAR) are calcium (Ca^{2+}) permeable ion channels that play important modulatory roles by regulating synaptic plasticity (section 1.1.3). Finally, the G-protein coupled metabotropic glutamate receptors, divided into several subclasses, act through diverse signalling pathways that function to modulate neurotransmission. Different types of glutamate receptors were shown to coincide at individual synapses and the additional variable expression and assembly of receptor subunits emphasises the complexity of glutamate-dependent signalling (Frerking and Nicoll, 2000; Rubio, 2000; Lujan et al., 2005).

The functional parameters vary between individual synapses, including a variability in neurotransmitter and receptor expression, the molecular composition of structural and signalling molecules, the synaptic structure and its size. This diversity becomes even morphologically apparent when the types of chemical synapses are compared. Inhibitory synapses appear as rather symmetrical structures with the postsynaptic sites mainly formed on dendritic shafts or the neuronal cell bodies (Keller, 2002). However, most of the CNS synapses are excitatory with distinct morphological properties. In strong contrast to inhibitory synapses, more than 90 percent of excitatory synapses form their postsynapse on a dendritic specialisation called the dendritic spine (Fig. 3A-C; (Nimchinsky et al., 2002)). Dendritic spines are thin protrusions from the dendritic shaft believed to create a micro-environment that restricts information flow between adjacent synapses on the same dendrite (Keller, 2002; Garner et al., 2006). The exact process of dendritic spine and therefore spine synapse formation is controversially discussed and three main hypotheses were formulated (Fig. 3D; (Ethell and Pasquale, 2005)). One model describes that dendritic spines originate from synapses that were originally formed on dendritic shafts, supported by the observation that the majority of synapses on young pyramidal neurons are mainly located on dendritic shafts (Fig. 3D, model 1). In line with this model, axonal filopodia may be involved in synaptic contact

formation by finding an appropriate region for synapse formation on the dendritic shaft. Another model considers that the formation of dendritic spines is independent of axonal contact (Fig. 3D, model 2). This is based on findings on distal branches of Purkinje cells that form spines before the establishment of synaptic contacts. The third model states that dendritic filopodia are precursors of dendritic spines. In this line of thought, filopodia are believed to probe the dendritic environment to find an appropriate axonal contact site and to form initial synaptic contacts that further mature into spine synapses (Fig. 3D, model 3; Fig. 4). This model is based on findings describing that dendrites extend a high number of filopodia during early stages of synapse formation and that, while synapse maturation proceeds, the number of filopodia decreases whereas the number of stable spine synapses increases. Owing to the potential of differential molecular compositions within different types of neurons or at specific neuronal sites, it is possible that dendritic spines emerge through different mechanisms. However, a multitude of recent findings, obtained with live imaging experiments in living animals, strongly support the hypothesis that dendritic filopodia are indeed precursors of dendritic spines (Ziv and Smith, 1996; Ethell and Pasquale, 2005; Holtmaat et al., 2005; Matus, 2005; Zuo et al., 2005a; Holtmaat et al., 2006; Knott et al., 2006; Toni et al., 2007).

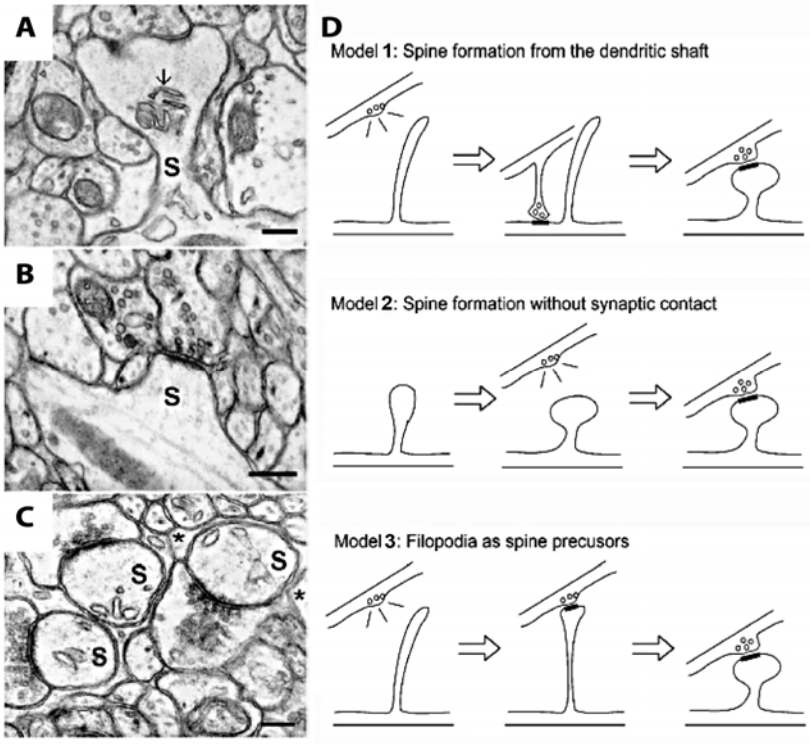

Figure 3. Ultra-structural appearance of dendritic spines. Characteristic electron micro-scopic appearance of several types of spines (S). ***A,*** A mushroom spine is shown. Note the constricted spine neck, the prominent irregular PSD, and the well-developed spine apparatus in this spine (*arrow*). Note also the density of the neuropil in this adult tissue. A stubby spine is illustrated in ***B***. Purkinje cell spines are very abundant (***C***) and are often seen in close contact with astrocytic processes (*asterisks*). The spine necks and their emergence from the parent dendrite are not shown in this photomicrograph. Note the presence of cisternae of SER in virtually all Purkinje cell spines. Micrographs (***A***) and (***B***) are from rat hippocampus; (***C***) is from mouse cerebellum. Scale bars: 300 nm (***A, B***), 250 nm (***C***). Electron micrographs from the *Atlas of Ultrastructural Neurocytology*, J. Spacek (http://www.synapses.bu.edu/atlas/contents.htm), with permission from the author. Panels ***A-C*** and text taken and modified from (Nimchinsky et al., 2002). ***D,*** Three models of dendritic spine genesis. Figure and text taken and modified from (Ethell and Pasquale, 2005).

Dendritic spines appear in variable shapes and are highly motile structures. Furthermore, morphology changes during synapse formation and at mature synapses are

correlated with changes in synapse efficacy and synaptic function (Hayashi and Majewska, 2005; Matus, 2005; Segal, 2005; Tada and Sheng, 2006). The spine head size correlates with synaptic strength, presumably related to the number of AMPAR levels within the postsynaptic membrane (Fig. 4, 7). In addition, smaller weaker spines are more prone to undergo changes in spine and synaptic structure while larger spines appear to be more stable (Tada and Sheng, 2006). It therefore becomes more and more apparent that dynamic rearrangements of dendritic spines are involved in changes of the synaptic circuitry. Several studies have confirmed that processes of learning and memory acquisition influence the generation of new spines, the disappearance of spines as well as the modulation of existing spines and synapses (Holtmaat et al., 2005; Zuo et al., 2005a; Zuo et al., 2005b; Holtmaat et al., 2006; Knott et al., 2006; Toni et al., 2007). Thus, the modulation of spine morphology leads to alterations in the synaptic transmission and contributes to neuronal plasticity, the precondition for processes such as learning and memory.

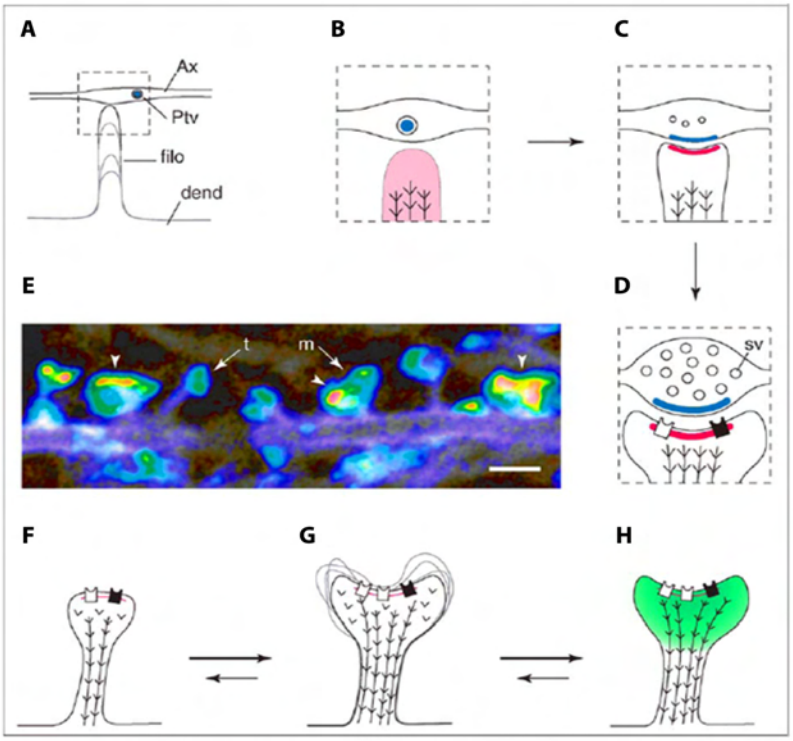

Figure 4. Actin-based motility in the lifetime of a dendritic spine. ***A,*** Growing dendrites (dend) produce motile filopodia (filo) that extend and retract (gray outlines) until they contact an axon (ax) containing presynaptic transport vesicles (ptv). The dashed box indicates the area shown in ***B-D***. ***B, C,*** Ptvs deliver molecular complexes of the structural proteins (blue) to the nascent presynaptic membrane, while molecules of the postsynaptic site (red) accumulate from a diffuse cytoplasmic pool. Herringbone lines indicate actin filaments, 'v' shapes indicate actin monomers. ***D,*** Spine maturation proceeds by the accumulation of synaptic vesicles (sv) in the presynaptic bouton, then NMDA receptors (black boxes) followed by AMPA receptors (white boxes) in the postsynaptic membrane. ***E,*** A composite confocal image of the surface of a pyramidal cell dendrite in a hippocampal slice culture, taken from a transgenic mouse expressing a membrane-targeted GFP construct. Thin spines with small heads (t) and large spines with mushroom-shaped heads (m) are identified. A superimposed motility plot, derived from a time-lapse recording of the same dendrite, shows local levels of motility on a psuedocolor scale ranging from blue (lowest) through green and yellow to red (highest). Note the prominent motility associated with the tips of large spines (arrowheads). Scale bar: 2 mm. ***F, G,*** LTP-type stimulation produces increases in both actin polymerisation and size of the spine head. This is coupled with increased expression of AMPA receptors (white boxes). Large spines are motile and show rapid lamellipodial ruffling of the spine head indicated by alternative gray outlines ***(G, E)***. ***H,*** Prolonged stimulation of NMDA receptors produces long-lasting blockade of head motility accompanied by targeting of actin binding proteins (green) to the spine head. Figure and text taken and modified from (Matus, 2005).

1.1.3 Synaptic plasticity

Single neurons form thousands of synapses and their pattern of connection and function determines the parameters of neuronal circuits, essential for the basic and higher functions of the brain. Each synapse can act as its own computational unit and its individual function is believed to be mainly regulated by changes in neurotransmitter release and neurotransmitter receptor function. It is therefore considered that synapses, in particular excitatory synapses located on dendritic spines, are the major sites of neuronal plasticity in the CNS and that fundamental brain processes like learning and memory involve plastic changes in synapse structure and function (Frotscher et al., 2007; Shepherd and Huganir, 2007). The structural and functional reconfiguration of synapses is termed synaptic plasticity (Juttner and Rathjen, 2005).

It is generally hypothesised that long-lasting activity-dependent changes in the efficacy of synaptic communication are of fundamental importance for the development of the neuronal circuitry and the storage of information in the mammalian brain. Model systems illustrating these changes in synaptic efficacy, thus synaptic plasticity, are long-term potentiation (LTP) and long-term depression (LTD) in the hippocampus, a brain region known to be involved in learning and memory processes (Bliss and Collingridge, 1993; Nicoll and Malenka, 1995; Akhondzadeh, 1999; Malenka and Nicoll, 1999).

The Hippocampus is a bilateral structure in the mammalian brain and it can be structurally divided into the Ammons horn, the dentate gyrus and the subiculum. The Ammons horn can be further separated into three subfields, termed the Cornu Ammonis (CA) 1-3. Viewed from the outer to the more medial layer, the Ammons horn includes alveus, strata oriens, oyramidal, radiatum, lacunosum and the molecular layer. The dendate gyrus is composed of closely packed cells that have dendritic brushes extending only towards the outer layer of the dentate gyrus. The subiculum is located at the distal borders of the CA1 region with the entorhinal cortex located ventrally and the retrosplenial cortex located dorsally to the hippocampal formation. Myelinated fibres, arising in part from the hippocampus, coat the surface of the hippocampus and mostly leave the region through a large efferent pathway, termed the fornix. Neuronal input reaches the hippocampus mainly in the dentate gyrus from the entorhinal cortex via a massive projection termed the perforant path. In turn, the dentate gyrus granule cells project via their Mossy fibres to the CA3 region. From the CA3 the Schaffer collaterals, parallel axons of CA3 pyramidal neurons, provide the major input to CA1. Other axons leave the cells of the CA3 via the fornix. Schaffer collaterals mainly form synapses with dendrites of CA1 pyramidal neurons in the stratum radiatum and stratum oriens layers (Fig. 5; (Akhondzadeh, 1999)).

Most information concerning LTP were gathered from experiments performed with rodent hippocampal tissue but similar phenomena have also been reported to occur in the human CNS (Cooke and Bliss, 2006). Experimentally induced LTP is characterised by an abrupt and long-lasting increase in the efficacy of synaptic transmission, induced by brief trains of high-frequency stimulation of monosynaptic excitatory pathways. Although LTP was

initially described for synaptic connections in the hippocampus, it can be observed at excitatory synapses throughout the mammalian brain. In contrast to LTP, LTD is a process resulting in long-lasting attenuation of synaptic strength and is stimulated by lower frequencies of stimulation when compared to LTP (Berninger and Bi, 2002). LTP is provoked rapidly but it lasts up to days, if stimulated *in vivo*. The later phases of LTP require gene transcription and protein synthesis, in line with the requirements for long-lasting forms of memory. Yet, it is still controversial whether LTP is stimulated during learning and related to memory formation (Malenka and Nicoll, 1999).

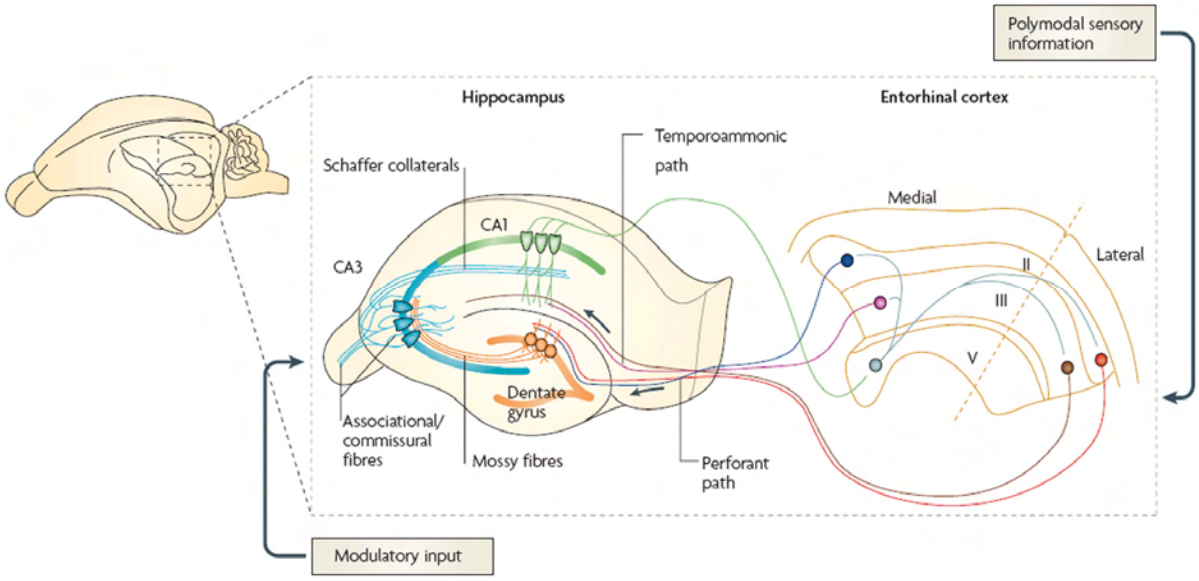

Figure 5. Basic anatomy of the hippocampus. The wiring diagram of the hippocampus is traditionally presented as a trisynaptic loop. The major input is carried by axons of the perforant path, which convey polymodal sensory information from neurons in layer II of the entorhinal cortex to the dentate gyrus. Perforant path axons make excitatory synaptic contact with the dendrites of granule cells: axons from the lateral and medial entorhinal cortices innervate the outer and middle third of the dendritic tree, respectively. Granule cells project, through their axons (the mossy fibres), to the proximal apical dendrites of CA3 pyramidal cells which, in turn, project to ipsilateral CA1 pyramidal cells through Schaffer collaterals and to contralateral CA3 and CA1 pyramidal cells through commissural connections. In addition to the sequential trisynaptic circuit, there is also a dense associative network interconnecting CA3 cells on the same side. CA3 pyramidal cells are also innervated by a direct input from layer II cells of the entorhinal cortex (not shown). The distal apical dendrites of CA1 pyramidal neurons receive a direct input from layer III cells of the entorhinal cortex. There is also substantial modulatory input to hippocampal neurons. The three major subfields have an elegant laminar organisation in which the cell bodies are tightly packed in an interlocking C-shaped arrangement, with afferent fibres terminating on selective regions of the dendritic tree. The hippocampus is also home to a rich diversity of inhibitory neurons that are not shown in the figure. Figure and text taken and modified from (Neves et al., 2008).

NMDA receptor-dependent (e.g., in the CA1 region) as well as independent (e.g., at mossy fibres synapses in CA3) forms of LTP have been described and both forms are characterised by a rise of intracellular Ca^{2+} levels. LTP generation or its modulation is further influenced by metabotropic G-protein-coupled receptors (an excerpt of components of the molecular machinery involved in LTP is shown in Fig. 6). Modulations of the size or dynamics of postsynaptic Ca^{2+} increases have a massive effect on synaptic plasticity because

Ca^{2+} levels that do not reach the threshold for LTP may elicit LTD or short-term potentiation (STP). STP is characterised by a brief synaptic enhancement that decays after 5 to 20 minutes (Malenka and Nicoll, 1999). The biochemical pathways that translate the Ca^{2+} signal into synaptic strength are hardly understood and seem to involve a large variety of different proteins. One of the best characterised key-components of the molecular machinery of LTP is the α-calcium-calmodulin-dependent protein kinase II (CaMKII). In addition, a whole variety of additional kinases and downstream signalling cascades as well as retrograde messengers affecting presynaptic functions are involved in LTP-dependent processes, indicating its molecular complexity (Fig. 6). The LTP-dependent increase in synaptic strength is directly connected to the increase in AMPA receptor responsiveness, its upregulation and its insertion at postsynaptic sites (Malenka and Nicoll, 1999; Shepherd and Huganir, 2007). Therefore, the long-lasting modification of synaptic structure and function is an accepted mechanism by which experiences contribute to learning and are translated into memories (Malenka and Nicoll, 1999).

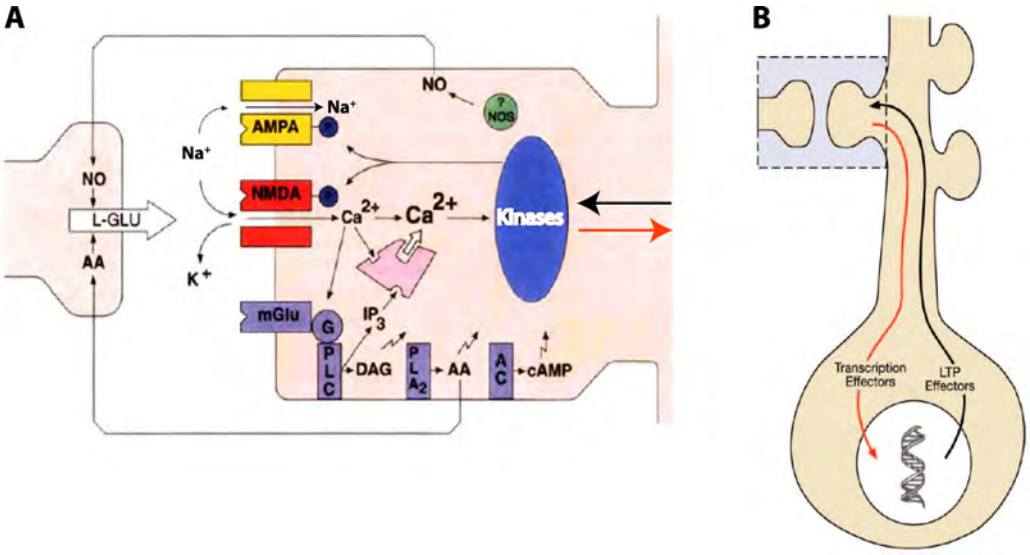

Figure 6. Intracellular signalling mechanisms mediating NMDA receptor-dependent long-term potentiation (LTP). ***A,*** The initial induction signal is a Ca^{2+} transient which permeates NMDAR. This signal is then amplified by the release of Ca^{2+} from Ca^{2+}/inositol triphosphate ($InsP_3$)-sensitive intracellular stores. A parallel pathway which may be important for the induction of LTP is provided by metabotropic glutamate receptors (mGluRs). These receptors can couple, through G-proteins, to the phosphoinositide-specific phospholipase C (PLC), phospholipase A_2 (PLA_2) and adenylate cyclase (AC), to produce diacylglycerol (DAG), arachidonic acid (AA), and to regulate the levels of cAMP, respectively, Note that the initial NMDAR-mediated Ca^{2+} transient may be necessary for the activation of these mGluR cascades by L-glutamate. The amplified Ca^{2+} signal, in association with the other activators of protein kinases (zig-zag arrows), then leads to the phosphorylation of substrate proteins including, probably, AMPAR and NMDAR. Other enzymes, such as nitric oxide synthase (NOS), if present, may also be activated by the Ca^{2+} transient. Biochemical changes in the presynaptic terminal may be initiated by the action of retrograde messengers, such as arachidonic acid (AA), nitric oxide (NO) and K^+, perhaps in conjunction with the action of L-glutamate on presynaptic mGluRs. ***B,*** Kinase-mediated signalling to the cell nucleus occurs via a number of intermediary steps, resulting in changes in transcription and eventual expression of proteins involved in long-lasting changes that mediate persistent LTP. Figures and text taken and modified from (Bliss and Collingridge, 1993; Cooke and Bliss, 2006).

The increase or decrease of synaptic strength is correlated with alterations in dendritc spine shape and size (Fig. 7). It has been shown that rapid tetanic stimulation, hence the induction of LTP, in hippocampal slices or cultures resulted in the rapid expansion of spine heads as well as the generation of new spines. In contrast, induction of LTD led to shrinkage of spines as well as a reduction in spine number (Segal, 2005; Tada and Sheng, 2006). The generation, destabilisation and morphology changes of dendritic spines rely on dynamics of the actin-cytoskeleton, in which actin polymerisation results in spine size increase and depolymerisation to shrinkage of spines (Fig. 7A). These processes are regulated by a variety of actin-binding proteins present in the spine, in turn regulated by signalling cascades. Actin polymerisation and thus spine structure is influenced by Ca^{2+}-dependent signalling, potentially regulated by CaMKII activity. Finally, it has been shown that NMDAR-dependent signalling and LTP are associated with a long-lasting increase of polymerised actin within dendritic spines, resulting in an increase of spine volume (Ethell and Pasquale, 2005; Hayashi and Majewska, 2005; Lippman and Dunaevsky, 2005; Matus, 2005; Segal, 2005; Tada and Sheng, 2006).

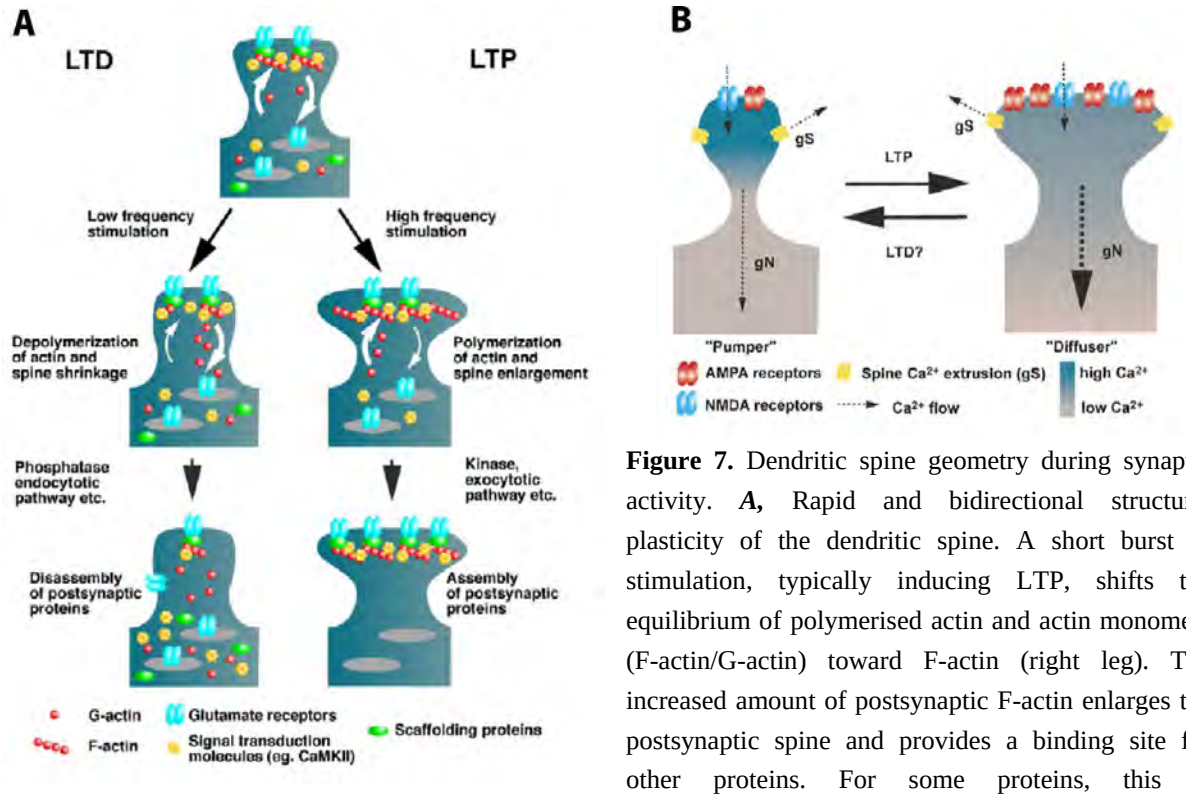

Figure 7. Dendritic spine geometry during synaptic activity. ***A,*** Rapid and bidirectional structural plasticity of the dendritic spine. A short burst of stimulation, typically inducing LTP, shifts the equilibrium of polymerised actin and actin monomers (F-actin/G-actin) toward F-actin (right leg). The increased amount of postsynaptic F-actin enlarges the postsynaptic spine and provides a binding site for other proteins. For some proteins, this is sufficient as an activity-dependent delivery mechanism to the postsynapse. For other proteins, synergistic activation of other mechanisms, such as phosphorylation or other posttranslational modifications, are necessary for postsynaptic delivery. In contrast, prolonged low-frequency stimulation, typically inducing LTD, shifts the F-actin/G-actin equilibrium toward G-actin (left leg). This reduces postsynaptic F-actin and, hence, other F-actin binding proteins, resulting in disassembly of the postsynaptic protein complex and a shrinkage of the dendritic spine. This will eventually disrupt anchorage of surface glutamate receptors, leading to loss of synaptic receptors. Other mechanisms, such as dephosphorylation or endocytosis, are likely involved as well. ***B,*** Ca^{2+} compartmentalisation and dendritic spine geometry during synaptic activity. Small dendritic spines (left) have relatively larger NMDA currents than AMPA currents, which may be electrophysiologically recorded as 'silent'

synapses (Groc et al., 2006). Ca^{2+} efflux from the spine is accomplished primarily through Ca^{2+} extrusion pumps (spine head conductance [gS]) located in the spine head. These spines are predominantly 'pumpers', as the spine neck is narrow and precludes Ca^{2+} diffusion into the dendrite (spine neck conductance [gN] is low). This results in large, prolonged Ca^{2+} signals in the spine and little Ca^{2+} increase in the dendritic shaft. Large dendritic spines (right), such as those observed after potentiation, have proportionally larger AMPA currents than NMDA currents. Ca^{2+} efflux from the spine head happens through two pathways: Ca^{2+} extrusion in the spine head (gS) and, due to the large radius of the spine neck, through Ca^{2+} diffusion in the dendritic shaft (gN). In these spines, Ca^{2+} increases are more moderate and transient, while dendritic Ca^{2+} concentrations are observed to change at the spine base. Figures and text taken and modified from (Hayashi and Majewska, 2005).

←

Studying the effects of LTP on a molecular and structural level have led to the identification of a wide variety of signalling cascades, influencing molecular as well as structural properties of the synapse. Plasticity-dependent changes of structural domains like dendritic spines and other plasticity-dependent modifications in synaptic structure are also directly influenced by ECM molecules. ECM molecules are known to be involved in synaptic development and plasticity, as signalling through their cell-surface receptors is known to modulate synaptic efficacy (Dityatev and Schachner, 2003; Pavlov et al., 2004; Dityatev and Schachner, 2006). Furthermore, rearrangements of cellular domains require the remodelling of the ECM, processes mediated by extracellular proteases. Extracellular proteolysis is implicated in general structural rearrangements at the synapse and proteases were shown to contribute directly to synaptic plasticity (Shiosaka, 2004; Juttner and Rathjen, 2005; Ethell and Ethell, 2007). Taken together, synaptic plasticity involves a large and diverse machinery of structural and functional rearrangements allowing the fine-tuning of synaptic contacts and thus neuronal circuit modification that is believed to be essential for processes involving learning and memory formation.

1.1.4 Mental retardation disorders

The brain's ability to process environmental stimuli and its ability to learn, remember and integrate this information for refined behavioural responses is mainly regulated at the level of the functional formation of neuronal networks. These networks are built and refined during development. Children show enhanced capacity for learning and memory compared to adults and the mechanisms for enhanced brain plasticity include postnatal neurogenesis in certain parts of the brain, the deletion of neurons, as well as changes at the synaptic level (Johnston, 2004). These synaptic changes include the generation or removal of synapses as well as activity-dependent refinement of synaptic contacts, summarised by the term synaptic plasticity (section 1.1.3). During the first two years of postnatal development in humans, approximately twice as many synapses are present in the cerebral cortex when compared to the adult. Further, synapse elimination and the refinement of synaptic circuits occurs mainly until around 16 years of age (Johnston, 2004). The complex molecular regulation of processes found to mediate, maintain or shape synaptic plasticity enable the refinement of the neuronal circuitry and are a precondition for processes such as learning and memory. However, the

demands for complex interactions and fine-tuning mechanisms render this system vulnerable to defects. Mutations or deletions of single proteins may provoke drastic phenotypes leading to the impairment of plasticity processes. Indeed, a diverse group of clinical disorders are caused by aberration or disruption of signalling cascades that have been implicated in learning and memory processes in animal models (Johnston, 2004).

Mental retardation (MR), also termed intellectual disability, is a common form of nonprogressive cognitive impairment, generally defined by an overall intelligence quotient (IQ) below 70. It includes deficits in adaptive behaviour which manifest before the age of 18. MR affects around 1-3 percent of the general population and is widely diverse in its causes. Several non-genetic factors are known to act prenatally or during early childhood. These include infectious diseases, very premature birth or excessive maternal alcohol consumption during pregnancy. Genetic causes of MR include chromosomal abnormalities, like chromosomal microdeletions and monogenic diseases (Chelly and Mandel, 2001; Basel-Vanagaite et al., 2007; Fernandez and Garner, 2007).

Nonsyndromic mental retardation (NSMR) is characterised by cognitive defects that are not accompanied by major physical anomalies or neurological abnormalities. Hence, aberrations in molecular processes implicated in neuronal differentiation or synaptic plasticity are believed to be involved in the development of MR (Chelly and Mandel, 2001; Basel-Vanagaite et al., 2007). Generally, genetically caused MR can be grouped into X-chromosome-linked MR (XLMR) and autosomal MR. The XLMR variant fragile X syndrome is the most commonly inherited MR, associated with an X-chromosomal fragile site in the fragile X mental retardation 1 (FMR1) gene (Chelly and Mandel, 2001). This mutation is characterised by the expansion of a trinucleotide repeat that results in transcriptional silencing of the FMR1 gene. The FMR1 protein (FMRP) is a messenger RNA (mRNA) binding protein involved in the regulation of local synaptic protein synthesis. Interestingly, mutation or absence of FMRP leads to aberrations in spine morphology. In fragile X syndrome patients, as well as in related animal models of the disease, dendritic spines appear morphologically immature as long and thin protrusions. Spines are dynamic structures that mature during development and their maturation depends on electric activity (sections 1.1.2 and 1.1.3) and it has been described that these morphological changes require local protein synthesis. However, FMRP was reported to bind a large number of mRNAs but the distinct targets involved in spine maturation remain elusive (Zalfa et al., 2006). Synapses on dendritic spines are the major targets for plasticity related phenomena involved in learning and memory formation and it is therefore not surprising that other genomic mutations have been described that cause mental disorders like MR by altering spine formation and morphology (Blanpied and Ehlers, 2004; Carlisle and Kennedy, 2005). An additional variant of XLMR shown to be linked to aberrant spine plasticity is caused by mutations in the PAK3 gene (Boda et al., 2004; Boda et al., 2006; Kreis et al., 2007).

A recently identified mutation in the autosomal gene PRSS12 was shown to cause autosomal NSMR in humans (Molinari et al., 2002). PRSS12 codes for the synaptic protease

neurotrypsin and the described mutation caused a frameshift mutation leading to a complete functional inactivation of the enzyme (section 1.2.2.3). This finding highlights the importance of proteolytic processes in fine-tuning events of CNS plasticity.

1.2 Proteases in the CNS

Enzymes function by efficiently catalysing and directing chemical reactions, enabling the rapid conversion of molecular properties essential for the function of biological systems. Proteases are a class of enzymes that catalyse the hydrolysis of peptide bonds of their respective protein substrates, resulting in substrate cleavage. Proteases are categorised into families depending on the composition of the enzyme's active site and therefore the mode of catalysis. In the CNS, members of several families of proteases are expressed, including serine proteases, matrix metalloproteinases (MMP), cysteine proteases and aspartic proteases. CNS-proteases are involved in almost all aspects of CNS development and maintenance, such as cell proliferation, migration, apoptosis, axonal growth, tissue and ECM remodelling, synaptogenesis as well as synaptic plasticity (Zhang et al., 2005; Shiosaka, 2004).

In the context of synaptic plasticity, important related processes are the structural and functional modification of established synapses as well as the structural reorganisation of synaptic circuits involving the formation of new synapses and the elimination of existing ones (Chklovskii et al., 2004). Both mechanisms have been reported to involve proteolysis by extracellular proteases (Shiosaka, 2004). Explained by their high efficiency in substrate conversion, proteolytic processes in the CNS have to be tightly regulated to reach spatially and temporally restricted substrate cleavage. This is partially achieved by their production as inactive precursors (zymogens) and regulated activation (Khan and James, 1998) as well as termination of the proteolytic activity by removal or degradation of the active enzyme (Binder et al., 2007). Regulation may further be mediated by the interaction with specific endogenously expressed inhibitors that exist for each set of protease families. Imbalances within these complex regulation patterns affect the events crucial for CNS development and function and have been implicated in a variety of neuropathological changes (Lukes et al., 1999; Zhang et al., 2005; Hook, 2006; Ethell and Ethell, 2007).

1.2.1 Serine Proteases

Serine proteases, named after the catalytic serine at their active site, are the largest family of proteases, as almost one-third of all proteases belong to this family. They are secreted enzymes and enzymatically characterised by the so called "catalytic triade", consisting of the three interacting amino acids serine, histidine and aspartate. These amino acids are positioned within the active-site cleft of the respective enzyme, enabling the optimised interaction with the substrate. Substrate peptide bond hydrolysis is initiated by a nucleophilic attack of the active-site serine on the carbonyl of the peptide substrate group (Fig. 8). The 4 existing clans of serine proteases mainly differ in the order and position of the

catalytic-triade amino acids within the primary structure of the respective enzyme (Hedstrom, 2002).

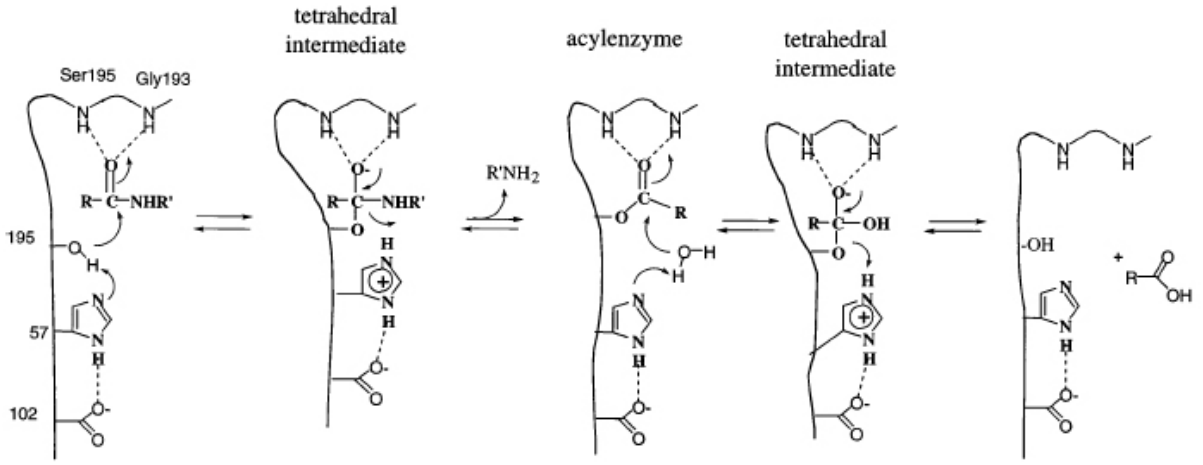

Figure 8: Catalytic mechanism of chymotrypsin-like serine proteases (Hedstrom, 2002). In the acylation half of the reaction, serine (Ser)195 attacks the carbonyl of the peptide substrate, assisted by histidine (His)57 acting as a general base, to yield a tetrahedral intermediate. The resulting His57-H+ is stabilised by the hydrogen bond to aspartate (Asp)102. The oxyanion of the tetrahedral intermediate is stabilised by interaction with the main chain NHs of the oxyanion hole. The tetrahedral intermediate collapses with expulsion of leaving group, assisted by His57-H+ acting as a general acid, to yield the acylenzyme intermediate. The deacylation half of the reaction essentially repeats the above sequence: water attacks the acylenzyme, assisted by His57, yielding a second tetrahedral intermediate. This intermediate collapses, expelling Ser195 and carboxylic acid product. The acylenzyme intermediate is well established, but the tetrahedral intermediates are inferred from solution chemistry. The transition states of the acylation and deacylation reactions will resemble the high energy tetrahedral intermediates, and the terms ‘transition state’ and ‘tetrahedral intermediate’ are often used indiscriminately in the literature. It is worth noting that a web of hydrogen bonding interactions links the substrate binding sites to the catalytic triad. As the reaction proceeds, changes in bonding and charge at the scissile bond will propagate to more remote enzyme-substrate interactions, and vice versa. Figure and text taken and modified from (Hedstrom, 2002).

The chymotrypsin-like serine proteases, represented by over 240 proteases, are by far the biggest clan within the family of serine proteases and its members are involved in many critical physiological processes. These include cascades of sequentially activated serine proteases to drive blood coagulation and fibrinolysis as well as developmental processes, such as matrix remodelling, differentiation and wound healing (Hedstrom, 2002). Some chymotrypsin-like proteases have also been implicated in CNS-plasticity, e.g., tissue type plasminogen activator, plasminogen, neuropsin and neurotrypsin (section 1.2.2). The stringent roles in these tightly regulated processes demands proteases with adjustable activities and distinct substrate specificities (Hedstrom, 2002). Serine proteases are synthesised as inactive precursors (zymogens) and are usually converted to the active enzyme by limited proteolysis of an inhibitory segment. Activation of these secreted enzymes may already occur within an intracellular compartment or in the extracellular environment where they are supposed to function (Khan and James, 1998). The substrate specificities are usually defined by the characteristics of a substrate binding site adjacent to the active site cleft (Hedstrom, 2002;

Page et al., 2005). However, further interactions of the substrate with additional exosites of the protease may enhance substrate specificity (section 1.3.2). Further regulatory mechanisms include the regulated interaction with endogenously expressed serine protease-specific inhibitors (Bode and Huber, 1992) as well as the removal or degradation of the active enzyme, hence terminating its proteolytic activity (Binder et al., 2007). Thus, substrate specificity and further regulatory mechanisms render serine proteases optimal for specific actions involved in plastic changes of the synaptic circuitry.

1.2.2 Chymotrypsin-like serine proteases and synaptic plasticity

Recent research has revealed the involvement of some chymotrypsin-like serine proteases as well as their inhibitors in CNS function, including synaptic plasticity (Shiosaka, 2004; Yepes and Lawrence, 2004; Zhang et al., 2005; Galliciotti and Sonderegger, 2006). Plastic changes of synapse-strength, involved in learning and memory processes, are connected with morphological changes of the individual synapse or associated structures (section 1.1.3). Furthermore, network-plasticity involves the reorganisation of synaptic circuits, including the formation of new synapses and the elimination of existing ones (Chklovskii et al., 2004). The synaptic cleft is filled with a network of polysaccharides and ECM molecules, connecting and stabilising pre- and postsynaptic elements (Dityatev and Schachner, 2006). It is speculated that adhesion and de-adhesion of cells in general is modulated by extracellular proteolysis and it is well documented that pericellular proteolysis of the ECM is involved in the formation or remodelling of the neuromuscular junction. Thus, the morphological rearrangements of CNS synapses or their elimination require the re-modulation of the ECM, mediated by proteases responsive to neuronal activity (Shiosaka, 2004). In addition, cleavage or interaction with extracellular substrates may also lead to direct activation or inhibition of signalling cascades involved in plasticity events (Samson and Medcalf, 2006; Stephan et al., 2008).

1.2.2.1 Tissue-type plasminogen activator and plasminogen

Tissue-type plasminogen activator (tPA) is a multidomain protein with a molecular mass (Mr) of 70 kilo Dalton (kDa) that contains a fibronectin type 1 domain, an epidermal growth factor domain, two kringle domains and the C-terminally located catalytic domain. The non-catalytic domains mediate protein-protein interactions, like the binding of tPA to fibrin. Because of its activation of Plasminogen, tPA was initially known as a fibrinolytic protease but its substrate spectrum extends to fibronectin and, more importantly, to the NR1 subunit of the NMDAR (Shiosaka, 2004). In the CNS, tPA is an immediate early gene that is highly responsive to chemical and electrical stimuli. Its expression pattern suggests roles as a modulator of neurotransmission as both tPA mRNA and tPA proteins have been localised to synapses. In addition, depolarisation was shown to induce exocytosis of tPA from intracellular stores, with its activation occurring directly after secretion. The overexpression of tPA in neurons of mice causes enhanced LTP and improved learning of the water maze

task. In contrast, tPA-deficient mice show selective interference with the late phase of hippocampal LTP. However, the involvement of tPA in hippocampal-dependent learning is still controversially discussed. tPA-deficient mice also revealed a reduced capacity to learn an active avoidance task, which implicates tPA function in striatum-dependent plasticity. When rats were trained for a complex motor task, tPA expression was increased in Purkinje cells of the cerebellar cortex, indicating that tPA may be involved in cerebellar motor learning.

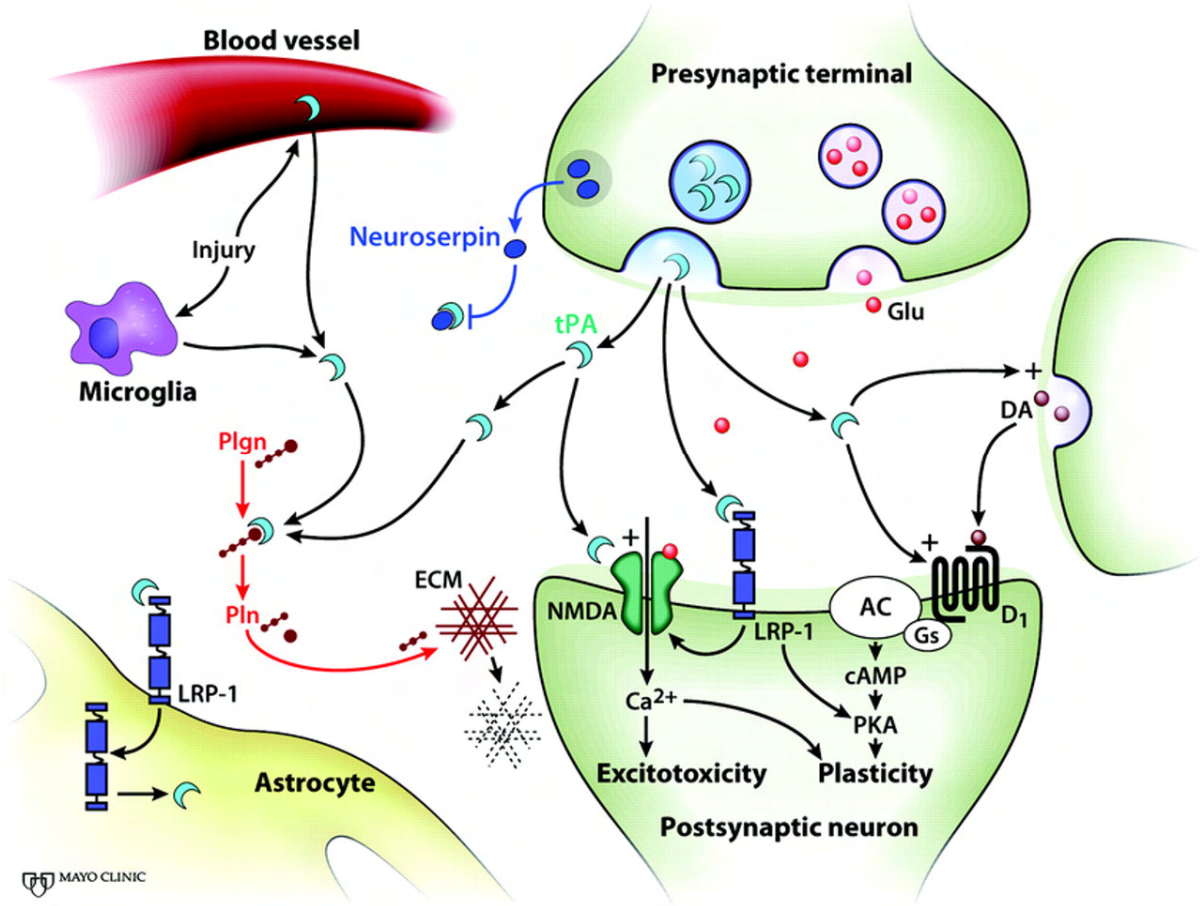

Figure 9. Tissue-type plasminogen activator (tPA) signaling in the CNS. tPA and its endogenous inhibitor, neuroserpin, are released from presynaptic terminals in response to depolarisation. tPA participates in mechanisms of synaptic plasticity by several mechanisms. Both directly and via its binding to the low-density lipoprotein–related receptor 1 (LRP-1), tPA increases calcium (Ca^{2+}) influx via NMDA receptors and potentiates dopamine (DA) D_1 receptors signaling via the adenylate cyclase (AC)–cyclic adenosine monophosphate (cAMP)–protein kinase A (PKA) pathway. tPA also triggers conversion of plasminogen (Plgn) into plasmin (Pln), which has a proteolytic effect on the extracellular matrix (ECM) that is important for synaptic remodeling. LRP-1 is involved in endocytosis of tPA by the astrocyte and in transcytosis of tPA through an intact blood–brain barrier. In the setting of acute injury, tPA is released from injured blood vessels and microglia and may contribute to ECM degradation and NMDA-mediated excitotoxicity. Neuroserpin inhibits these effects. Figure and text taken and modified from (Benarroch, 2007).

How tPA influences all these plasticity-related phenomena is not completely clear but several reported actions may explain tPA's functions. As mentioned above, tPA cleaves the NR1 subunit of the NMDAR but direct functional implications of this cleavage are so far not known. It is possible that this interaction leads to downstream effects of altered Ca^{2+}-

dependent signalling, modifying LTP. It was also reported that tPA interacts with the NR2B subunit of NMDAR. This interaction does not involve cleavage, however, binding of tPA to NR2B resulted in the ablation of NMDAR-dependent phosphorylation of the extracellular signal-regulated kinase 1/2 (ERK1/2) that is known to be involved in LTP and LTD (Ito-Ishida et al., 2006). Additional functions of tPA include binding to and signalling through the low-density lipoprotein receptor-related protein 1 (LRP-1). Again, catalytic activity of tPA is not required for this process. The interaction of tPA and LRP-1 induces an increase of cyclic adenosine monophosphate (cAMP) levels and protein kinase A (PKA) activity, resulting in synaptic potentiation. The involvement of the tPA/LRP-1 interaction in synaptic plasticity-related processes is supported by the general finding that low-density lipoprotein receptor (LDLR) family members, like LRP-1, are crucial for hippocampal CA1-dependent LTP. Theoretically, also a potential tPA-dependent proteolytic activity on ECM molecules could contribute to tPA's role in synaptic plasticity. Importantly, tPA converts plasminogen into active plasmin also in the CNS, therefore activating another protease involved in synaptic plasticity (see below). Finally, extracellular tPA activity is regulated by inhibitors like neuroserpin and plasminogen activator inhibitor-1 (PAI-1), increasing the complexity of potential tPA-dependent functions (Shiosaka, 2004; Samson and Medcalf, 2006). Taken together, many different actions of tPA may explain its involvement in processes contributing to synaptic plasticity. These processes possibly occur independent as well as dependent on plasminogen activation (Fig. 9).

Plasminogen is a multidomain glycoprotein with a Mr of 92 kDa, consisting of an N-terminal activation peptide, five kringle domains and a C-terminal catalytic domain. Again, the kringle domains mediate protein-protein interactions, such as substrate recognition, membrane association and inhibitor binding. Plasminogen can be activated by tPA, urokinase-type plasminogen activator (uPA), kallikrein as well as by several coagulation factors and it plays an important role in fibrin clot degradation. In the CNS, plasminogen is highly expressed in the hippocampus, the cerebral cortex and the cerebellum and is most likely activated by tPA and uPA, both known to be expressed in the CNS. Activated plasminogen, termed plasmin, has a broad spectrum of substrates, including the ECM proteins laminin and fibronectin. Furthermore, plasmin was shown to activate MMPs, which can degrade other ECM molecules that are involved in synaptic plasticity (section 1.2). Several effects downstream of tPA-activation (see above) have been shown to involve plasmin activation, mediating processes involved in synaptic plasticity. The tPA-mediated activation of plasmin triggers dopamine release in the nucleus accumbens upon morphine injection, implicating the tPA-plasmin system in drug-dependent synaptic plasticity. Additionally, hippocampal CA1-dependent LTP, triggered by tPA, was reported to depend partially on plasmin-mediated generation of neurotrophins. And finally, plasmin has been shown to enhance NMDAR-dependent intracellular Ca^{2+} levels (Zhang et al., 2005; Samson and Medcalf, 2006). As already mentioned in the context of tPA functions, plasmin activity is also regulated by

inhibitors like neuroserpin and plasminogen activator inhibitor-1 (PAI-1), potentially regulating plasticity-dependent effects of plasmin (Zhang et al., 2005).

1.2.2.2 Neuropsin

Neuropsin is a simple neuronal serine protease with a Mr of around 30 kDa, containing only one characteristic domain that mediates neuropsin's proteolytic activity. This protease is mainly expressed in the hippocampus, the amygdala and the entorhinal cortex and its expression is caused by neuronal stimulation such as stimuli-induced epilepsy or LTP. Neuropsin is believed to be secreted by both synaptic activity-dependent and -independent mechanisms and stored extracellularly in its inactivated form, mostly within the synaptic cleft. Activation of neuropsin is dependent on synaptic activity and probably mediated by NMDAR-dependent signalling pathways. The inhibition of neuropsin activity by application of neutralising antibodies caused stimulus-induced progression of kindling epileptogenesis *in vivo*. In contrast, the bath application of neuropsin revealed a regulatory effect of early phase Schaffer collateral synapse LTP. In line with this evidence, neuropsin cleaves the synaptic cell-adhesion molecule L1 (L1CAM) upon stimulation of synaptic activity and cleavage occurs during early phase LTP. As blockage of L1CAM by specific antibodies as well as application of L1CAM fragments were shown to block early phase LTP, these data argue for a specific proteolysis-dependent effect of neuropsin on synaptic plasticity, maybe specific to the Schaffer collateral synapses (Shiosaka, 2004).

1.2.2.3 Neurotrypsin

Neurotrypsin is a multidomain serine protease and human neurotrypsin, with a Mr of around 97 kDa, contains a proline-rich basic domain, a kringle domain, 4 scavenger receptor cysteine-rich (SRCR) domains and the C-terminal protease domain (Fig. 10A; (Proba et al., 1998)). In contrast, murine neurotrypsin protein has a Mr of approximately 85 kDa, because of the expression of only 3 SRCR domains (Fig. 10B; (Gschwend et al., 1997)). By comparison of primates with other mammalian orders it was shown that a deletion of the exons encoding the first SRCR domain occurred in the murine lineage only (Xu and Su, 2005). The non-catalytic domains of neurotrypsin are believed to mediate protein-protein interactions, similar to the previously mentioned roles for the noncatalytic domains of tPA and plasminogen. These domains may mediate interactions with proteins involved in neurotrypsin targeting within the cell, its binding to the cell surface or ECM molecules, its interaction with substrates and/or the interaction with regulators of activation.

Details about the mode of catalytic activation of neurotrypsin are so far not known. However, its zymogen activation site (Fig. 10, arrow) is located proximal to the protease domain and proposes an activation mechanism similar to other proteases of its clan. Proteolytic cleavage at the zymogen activation site is supposed to separate the protein into two chains that are linked via a disulfide bridge. The removal of an 'activation segment' or the induction of structural changes by activation cleavage are believed to unlock the

proteolytic activity (Khan and James, 1998). A potential candidate for neurotrypsin activation is the protease furin (unpublished observations), a member of the subtilisin superfamily of serine endoproteases (Thomas, 2002). Furin is an ubiquitously expressed enzyme localised to the secretory pathway and potentially activates neurotrypsin during its secretion.

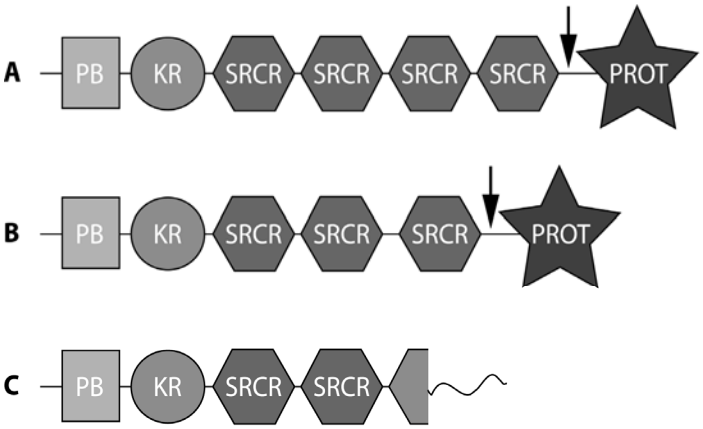

Figure 10. Schematic overview of neurotrypsin's protein structure. ***A,*** human neurotrypsin (Proba et al., 1998); ***B,*** mouse neurotrypsin (Gschwend et al., 1997); ***C,*** truncated human neurotrypsin (Molinari et al., 2002). PB – proline-rich basic domain; KR – kringle domain; SRCR – scavenger receptor cysteine-rich domain; PROT – protease domain. The arrow indicates the approximate position of the zymogen activation site of neurotrypsin.

Neurotrypsin is expressed in endothelial cells of the blood vasculature, in the kidney, in the lung and is expressed in the nervous system (Gschwend et al., 1997; Yamamura et al., 1997; Iijima et al., 1999; Wolfer et al., 2001; Aimes et al., 2003; Reif et al., 2007). Within the nervous system, neurotrypsin is expressed in a wide variety of regions (Fig. 11). This includes prominent expression in motorneurons of the spinal cord (Fig. 11E) and, concerning its expression in the brain, the cerebral cortex, the hippocampus and the amygdala (Fig. 11A-D; Fig. 12; (Gschwend et al., 1997; Iijima et al., 1999; Wolfer et al., 2001)). Neurotrypsin mRNA expression in the CNS is developmentally regulated and peaks around the first postnatal week in mice (Fig. 12; (Wolfer et al., 2001)). Furthermore, it was recently reported that neurotrypsin expression in motorneurons was downregulated after interruption of target contact by facial nerve axotomy and that its expression was re-established after facial motorneuron recovery and reinnervation of target muscles (Numajiri et al., 2006). Its prominent expression in CNS structures involved in learning and memory processes as well as its developmental and target contact regulated expression suggests a potential involvement of neurotrypsin function in crucial steps of CNS development and neuronal circuit refinement, hence synaptic plasticity. In support of this notion, neurotrypsin protein expression, analysed by immunoelectron microscopy, was localised to synapses in the cerebral cortex as well as in the hippocampus. Here, neurotrypsin was detected in presynaptic terminals, within vesicular structures in the area lining the synaptic cleft (Fig. 13; (Molinari et al., 2002; Stephan et al., 2008)). Further analyses in cultured hippocampal neurons revealed that its synaptic recruitment as well as its exocytosis from synaptic terminals is regulated by neuronal activity. Depolarisation of neurons leads to the exocytosis of synaptic neurotrypsin and the externalised protease was shown to linger at the synapse for minutes before disappearing due to diffusion or degradation (Frischknecht et al., 2008). These observations suggest an activity-dependent extracellular proteolytic function of neurotrypsin at the synapse.

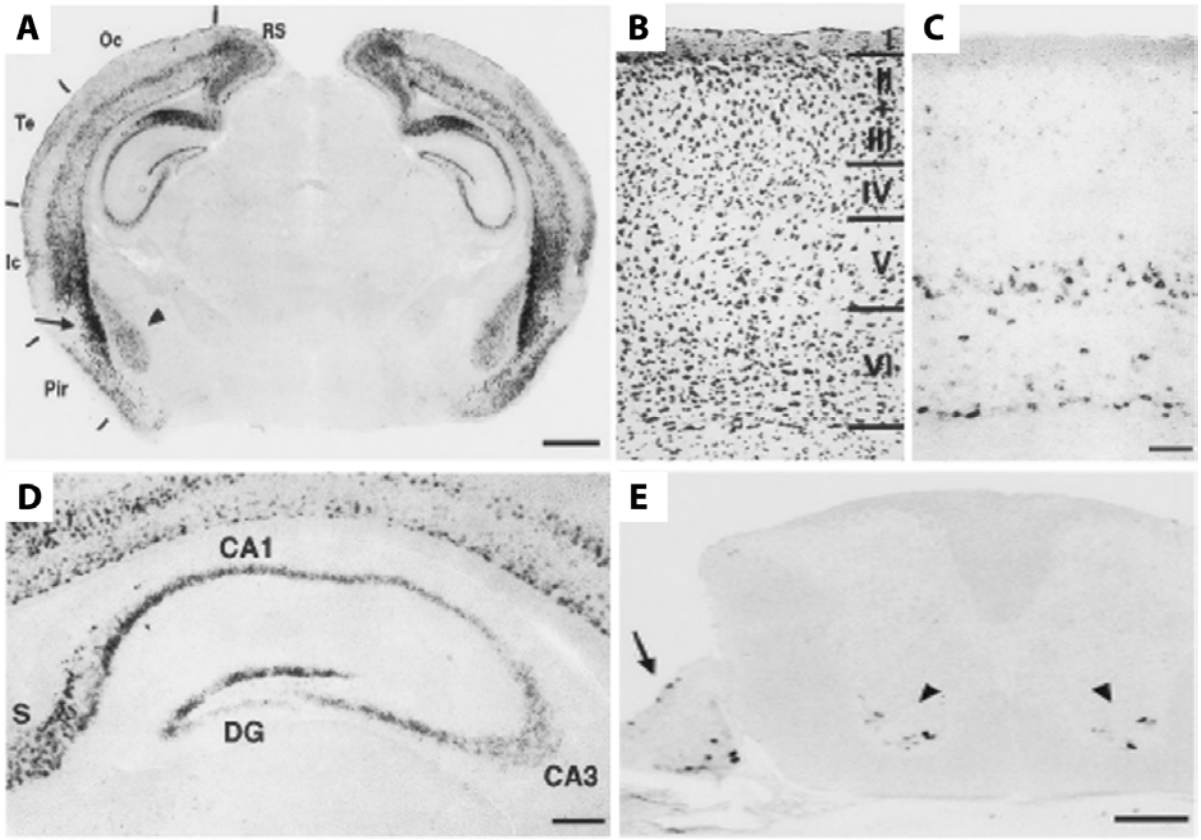

Figure 11. *In situ* hybridisation of sections from different CNS regions of adult mice using DIG-labeled neurotrypsin antisense cRNA. ***A,*** Brain section cut in a dorsocaudal-rostroventral plane (angle: approximately 30° to the coronal plane). The section was hybridised with a neurotrypsin antisense riboprobe. Labeling is seen in distinct layers throughout the neocortex (Te, temporal cortex; Oc, occipital cortex) with a more widespread labeling in the transition zones between iso- and allocortex (Ic, insular cortex; RS, retrosplenial cortex). In the allocortex, labeling is detected in the piriform cortex (Pir), with a strong labeling in the endopiriform nucleus (arrow), and in the hippocampal formation (see also ***D***). Neurotrypsin expression is also seen in the lateral amygdala (arrowhead). Scale bar: 1 mm. ***B, C,*** Consecutive coronal sections of the parietal cortex, either stained with cresyl violet (***B***) or hybridised with neurotrypsin antisense riboprobe (***C***). Cortical layers are marked in (***B***). ***C,*** Large positive neurons are seen in the lower half of layer V. In layer VI, positive cells are found throughout the layer, but concentrated at the border to the white matter. Weak labeling is associated with cells scattered in layers II and III. No labeling is detected in layers I and IV. Scale bar in ***C*** represents 100 µm. ***D,*** Coronal section of the hippocampus. Labeling is detected in neurons of the subiculum (S), in pyramidal neurons of CA1 and CA3, and in granule neurons of the dentate gyrus (DG). Scale bar: 300 µm. ***E,*** Cross section of the cervical spinal cord. Large cells are labeled in the motor columns (arrowheads). Labeling is also detected in the DRG (arrow). Scale bar: 300 µm. Figure and text taken and modified from (Gschwend et al., 1997).

Neurotrypsin was recognised to play an indispensable role for cognitive processes in humans when a four-nucleotide deletion in its coding region was identified as the cause of severe autosomal recessive nonsyndromic MR (Molinari et al., 2002). This frameshift mutation resulted in complete functional inactivation of neurotrypsin by causing the translation of a truncated enzyme lacking the protease domain (Fig. 10C). The affected children exhibited severe deficits in cognitive development after normal psychomotor development during the first 18 months, indicating that neurotrypsin does not play a critical role in early neural development or for the formation of synapses. Rather, neurotrypsin may

be crucial for the reorganisation of synapses and neuronal circuits which are required to establish and maintain higher cognitive functions during later developmental and adult stages.

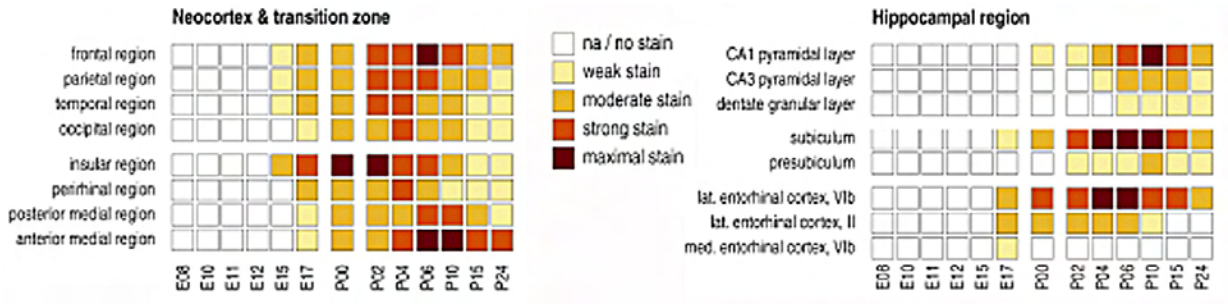

Figure 12. Semiquantitative synopsis of the time course of neurotrypsin mRNA expression in neural and nonneural tissues during pre- and postnatal development. Columns represent developmental stages. Rows represent cell populations, regions, or tissues. The shading pattern of each box indicates the average signal intensity, assigned to one of the four staining levels listed in the middle of the figure. Figure and text taken and modified from (Wolfer et al., 2001).

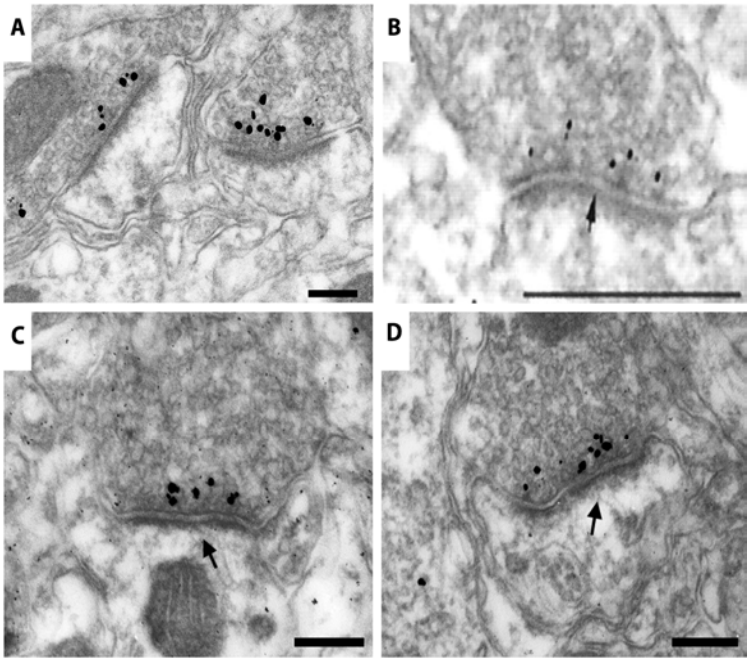

Figure 13. Subcellular localisation of neurotrypsin in hippocampus and cerebral cortex of wildtype mice and humans. ***A-D,*** Immuno-electron microscopy of the neuropil of the human cerebral cortex (***A, B***), the neuropil of the murine hippocampal CA1 area (***C***) and the murine cerebral cortex (***D***) localised neurotrypsin in presynaptic terminals, close to presynaptic membranes lining the synaptic cleft. Silver intensified gold particles reporting neurotrypsin immuno-reactivity were accumulated at vesicles close to the presynaptic membrane opposite to the postsynaptic density (arrows). Scale bars: 0.2 µm. ***A, B,*** taken and modified from (Molinari et al., 2002); ***C-D,*** taken and modified from (Stephan et al., 2008).

The so far unique proteolytic target of neurotrypsin is agrin, a protein well known because of its crucial function in neuromuscular synapse (neuromuscular junction, NMJ) maturation and maintenance (Sanes and Lichtman, 2001; Kummer et al., 2006). However, recent reports also implicate agrin as a regulator of CNS synapses ((Annies et al., 2006; Hilgenberg et al., 2006; McCroskery et al., 2006; Ksiazek et al., 2007); section 1.3). Thus, assuming that agrin is also a substrate of neurotrypsin in the CNS, cleavage by neurotrypsin could regulate agrin's action at the CNS synapse, which implicates neurotrypsin as an important regulator of structural and functional reorganisation of the synaptic circuitry.

1.3 Agrin is a substrate of neurotrypsin

1.3.1 Agrin at the NMJ and in the CNS

Agrin was initially isolated from the basal lamina of the synapse rich electric organ of *Torpedo californica* (Nitkin et al., 1987). The synaptic basal lamina is formed by a thin sheet of ECM molecules within the synaptic cleft of the NMJ. Initial interest in proteins expressed in the ECM of vertebrate muscles originated from findings that synaptic ECM factors were able to reinstruct the generation of synapses after muscle denervation. It was hypothesised that one or several factors immobilised in the synaptic basal lamina were able to induce pre- and postsynaptic differentiation (Bezakova and Ruegg, 2003). The first identified was agrin, named after its ability to aggregate acetylcholine receptors (AChR) in the postsynaptic membrane (Nitkin et al., 1987). The indispensable role for agrin in vertebrate NMJ function was confirmed by the generation of agrin-deficient mice. These mice developed a strong reduction in the number, size and density of postsynaptic AChR aggregates as well as abnormal intramuscular nerve branching and defective presynaptic differentiation in the muscle fibre membrane (Fig. 14). Agrin-deficient mice die at birth because of muscular defects resulting in an inability to breathe, indicating the importance of agrin in neuromuscular development (Gautam et al., 1996). The additional finding that the injection of agrin expression plasmids or purified agrin protein into non-synaptic regions of murine muscles induced the formation of fully functional and mature postsynaptic structures, placed agrin as a critical nerve-derived organiser of NMJ postsynaptic development (Sanes and Lichtman, 1999; Bezakova and Ruegg, 2003). More recent findings, however, have redefined the important role of agrin in the process of NMJ development and point to a function in NMJ maturation and maintenance, rather than in NMJ formation (Kummer et al., 2006).

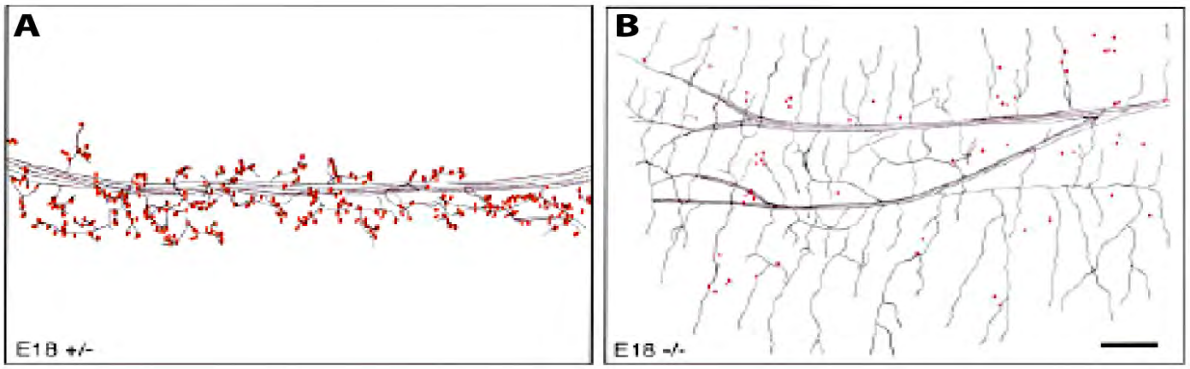

Figure 14. Development of pre- and postsynaptic structures in agrin mutant mice. Diaphragm muscles from control (***A***) and agrin-deficient (***B***) embryos at E18 were doubly stained for AChRs and axons, then drawn with a camera lucida. Myotubes run vertically. In controls, axonal branches (black) and AChR clusters (red) are confined to a central endplate band. In the mutant, AChR aggregates are smaller, less dense, and less numerous; axons form fewer but longer branches; and synaptic relationships are disorganised. Some of the dimmest, smallest AChR aggregates in mutant muscle are not shown. Scale bar: 100 µm. Figure and text taken and modified from (Gautam et al., 1996).

Agrin is a large multidomain chimeric proteoglycan because its protein backbone alone has a predicted Mr of 225 kDa. However, mature forms of agrin have a Mr of up to around 600 kDa

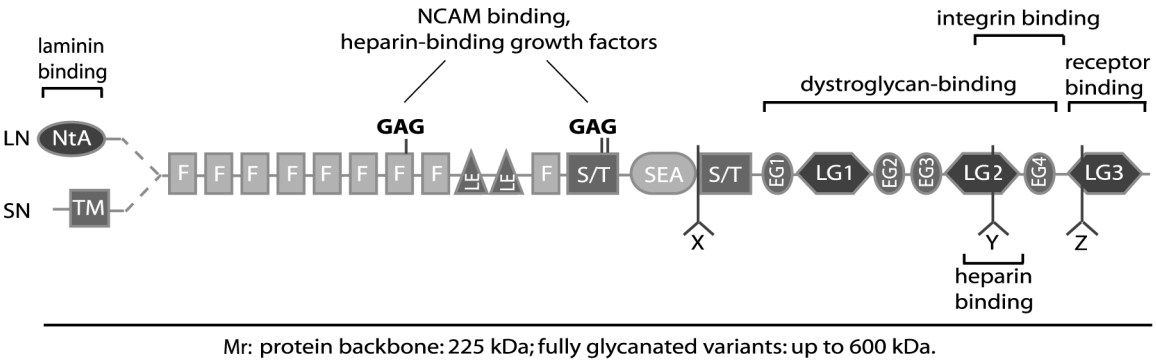

Figure 15. Schematic overview of agrin's protein structure (modified from (Hoch et al., 1993; Bezakova and Ruegg, 2003)). Alternative splicing leads to the expression of a variety of transmembrane (SN) or secreted (LN) agrin variants, containing variable inserts of several amino acids at the x, y, and z splice sites. Binding sites of agrin are indicated. NtA - N-terminal agrin domain; TM - transmembrane domain; F - follistatin-like domains; GAG - glycosaminoglycan side chains; LE - laminin-epidermal growth factor (EGF)-like domains; S/T - serine-threonine-rich region; SEA - sperm protein, enterokinase and agrin domain; EG - EGF-like domains; LG - laminin-globular domains.

due to attachment of chondroitin sulphate and heparan sulphate glycan sidechains and other additional N- and O-linked glycosylations (Fig. 15; (Rupp et al., 1991; Tsen et al., 1995; Parkhomovskiy et al., 2000; Xia and Martin, 2002; Bezakova and Ruegg, 2003; Winzen et al., 2003)). In addition to its extensive and complex structure, several alternative splice variants of agrin have been identified, altering its structural as well as functional properties. Alternative splicing within the N-terminal region of agrin results in the expression of both secreted and transmembrane isoforms (Denzer et al., 1995; Neumann et al., 2001). The N-terminal domain responsible for secretion of agrin variants was shown to bind to laminin and to mediate integration of agrin into the ECM. This interaction with laminin is crucial for agrin's function at the NMJ as it mediates agrin's integration in the synaptic basal lamina. In contrast, the transmembrane domain is believed to target agrin to alternative domains of cells that do not contain basal laminae (Bezakova and Ruegg, 2003). Secreted and transmembrane variants are further alternatively spliced at three independent sites within agrin's C-terminal half (Fig. 15). Alternative splicing at these sites, termed x, y and z splice sites for rat agrin isoforms, have additional impact on agrin's structural and functional complexity. The x-splice site is located in front of the second serine-threonine-rich region and alternative insertion of either 12 amino acids, 3 amino acids or no insertion have been described (x_{12}, x_3 or x_0; (Hoch et al., 1993)). The y-splice site is located within the second laminin-globular (LG) domain and no insertion (y_0) or a 4 amino acid insertion (y_4) is possible. The y_4-splice insert is required to enable heparin (heparan sulphate glycan) binding and modulates agrin's interaction with the α-subunit of the dystroglycan complex (Gesemann et al., 1996). The dystroglycan complex is composed of an extracellular α-subunit and a transmembrane β-subunit and was shown to connect the ECM to the intracellular actin cytoskeleton (Henry and Campbell, 1996). Binding to heparan sulphate proteoglycans as well as interaction with dystroglycan have been shown to contribute to agrin's function at the NMJ (Bezakova and Ruegg, 2003). The z-splice site is located within the third LG domain (LG-3) and no insertion (z_0) or alternative inserts of either

8, 11 or 19 amino acids (z_8, z_{11}, z_{19}) have been described (Ferns et al., 1992; Tsim et al., 1992; Ferns et al., 1993; Hoch et al., 1993; Ngo et al., 2007). It was shown that agrin's NMJ function relied strictly on isoforms that contained any positive insert at the molecules z-splice site (Bezakova and Ruegg, 2003).

Agrin variants are expressed in a wide variety of tissues, including the lung, muscle, peripheral nervous system (PNS) and CNS. Non-neuronal tissues as well as CNS glial cells are believed to exclusively express secreted variants, whereas the transmembrane isoforms are predominantly expressed by CNS neurons (Bezakova and Ruegg, 2003). Also C-terminal splicing is regulated in a tissue-dependent manner. Although the x_{12}-splice variant predominates in all tissues (Hoch et al., 1993), z-insert containing variants are exclusively expressed by PNS and CNS neurons as well as by adult Schwann cells. The y4 insert-containing splice variants are mainly expressed by PNS and CNS neurons as well as by CNS glia (Bezakova and Ruegg, 2003).

. The receptor mediating agrin's function in postsynaptic development was identified as the 'muscle-specific' receptor tyrosine kinase (MuSK). Mice with a targeted disruption of the gene for MuSK developed profound defects in NMJ formation, similar to agrin-deficient animals (DeChiara et al., 1996; Glass et al., 1996). The MuSK-mediated effects on post-synaptic development were shown to be maximally induced by a 95-kDa C-terminal agrin fragment. Although several hundred-fold less potent, a 21-kDa C-terminal agrin fragment, consisting of only the last LG-3 domain with any positive z-splice site insertion, is sufficient to induce the maximal numbers of AChR clusters on the muscle surface *in vitro*. This suggests that agrin interacts with its receptor at the NMJ via the LG-3 domain, additionally supported by further N-terminal domains of agrin (Bezakova and Ruegg, 2003). However, a direct interaction between MuSK and agrin was never shown and has led to the hypothesis that agrin binds to a MuSK receptor complex via a so far unidentified 'myotube-associated specificity component' (MASC) (Glass et al., 1996; Glass et al., 1997).

In the murine CNS, agrin is broadly expressed by neuronal as well as non-neuronal cells and localises to perisynaptic as well as extrasynaptic sites (Fig. 16; (Stephan et al., 2008)). Its expression is developmentally regulated with peak expression around birth (Cohen et al., 1997; Halfter et al., 1997; Li et al., 1997; Smith and Hilgenberg, 2002). Owing to its complex structure, broad expression pattern and interaction with a wide variety of molecules (Burgess et al., 2002), agrin has been implicated in a multitude of processes in the CNS, including neurite outgrowth and blood-brain barrier function (Kroger and Schroder, 2002; Smith and Hilgenberg, 2002). Agrin has also been shown to function in PNS interneuronal synapses (Gingras and Ferns, 2001; Gingras et al., 2002; Bezakova and Ruegg, 2003; Gingras et al., 2007) but its involvement in CNS synapse development and function are just emerging. Initial studies, mainly performed with cultured neurons, created a controversial picture by supporting a role for agrin in CNS synapse development (Ferreira, 1999; Bose et al., 2000) as well as contradicting its contribution to this process (Li et al., 1999; Serpinskaya et al., 1999). However, it has recently been reported that agrin-deficient mice, rescued from perinatal death

by transgenic expression of agrin in motorneurons, exhibited a reduced number of synapses in the cerebral cortex. The signalling events contributing to agrin's role in the formation and/or maintenance of CNS synapses potentially involve the mitogen-activated protein (MAP) kinase signalling pathway (Ksiazek et al., 2007). The receptor mediating this function is not known but MuSK, whose expression in the CNS was recently reported (Cheusova et al., 2006; Garcia-Osta et al., 2006; Ksiazek et al., 2007), was suggested as a potential candidate (Ksiazek et al., 2007). Other recent findings suggest that agrin may be involved in the generation of dendritic filopodia, structures considered to be precursors of dendritic spines, and thus in spine synapse formation (section 1.1.2). Both antibody-mediated clustering of agrin and the overexpression of agrin in neurons stimulated the formation of dendritic as well as axonal filopodia (Annies et al., 2006; McCroskery et al., 2006), dependent on the N-terminal domain of transmembrane agrin variants (McCroskery et al., 2006).

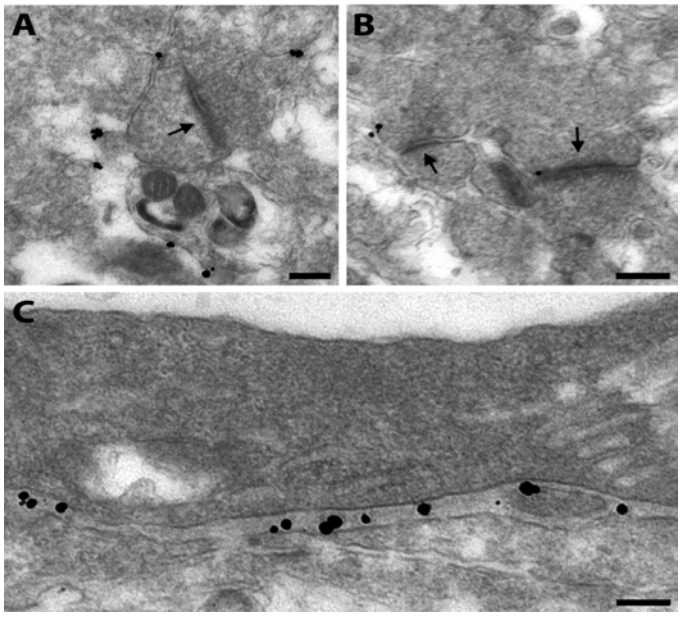

Figure 16. Subcellular localisation of agrin in hippocampus and cerebral cortex of wildtype mice. ***A, B,*** Silver intensified gold particles indicating agrin immuno-reactivity were found at perisynaptic as well as extrasynaptic locations in the neuropil of the hippocampal CA1 area and the cerebral cortex. ***C,*** The basal lamina of blood vessels in the stratum radiatum in the CA1 area of the hippocampus was strongly labelled with agrin-specific antibodies. The complete absence of gold particles in the adjacent tissue indicates a high specificity of the antibody. Arrows point to postsynaptic densities. Scale bars: 0.2 μm. Figure and text taken and modified from (Stephan et al., 2008).

First evidence for a direct role of agrin in CNS synapse function emerged when a synaptic receptor for agrin was discovered in cultured cortical neurons (Hoover et al., 2003). Similar to signalling processes at the NMJ, a 20-kDa C-terminal agrin fragment was shown to be sufficient for receptor-binding although independent of z-splice insertions. This striking difference suggests that the agrin-binding component of the neuronal CNS receptor is distinct to its receptor at the NMJ (Hoover et al., 2003). Binding of the 20-kDa agrin fragment to its receptor resulted in increased intracellular Ca^{2+}-levels and subsequent stimulation of CaMKII and MAP kinase activity, eventually resulting in the stimulation of early immediate gene expression, i.e., c-fos and cAMP-response element-binding protein (Ji et al., 1998; Hilgenberg and Smith, 2004). This synaptic agrin receptor was finally identified as the α3-subtype of the Na^+/K^+ ATPase and inhibition of its ATPase function by binding of the C-terminal agrin fragment was shown to evoke synaptic depolarisation (Hilgenberg et al., 2006).

Taken together, the molecular mechanisms of agrin function in the CNS appear to be fundamentally distinct from those found at the NMJ, covering a wide variety of distinct

processes including synapse formation/maintenance and synapse function. However, further research is required to elucidate the exact mechanisms by which agrin elicits its varied CNS functions.

1.3.2 Agrin is a substrate of neurotrypsin

Neurotrypsin is a serine-protease mainly expressed in the nervous system and serves an important role in cognitive functions (section 1.2.2.3). The NMJ is considered as a model system for neuron-neuron synapses (Sanes and Lichtman, 1999), owing to its size, accessibility and simplicity. To initially determine a potential synaptic function for neurotrypsin, transgenic mice were generated that overexpressed neurotrypsin in motorneurons and analysed for potential NMJ phenotypes. It was found that these mice developed a phenotype that strongly resembled the phenotype found in the diaphragm of agrin-deficient mice (section 1.3.1, Fig. 14; Bolliger, M. *et al.*, unpublished observations). Because both neurotrypsin and agrin are endogenously expressed in motorneurons *in vivo* it was speculated that agrin is a substrate of neurotrypsin.

Co-expression of neurotrypsin and agrin in transiently transfected cos7 cells indeed confirmed that agrin is a substrate of neurotrypsin. Neurotrypsin-dependent cleavage of agrin occurs at two homologous sites, termed α- and β-cleavage sites and results in the release of an intermediate 90-kDa and a C-terminal 22-kDa fragment from the N-terminal moiety of agrin ((Reif et al., 2007); see also Fig. 19). Detailed *in vitro* analyses confirmed the high specificity of neurotrypsin activity. Several highly conserved amino acids in the sequences flanking both cleavage sites of agrin are required for neurotrypsin-dependent cleavage. In addition, further exosite interactions between neurotrypsin and agrin are believed to be necessary for cleavage, supporting the high specificity of this interaction and suggesting only few, if any, additional substrates for neurotrypsin (Reif et al., 2007). Neurotrypsin localises to synapses *in vivo* and its secretion is caused by synaptic activity ((Molinari et al., 2002; Frischknecht et al., 2008; Stephan et al., 2008); section 1.2.2.3). Furthermore, the development of nonsyndromic MR upon functional inactivation of neurotrypsin places it as an important regulator of adaptive reorganisations of the synaptic circuitry ((Molinari et al., 2002); section 1.2.2.3). Given agrin's emerging important role in the formation, maintenance and function of CNS synapses (section 1.3.1), it was tempting to speculate that agrin is a substrate of neurotrypsin also in the CNS, potentially regulating agrin's synaptic functions.

1.4 Aim of this study

Agrin is a substrate of neurotrypsin *in vitro* and at the NMJ *in vivo* (section 1.3.2). The aim of this study was to analyse the possible functional interaction of neurotrypsin and agrin in the CNS. This was supposed to be achieved by two fundamentally different approaches. 1) By performing a detailed biochemical *in situ* analysis of the potential neurotrypsin-dependent cleavage of agrin in the murine CNS. 2) By determining its potential functional implications with cell biological analyses *in vitro*.

2. Material and Methods

2.1 *In situ* analyses in the murine brain

2.1.1 Generation of transgenic mice.* To generate the pThy1-loxP-STOP-loxP-neurotrypsin constructs, either mouse or human neurotrypsin cDNA was subcloned into the *Xho*I site of the murine Thy1.2 genomic expression cassette (Caroni, 1997). The loxP-flanked transcription termination cassette from the pBS302 vector (Invitrogen AG, Basel, Switzerland) was inserted between the Thy1 promoter and the translational start codon of neurotrypsin. To generate the pThy1-neurotrypsin construct containing the serine-to-alanine mutation, a PCR fragment was amplified using mouse neurotrypsin cDNA as a template and 5'-CGTGTGGACAGCTGCCAGGGAGACGCTGGAGGA-3' and 5'-CTCAAGCTTAGTTAC-AGACTGGTGACACTTTTTATC-3' as primers. This fragment was reintroduced into the vector containing full-length mouse neurotrypsin. The mutated neurotrypsin cDNA was excised and subcloned into the *Xho*I site of the Thy1.2 cassette. The two resulting vectors were digested with *Pvu*I, and the fragments were purified from agarose gels for pronuclear injections into fertilised oocytes according to standard protocols (Rulicke, 2004). Zygotes were produced by mating B6C3F1 hybrids. The offspring of transgenic founders of each transgenic line (mouse neurotrypsin, *Tg(Prss12)*533.1Zbz; human neurotrypsin, *Tg(PRSS12)*491.1Zbz; inactive mouse neurotrypsin, *Tg(Prss12^{S785A})*785.1Zbz were mated with C57BL/6-*Tg(CMV-cre)* mice (Schwenk et al., 1995) to delete the floxed transcription termination cassette (Sauer, 1998) and activate the dormant transgene. Subsequent offspring of constitutively overexpressing mice were backcrossed for more than 10 generations to C57BL/6 to produce congenic lines. For genotyping, animals were screened by PCR on genomic DNA using the primers 5'-CCCATCCACATGGATAATGTGAA-3' and 5'-CCCATGTTCTGAGATATTGGAAG-3' (and see section 2.2.11). Neurotrypsin deficient mice were generated as described before (Reif et al., 2007). In brief, a targeting vector, containing the genomic DNA segment comprising exons 10 and 11 of murine neurotrypsin, was generated by inserting a loxP site 0.22 kb upstream of neurotrypsin exon 10 and a floxed neomycin resistance sequence 0.12 kb downstream of neurotrypsin exon 11. In addition, homology arms of 7.5 kb and 3.5 kb were added at the 5'- and 3'- regions, respectively. For negative selection, a diphtheria toxin cassette was inserted at the 3' end. The linearised targeting vector was electroporated into C57BL/6-derived embryonic stem cells. Stem cell lines with homologous recombination were injected into blastocysts and a germ-line chimeric male was crossed with C57BL/6 females to generate heterozygous animals. These animals were crossed with CMV-Cre mice to excise the floxed region, resulting in a truncated neurotrypsin gene lacking the region encoding the proteolytic domain. Agrin-deficient animals, lacking the region from exon 6 to 33 of the agrin gene, were obtained from J. Sanes

and generated as described previously (Lin et al., 2001). All experimental protocols were approved by the Veterinary Department of the Canton of Zurich, Switzerland.

* mice were generated by Serguei V. Kozlov, Paolo Cinelli or Andreas Zurlinden (all Department of Biochemistry, University of Zurich, Zurich, Switzerland) with additional help by Thomas Rülicke (Institute of Laboratory Animal Science, University of Zurich, Zurich, Switzerland), unless otherwise stated. Animal breedings were maintained by Beat Kunz and Daniel Blaser (Department of Biochemistry, University of Zurich, Zurich, Switzerland).

2.1.2 Antibodies. The rabbit antiserum SZ177 was raised against two synthetic peptides corresponding to Asp_{22}-Gln_{40} and Leu_{45}-Phe_{57} of mouse neurotrypsin (CAA73646) and goat antiserum G93 was raised against full-length mouse neurotrypsin (Reif et al., 2007). Rabbit antiserum R132 (C-90-1) and goat antiserum G91 (C-90-2) were raised against the C-90-kDa fragment of agrin. Goat antiserum G92 (C-22-1) and rabbit antiserum R139 (C-22-2) were raised against the C-22-kDa fragment of agrin (Reif et al., 2007). The C-90 and C-22 anti-agrin sera were purified by affinity chromatography. *Western blotting:* Depending on the goal of the analysis, either the anti-C-22 or the anti-C-90 antibodies were used. The anti-C-22 antibodies were used to make sure that the detected signals corresponded to full-length agrin, because they were directed versus the most C-terminal domain of agrin. Because of their higher affinity, the anti-C-90 antibodies were superior to the anti-C-22 antibodies when detection of low amounts of antigen was the primary goal. In Western blotting experiments, both the anti-C-90 and the anti-C-22 antibodies detected the variants of full-length agrin in an identical band pattern (Fig. 19). The slight differences in the relative intensity of the upper, middle, and lower variants obtained with the anti-C-22, compared to the anti-C-90 antibodies, most likely reflected a differential preference of the antibodies for distinct variants of agrin rather than contributions from neurotrypsin-dependent cleavage fragments, although fragments that originate from cleavage only at the β site are expected to co-localise with the full-length forms of agrin on Western blots in the Mr range above 250 kDa. Co-expression of agrin and neurotrypsin in HeLa cells resulted in the release of not only the 22-kDa and the 90-kDa, but also the 110-kDa fragment that originated from partial cleavage at the α site (Reif et al., 2007). This pattern demonstrated that neurotrypsin-dependent cleavage at the β site was not a necessary condition for cleavage at the α site and suggested that agrin cleavage at the α site preceded β site-cleavage, or that cleavage occurred at both sites in parallel. Therefore, we assumed that the large agrin fragment generated by partial cleavage at the β site and, thus, lacking only the 22-kDa fragment, occurred only in negligible amounts if at all. The anti-C-22-1 antibody was used for detection of full-length agrin in the initial analyses of neurotrypsin-dependent agrin cleavage in brain homogenates of both neurotrypsin-overexpressing and neurotrypsin-deficient mice (Fig. 21), in order to exclude detection of partially cleaved agrin variants. As these analyses were done with P9 mouse brain tissue, the agrin signals were sufficiently strong to be detected by this relatively low affinity antibody. In contrast, for all experiments that required sensitive detection of weak signals, including the

analysis of the time course of agrin cleavage (Fig. 20) and the analyses of synaptosomal preparations from wild-type or transgenic animals overexpressing neurotrypsin (Fig. 23, 24), the anti-C-90-1 antibody that has a higher affinity was used. *Immunocytochemistry:* Mainly the anti-C-90 antibodies were used for immunofluorescence detection of agrin variants, because of their higher affinity.

Table 1: Antibodies

name/antigen	antibody species	type	concentration/dilution for Western blotting	concentration/dilution for immunocytochemistry
SZ177	rabbit	serum	1:1000	1:200
G93	goat	serum	1:2,000	1:2,000
R132 (C-90-1)	rabbit	serum	1:1,000	--
R132 (C-90-1)	rabbit	affinity purified	1 μg/ml	1 μg/ml
G91 (C-90-2)	goat	serum	--	1:10,000
G91 (C-90-2)	goat	affinity purified	1 μg/ml	--
G92 (C-22-1)	goat	affinity purified	2.5 μg/ml	--
R139 (C-22-2)	rabbit	affinity purified	2.5 μg/ml	--
R149 (NtA)	rabbit	serum	1:1000	1:1000
PSD-95	mouse	IgG	1:2,000	--
beta-actin	mouse	IgG	1:7,000	--
synaptophysin	rabbit	serum	--	1:200
synaptophysin	mouse	IgG	1:1000	1:1,000
MAP-2	mouse	IgG	--	1:1,000
Lamp-1	mouse	IgG	--	1:200
Peroxidise-conjugated secondary anti-mouse	goat	IgG	1:20,000	--
Peroxidise-conjugated secondary anti-goat	rabbit	IgG	1:30,000	--
Peroxidise-conjugated secondary anti-rabbit	goat	IgG	1:20,000	--
FITC/Cy3-labeled secondary antibodies	donkey	IgG	--	1:400
AMCA/Cy5-labeled secondary antibodies	donkey	IgG	--	1:200

Rabbit antiserum R149 was raised against the N-terminal domain of the secreted agrin isoform (anti-NtA antibody). The monoclonal anti-β-actin antibody (clone AC-74) and the monoclonal antibody against microtubuli-associated protein 2 (MAP-2, clone HM-2) were purchased from Sigma-Aldrich Co. (Saint Louis, MO, USA). The monoclonal anti-PSD-95 antibody (clone10) was purchased from BD Biosciences (Allschwil, Switzerland). The polyclonal antibody against synaptophysin (A00010) was purchased from DAKO GmbH (Hamburg, Germany) and the monoclonal antibody against synaptophysin (MAB5258) was purchased from Chemicon International (Millipore AG, Zug, Switzerland). The monoclonal

antibody against human lysosomal membrane-associated protein 1 (Lamp-1) was kindly provided by Dr. Jack Rohrer (University of Zurich, Zurich, Switzerland). The peroxidase-conjugated secondary antibodies for immunoblotting were purchased from Sigma Aldrich Co. (Saint Louis, MO, USA). The Fluorescence-labeled secondary antibodies for immunocytochemistry were purchased from Jackson ImmunoResearch Europe Ltd. (Newmarket, Suffolk, UK).

2.1.3 Brain tissue preparation. *Embryonic tissue:* Embryos were removed from pregnant mice (C57BL/6 wild type, agrin-deficient or neurotrypsin-deficient mice) at defined time points and whole brains were dissected under a stereomicroscope (Wild, Heerbrugg, Switzerland), using micro-scissors and Dumont Tweezers #55 (World Precision Instruments Inc., Sarasota, FL, USA). Isolated brains were mmediately transferred into 35 mm dishes (Corning B.V. Life Sciences, Schiphol-Rijk, The Netherlands) containing Hank's balanced salt solution (HBSS, Invitrogen AG, Basel, Switzerland) or phosphate-buffered saline (PBS; 137 mM NaCl, 2.7 mM KCl, 8 mM Na_2HPO_4, 1.5 mM KH_2PO_4, pH 7.4). Forebrain/midbrain sections were further isolated and processed as stated below.

Tissue from postnatal animals: Whole brains of C57BL/6 wild-type mice, neurotrypsin-deficient mice, mice overexpressing catalytically active human neurotrypsin or catalytically inactive mouse neurotrypsin were carefully removed from the animals scull. The anterior part of the brain, obtained by vertical dissection directly behind the cortex, was labelled the forebrain/midbrain section. Forebrain/midbrain tissue was further processed by homogenisation in a glass-teflon homogeniser (1,000 rpm, 10 strokes) in ice-cold buffer A (320 mM Sucrose, 5 mM HEPES, pH 7.5, containing protease inhibitors (1:100 dilution, P-8340, Sigma Aldrich Co., Saint Louis, MO, USA)). After brief centrifugation of the homogenates at 1,000 x g, 4 °C, supernatants were collected and protein concentrations were measured by a Bradford assay (Bio-Rad Laboratories, Inc., Hercules, CA, USA).

2.1.4 SDS-PAGE and Western blotting. Samples with equal protein concentrations were resolved by SDS-PAGE on 4-12 % NUPAGE gels using MOPS running buffer or on 10-20 % NOVEX Tricine gels (both from Invitrogen AG, Basel, Switzerland), following the manufacturers instructions. These pre-cast gels were mainly used for optimised full-length agrin separation and simultaneous detection of full-length agrin variants and agrin cleavage fragments. Alternatively, samples with equal protein concentrations were resolved by SDS-PAGE on conventional, discontinuous 10 % or 12.5 % gels (Laemmli, 1970). Proteins were subsequently blotted to polyvinylidene fluorid membranes (Immobilon P membrane, Millipore AG, Zug, Switzerland). Mainly for full-length agrin detection and neurotrypsin detection in brain tissues, proteins were transferred by wet blotting in a Criterion blotter (Bio-Rad Laboratories, Inc., Hercules, CA, USA) using 0.5 x blotting buffer (12.5 mM Tris, 91 mM Glycine, 10 % Methanol) or 1x NUPAGE transfer buffer (Invitrogen AG, Basel,

Switzerland) at 20 volts for 16-24 hours at 4 °C. Otherwise, proteins were semi-dry blotted in a Trans-Blot SD Transfer Cell (Bio-Rad Laboratories, Inc., Hercules, CA, USA) using 1 x blotting buffer (25 mM Tris, 192 mM Glycine, 20 % Methanol) at 24 Volts for 1 hour at room temperature. The membranes were stained with Ponceau-solution (2 % Ponceau-S, 30 % trichloric acid, 30 % sulfosalicylic acid), destained in distilled water and dried to finalise blocking of the membranes. Primary antibodies were diluted in Tris-buffered saline (TBS; 10 mM Tris/HCl, 150 mM NaCl, pH 8.0) containing 0.1 % Tween-20 (TBST) and 2.5 % Western blocking reagent (Roche Diagnostics (Schweiz) AG, Rotkreuz, Switzerland), and incubated with the membranes for 60 min. After washing with TBST, the blots were incubated with peroxidase-conjugated secondary antibodies for 45 min, and washed again. Immunoreactive protein bands were detected using ChemiGlow (Alpha Innotech GmbH, Kasendorf, Germany) and a LAS-3000 Fujifilm imager (Fujifilm Europe GmbH, Düsseldorf, Germany). For reprobing, membranes were incubated twice for 30 min in stripping solution 1 (0.1 % SDS, 1 % Tween-20, in 200 mM glycine-HCl, pH 2.2) or trice for each 10 min in stripping solution 2 (200 mM NaOH) and afterwards extensively washed in TBST before incubation with primary antibodies.

2.1.5 Heparitinase digestion. The forebrain/midbrain regions of one P6 C57BL/6 mouse were homogenised with a glass-teflon homogeniser (1,000 rpm, 10 strokes) in enzyme buffer (20 mM Tris, 0.1 mg/ml BSA, 4 mM $CaCl_2$, protease inhibitors, pH 7.5). After brief centrifugation of the homogenate at 1,000 x g, the supernatant was collected and the protein concentration was measured by a Bradford assay (Bio-Rad Laboratories, Inc., Hercules, CA, USA). Aliquots of 150 µg protein were incubated with 1 U heparitinase (heparinase III, reconstituted in enzyme buffer, Sigma-Aldrich Co., Saint Louis, MO, USA) for either 2 or 5 hours at 37 °C. For the control sample, 150 µg protein were incubated in enzyme buffer alone. Reactions were stopped by freezing the samples in liquid nitrogen. Samples were finally analysed by SDS-PAGE and Western blotting for full-length agrin detection (section 2.1.4).

2.1.6 Preparation of synaptosomes. The data presented were obtained with synaptosomal preparations from P12 animals or older. Preparations from brain tissue of younger animals yielded synaptosomal samples of minor purity, as confirmed by electron microscopy, and were therefore not considered. Therefore, synaptosomes were prepared from P12 to P15 neurotrypsin-overexpressing transgenic mice or from P13-P16 neurotrypsin-deficient mice and their corresponding wild-type littermates as described before (Phelan and Gordon, 1997). In brief, the forebrain/midbrain regions from 6 mice were homogenised with a glass-teflon homogeniser (800 rpm, 12 strokes) in buffer A (320 mM Sucrose, 5 mM HEPES, pH 7.5, containing protease inhibitors (1:100 dilution, P-8340, Sigma Aldrich Co., Saint Louis, MO, USA)) and centrifuged at 1,000 x g for 5 minutes. The resulting supernatant was further centrifuged at 12,000 x g for 20 minutes to produce the crude synaptosomal pellet. To reduce

the content in mitochondria, only the upper part of the pellet was resuspended and re-homogenised in buffer A using a handheld glass-homogeniser (5 strokes) and the centrifugation at 12,000 x g was repeated. Again, only the upper part of the pellet was resuspended and re-homogenised in buffer A, loaded on a 7.5 %/12 % Ficoll step gradient and centrifuged at 68,000 x g for 1 hour. The synaptosomes, concentrated at the 7.5 % /12 % Ficoll gradient interphase, were well separated from a mainly myelin-containing band in the upper part of the 7.5 % Ficoll phase and the mainly mitochondria-containing pellet. The synaptosomal fraction was collected by puncturing the tube with a 18 g needle and further analysed by Western blotting or electron microscopy. To prepare samples for electron microscopy, purified synaptosomes were washed and resuspended in Krebs solution (20 mM HEPES, 145 mM NaCl, 5 mM KCl, 1.3 mM $MgCl_2$, 1.2 mM NaH_2PO_4, 10 mM Glucose, pH 7.5), incubated for 10 minutes at 37 °C and fixed overnight at 4 °C in 4 % formaldehyde and 0.05 % glutaraldehyde in phosphate buffer (PB, 0.1 M, pH 7.4).

2.1.7 Electron microscopy of the synaptosomal fraction.[**] After several washes of the purified and fixed synaptosomes (see above) in PB the samples were osmicated in 1 % OsO_4 in PB for 30 minutes, washed thoroughly with PB and dehydrated in increasing concentrations of ethanol. Subsequently, fractions were embedded in Epon resins (Epon 812, Fluka, Buchs, Switzerland). Ultrathin sections from synaptosomes were imaged using a digital camera (Gatan 791 multiscan; Gatan Inc., Pleasanton, CA, USA) attached to a EM10C electron microscope (Zeiss, Oberkochen, Germany).

[**] Electron microscopy experiments were performed by José María Mateos.

2.1.8 Mass spectrometric analysis. Both agrin C-90 fragments were affinity purified from P25 to P50 neurotrypsin-overexpressing transgenic mouse brains. At this age, both bands appear with almost equal intensity and, due to overexpression of active neurotrypsin, in substantial amounts. In addition, at ages above P15, bands detected in mouse brain tissue appear well separated (Fig. 20A). In brief, forebrain/midbrain tissue (section 2.1.3) from 53 brains was homogenised in purification buffer (20 mM HEPES, 80 mM NaCl, pH 7.5, including protease inhibitors (1:100 dilution, P-8340, Sigma Aldrich Co., Saint Louis, MO, USA)) with a 15 % tissue to buffer ratio. The soluble fraction, obtained by ultracentrifugation at 100,000 x g for 1 hour at 4 °C (Sorvall T865 rotor, Thermo Fisher Scientific Inc., Waltham, MA, USA), was used for heparin-sepharose CL-6B affinity chromatography (Amersham Biosciences, GE Healthcare UK Ltd., Buckinghamshire, UK). Proteins were eluted with 1M NaCl, in 20mM HEPES, pH 7.5, and the eluate was concentrated with VIVASPIN20 centrifuge cartridge concentrators (MWCO: 50 kDa; Sartorius AG, Goettingen, Germany). Samples were further purified by immunoaffinity chromatography, using immobilised affinity-purified antibody R132. Bound proteins were eluted by boiling the affinity-matrix in 10 % SDS/PBS (137 mM NaCl, 2.7 mM KCl, 8 mM Na_2HPO_4, 1.5 mM KH_2PO_4, pH 7.4,

containing 10 % (w/v) SDS). The eluted proteins were concentrated by methanol/chloroform protein precipitation (Wessel and Flugge, 1984), resuspended in Laemmli buffer (Laemmli, 1970) and separated by 10 % SDS-PAGE to yield maximal partition of the upper and lower 90-kDa agrin bands. Separated proteins were visualised using the colloidal blue staining kit (Invitrogen AG, Basel, Switzerland). Bands corresponding to both upper and lower 90-kDa agrin (see results, Fig. 20) were analysed by LC-ESI-MS/MS analysis on a Qutof Ultima API (Waters S.A.S., Saint-Quentine, France) at the Functional Genomics Center Zurich, University and ETH Zurich, Switzerland.

2.1.9 Quantification and statistical analysis. Western blots were recorded with a LAS-3000 Fujifilm imager (Fujifilm Europe GmbH, Düsseldorf, Germany) and densitometric analyses of the protein bands were performed using AIDA software (Raytest GmbH, Straubenhardt, Germany). I was careful to avoid measurement of saturated signals. For analysis of P9 mouse brain homogenates, at least 3 animals per genotype were analysed and compared to signals of at least 3 different corresponding wild-type littermates. Signals of two independent blots per genotype were quantified and used for statistical analyses. For densitometric analyses of synaptosomal preparations, five separate preparations were analysed. For all analyses, agrin signals were first normalised to actin signals of the corresponding sample, serving as an internal loading control. Then, adjusted values obtained from transgenic or neurotrypsin-deficient samples of each experiment were compared to the corresponding adjusted signals from the samples of wild-type littermates, whereby the wild-type signal was set to 100 percent. Data are presented as mean ± S.E.M. Statistical analyses were performed using unpaired Student's *t*-test (Sigmaplot, Systat Software, Inc., San Jose, CA, USA).

2.2 Molecular biology techniques

2.2.1 Generation of competent bacteria. *Heat shock Ca^{2+} competent E. coli DH-5α or XL-1 blue bacteria* were generated as follows: 20 ml sterile LB-medium (10 g bacterial peptone, 5 g yeast extract, 5 g NaCl in 1 l distilled H_2O) was inoculated with bacteria and grown overnight at 37 °C. Then, 4 ml preculture were added to 400 ml LB-medium and incubated at 37 °C, 180 rpm shaking until an OD_{600} of about 0.375 (Kontron Spectrophotometer Uvikon 810, Kontron AG, Eching, Germany). The culture was then distributed to 8 x 50 ml tubes (Sarstedt AG & Co., Nümbrecht, Germany) and kept on ice for 10 min. Bacteria were afterwards pelleted at 3,000 rpm, 7 min, 4 °C (Sorvall RT6000D, Thermo Fisher Scientific Inc., Waltham, MA, USA), supernatant was discarded and pellets were resuspended in each 10 ml ice-cold $CaCl_2$ solution (60 mM $CaCl_2$, 15 % glycerol, 10 mM PIPES, pH7.0). Bacteria solutions were pooled to 2 x 50 ml tubes and kept on ice for 1 hour. Cells were pelleted at 3,000 rpm, 5 min, 4 °C, resuspended in each 10 ml ice-cold $CaCl_2$ solution and pooled to a 50 ml tube. Cells were pelleted again as described above and the final pellet was resuspended in

2 ml ice-cold $CaCl_2$ solution, distributed into pre-chilled sterile 1.5 ml tubes (Eppendorf AG, Hamburg, Germany), frozen immediately on dry ice and stored at -80 °C.

Electro competent E. coli BM25.8 bacteria were generated as follows: 50 ml sterile LB-medium (see above but containing 10 µg/ml Kanamycin) was inoculated with bacteria and grown overnight at 37 °C. Then, the preculture was added to 800 ml LB-medium and incubated at 37 °C, 180 rpm shaking until an OD_{600} of about 0.5 (Kontron Spectrophotometer Uvikon 810, Kontron AG, Eching, Germany). The culture was then chilled on ice for about 20 min, distributed to 16 x 50 ml prechilled tubes (Sarstedt AG & Co., Nümbrecht, Germany) and centrifuged at 4500 rpm, 10 min, 4 °C to pellet bacteria. The supernatant was discarded, cells were resuspended in 10 ml/tube ice-cold sterile distilled water and bacteria solutions were pooled to 4 x 50 ml tubes. Cells were pelleted again at 4500 rpm, 10 min, 4 °C, resuspended in 10 ml/tube sterile ice-cold 10 % glycerol/distilled water and pooled to one 50 ml tube. Cells were pelleted once more at 3000 rpm, 4 °C, 10 min, finally resuspended in 2 ml sterile 10 % glycerol/distilled water, distributed to pre-chilled sterile 1.5 ml tubes (Eppendorf AG, Hamburg, Germany), frozen immediately in liquid nitrogen and stored at -80 °C.

2.2.2 Transformation of bacteria. *Heat-shock Ca^{2+} competent bacteria:* 50 µl Competent *E. coli* DH5α or XL-1 blue bacteria (section 2.2.1) were thawed on ice, mixed with either 5 µl ligation sample (section 2.2.7) or 10 ng vector DNA and kept on ice for further 30 min. Heat shock transformation was achieved by incubation of the samples for 1 min at 42 °C. Afterwards, 800 µl LB-medium (10 g bacterial peptone, 5 g yeast extract, 5 g NaCl in 1 l distilled H_2O) were added to the transformation sample and the bacteria were further incubated for 30 min at 37 °C, shaking. Bacteria were pelleted at 1,000 g for 3 min and resuspended in 100 µl supernatant. The final suspension was then plated onto LB/Agar-plates (10 g bacterial Peptone, 5 g yeast extract, 5 g NaCl, 13 g Agar in 1 l H_20) containing suitable antibiotics for selective growth of transformed bacteria and incubated overnight at 37 °C.

Electro competent bacteria: 100 µl electro-competent *E. coli* (e.g., *E. coli* BM25.8; section 2.2.1) bacteria were thawed on ice, mixed with respective plasmid DNA and transferred to pre-chilled electroporation cuvettes (0.1 cm gap, Bio-Rad Laboratories, Inc., Hercules, CA, USA). Electroporation was performed in a Gene Pulser (Bio-Rad Laboratories, Inc., Hercules, CA, USA) at 1.6 V, 200 µOhm, 25 µFD (960 µFD extended). Immediately afterwards, the sample was diluted with 800 µl LB medium (10 g bacterial peptone, 5 g yeast extract, 5 g NaCl in 1 l distilled H_2O) within the cuvette, transferred to an 1.5 ml tube (Eppendorf AG, Hamburg, Germany) and further incubated shaking for 30 min at 37 °C. Cells were pelleted (1000 x g, 3 min), resuspended in 100 µl supernatant and plated onto LB/Agar-plates (10 g bacterial Peptone, 5 g yeast extract, 5 g NaCl, 13 g Agar in 1 l H_20) containing suitable antibiotics for selective growth of transformed bacteria and incubated overnight at 37 °C.

2.2.3 Working concentrations of antibiotics. The following antibiotics (Invitrogen AG, Basel, Switzerland) were applied for selective growth of transformed bacteria, dependent on the respective plasmid properties: Ampicilline (100 μg/ml; 60 μg/ml in combination with 30 μg/ml Zeocin for pAd selection); Zeocin (30 μg/ml); Kanamycin (10 μg/ml);

2.2.4 Mini-preparation and Midi-preparation production of vector-constructs. For low yield vector amplification and analyses of plasmid clones, mini-preparations were performed using the QFX microprep kit (QE Healthcare UK Ltd., Buckinghamshire, England). Briefly, 3 ml of LB-medium (10 g bacterial peptone, 5 g yeast extract, 5 g NaCl in 1 l distilled H_2O), containing suitable antibiotics for selective growth of transformed bacteria, were inoculated in 15 ml Falcon tubes (BD Biosciences, Allschwil, Switzerland) with bacteria from a colony grown on a LB/Agar plate (section 2.2.2) or from a glycerol stock (see below) and incubated for 16 hours at 37 °C, shaking. Bacteria were pelleted and isolation, purification and elution of plasmid DNA were performed according to the manufacturers protocol. Purified plasmid DNA was analysed by restriction digest analysis (section 2.2.5) and DNA sequencing (Microsynth AG, Balgach, Switzerland). Plasmid DNA was stored at -20 °C and mini-cultures of positive clones were stored as glycerol stocks (final 20 % glycerol) in Cryo tubes (Nunc GmbH & Co. KG, Wiesbaden, Germany) at -80 °C.

To produce highly pure and high yield plasmid DNA, midi-preparations were performed with the Qiafilter midi kit (Qiagen AG, Hombrechtikon, Switzerland). In brief, 50 ml of LB-medium, containing suitable antibiotics for selective growth of positive bacteria clones, were inoculated in 50 ml tubes (Sarstedt AG & Co., Nümbrecht, Germany) with bacteria from a mini-culture (see above) or from a glycerol stock (see above) and incubated for 16 hours at 37 °C, shaking. Bacteria were pelleted and isolation, purification and elution of plasmid DNA were performed according to the manufacturers protocol. Purified plasmid DNA was analysed by restriction digest analysis and DNA sequencing (Microsynth AG, Balgach, Switzerland) and stored at -20 °C.

2.2.5 Restriction digest analyses and gel extraction of DNA samples. Restriction enzymes were obtained from New England Biolabs (Ipswich, MA, USA), Promega AG (Dübendorf, Switzerland) or Fermentas International Inc (Burlington, Ontario, Canada) and digests of PCR products or plasmid DNA were performed according to standard manufacturers protocols in 1.5 ml tubes (Eppendorf AG, Hamburg, Germany). DNA was purified using the 'PCR product purification kit' (Qiagen AG, Hombrechtikon, Switzerland). Alternatively, if separation of digested fragments was desired, samples were constituted with 6x loading buffer (10 mM Tris/HCl pH 7.5, 30% glycerol, 0.1 % Xilene cyanol, 0.1 % bromphenol blue) and separated by agarose gel electrophoresis (0.8-2 % agarose in TAE buffer (40 mM Tris-acetate, 2 mM Na_2EDTA, pH 8.5), containing 1 μg/ml ethidium bromide). Desired bands were excised from the gel and finally eluted in TE buffer (10 mM Tris/HCl pH 7.5, 1 mM EDTA)

using the ‘gel extraction kit’ (Qiagen AG, Hombrechtikon, Switzerland). In case of fragments bigger than 10 kb, the ‘QiaExII kit’ (Qiagen AG, Hombrechtikon, Switzerland) was used for gel-extraction and purification of DNA fragments.

2.2.6 Ethanol precipitation. To change buffer conditions for further enzymatic processing of plasmid DNA or to concentrate DNA, the DNA was precipitated by adding 10 mM EDTA, 300 mM sodium acetate and 100 % ethanol (precooled to -20 °C; final concentration: 70 %). Samples were incubated for 60 min or overnight at -20 °C and DNA was subsequently pelleted in a table-top centrifuge (Eppendorf AG, Hamburg, Germany) at 14,000 rpm for 20 min at 4 °C. The pellet was washed once with 70 % ethanol, centrifuged for 2 min at 14,000 rpm and air-dried for 10 minutes at room temperature. Finally, DNA was resuspended in TE buffer (10 mM Tris/HCl pH 7.5, 1 mM EDTA) or elution buffer (Qiagen AG, Hombrechtikon, Switzerland) by incubating the sample for 10 min at 50 °C, shaking.

2.2.7 Ligation. Ligation of double stranded DNA ends was performed using the DNA ligation kit ‘mighty mix’ (Takara Bio Inc., Shiga, Japan) according to the standard manufacturers protocol. Briefly, linearised plasmid vector backbone DNA and DNA fragment inserts were mixed in a molecular ratio of 1:3 in total 5 µl volume and incubated with 5 µl of Takara ligation mix for 30 min at 16 °C in a Thermocycler T3 (Biometra biomedizinische Analytik GmbH, Göttingen, Germany). Ligation samples were stored at -20 °C or directly used for transformation of competent bacteria (section 2.2.2). In case of electro-shock transformation of electro competent bacteria, ligation samples were dialysed and therefore desalted on MF-Millipore Membranes (VSWP01300, 0.025 µm, 13 mm; Millipore AG, Zug, Switzerland) floating on distilled H_2O in a Petri dish (Sarstedt AG & Co., Nümbrecht, Germany) for 30 minutes, prior to transformation.

2.2.8 Generation of neurotrypsin and membrane targeted eGFP expression constructs. The following neurotrypsin (all *mus musculus*) expression constructs were generated in our lab: Wild-type neurotrypsin, catalytically inactive neurotrypsin (mutation of the catalytic serine, at amino acid position 711, to alanine) and either catalytically active or inactive variants of neurotrypsin-enhanced green fluorescent protein (eGFP (Cubitt et al., 1995; Heim et al., 1995), Clontech, Takara Bio Inc., Shiga, Japan) fusion proteins. These variants were generated by fusing the eGFP cDNA sequence in-frame to the 3’-end of neurotrypsin. The respective coding sequences were subcloned into the pCDNA3.1(-)A vector (Invitrogen AG, Basel, Switzerland) or into the transfer vector for adenovirus production (pCMVtransfer; section 2.3; (Frischknecht et al., 2008)).

A construct coding for amino acids 1-41 of myristoylated alanine-rich C-kinase substrate (MARCKS; homo sapiens) fused at its 3’-end in-frame via a linker (coding for the two amino acids glycine and serine) to eGFP (MARCKS-eGFP) was kindly provided by P.

Caroni (FMI Basel, Basel, Switzerland). This construct targets eGFP to cellular membranes (De Paola et al., 2003). The MARCKS-eGFP sequence was excised with XhoI and subcloned into the pCDNA3.1(+) vector (Invitrogen AG, Basel, Switzerland) or into the transfer vector for adenovirus production (pCMVtransfer; section 2.3).

2.2.9 Generation of agrin expression constructs. The transmembrane agrin-x12, y4, z8 isoform (SN-agrin (*rattus norvegicus*), kindly provided by M. Rüegg, Biozentrum, Basel, Switzerland), was selected, because SN-agrin is strongly expressed in CNS neurons both *in vitro* and *in vivo* (O'Connor et al., 1995; Lesuisse et al., 2000). In addition, this isoform has been used in most of the studies analysing agrin functions in CNS neurons (Hilgenberg et al., 1999; Bose et al., 2000; Gingras et al., 2002; Hilgenberg et al., 2002; Hoover et al., 2003). eGFP-tagged variants of neurotrypsin were generated in our lab (section 2.2.8). Therefore, a wild-type SN-agrin expression construct and, for simultaneous microscopic analyses of co-expressed neurotrypsin and agrin variants in living neurons, monomeric red-fluorescent protein (mRFP (Campbell et al., 2002)) tagged SN-agrin variants were produced. These constructs contained mRFP in-frame either at agrin's N-terminus or its C-terminus. Concerning the analysis of neurotrypsin-dependent cleavage of agrin, these mRFP-agrin and agrin-mRFP constructs were believed to also enable the tracking of agrin parts after neurotrypsin-dependent cleavage. In addition, SN-agrin expression constructs were generated that are not cleavable by neurotrypsin (SN-agrin-mutant). Several modified parts of SN-agrin, carrying a mutation in the P1-position of the α cleavage site (arginine to alanine mutation) or the β cleavage site (lysine to alanine mutation), respectively (Reif et al., 2007), were assembled to yield the final SN-agrin-mutant construct. Again, untagged as well as mRFP-tagged variants were generated. Furthermore, as a control for experiments performed to analyse SN-agrin's function to generate filopodia, the secreted variant of the agrin-x12, y4, z8 isoform (LN-agrin) was generated. All constructs were assembled in the pCDNA 3.1(+) vector (Invitrogen AG, Basel, Switzerland) for ectopic expression in transiently transfected eukaryotic cells and identically subcloned into the transfer vector for adenovirus production (pCMVtransfer; section 2.3), unless otherwise stated.

SN-agrin-mRFP: Two fragments of about 3.5 kb, covering the total SN-agrin sequence and lacking the original agrin stop codon, were generated by PCR using the PfuUltra hot start DNA Polymerase (Stratagene, La Jolla, CA, USA) and pCDNA3.1-SN-agrin (M. Rüegg, Biozentrum, Basel, Switzerland) as template DNA for final assembly in the pCDNA3.1(+) vector. The first fragment, flanked by NotI and NdeI restriction sites, was ligated with the second fragment, flanked by NdeI and BglII restriction sites, at the agrin-internal NdeI site. mRFP was modified and amplified by PCR from the vector pRSETB-mRFP (kindly provided by J. Rohrer, University of Zurich, Zurich, Switzerland) for in-frame ligation to the modified 3'-end of SN-agrin via its BglII restriction site (see above). The whole construct was inserted into the multiple cloning site of the linearised pCDNA 3.1(+) vector via NotI and XbaI

restriction sites. The final construct was analysed by sequencing (Microsynth AG, Balgach, Switzerland) and also subcloned into the pCMVtransfer vector via NotI and XbaI restriction sites.

Wild-type SN-agrin: The 5' PCR fragment used for SN-agrin-mRFP generation (see above) was ligated with a NdeI to XbaI fragment, obtained by restriction digest from pCDNA3.1-SN-agrin template DNA (M. Rüegg, Biozentrum, Basel, Switzerland), and inserted via NotI and XbaI restriction sites into pCDNA3.1(+). This step was performed to generate matching restriction sites for virus-vector assembly. Due to usage of the NdeI/XbaI restriction fragment from the original template vector, this construct contained an approximately 1,000 bp long stretch of the original agrin 3' UTR sequence at its 3'-end.

mRFP-SN-agrin: An approximately 3.5 kb fragment covering the 5' SN-agrin sequence and lacking the original agrin translation initiation codon was generated by PCR using the PfuUltra hot start DNA Polymerase (Stratagene, La Jolla, CA, USA) and pCDNA3.1-SN-agrin (M. Rüegg, Biozentrum, Basel, Switzerland) as template DNA. This construct, flanked by NotI and NdeI restriction sites, was ligated with the 3' agrin NdeI to XbaI fragment, obtained by restriction digest from pCDNA3.1-SN-agrin template DNA (M. Rüegg, Biozentrum, Basel, Switzerland), into pCDNA 3.1(+) via its NotI and XbaI restriction sites. mRFP was modified and amplified by PCR from the vector pRSETB-mRFP (kindly provided by J. Rohrer, University of Zurich, Zurich, Switzerland), in this case lacking the original mRFP stop codon and containing NotI restriction sites at both ends. This fragment was then ligated in-frame with the modified 5'-end of SN-agrin via the NotI site of the previously assembled agrin construct. The final construct was analysed by sequencing (Microsynth AG, Balgach, Switzerland). Lastly, this construct was subcloned into the multiple cloning site of the pCMVtransfer vector via PmeI restriction sites flanking the mRFP-SN-agrin construct. Due to usage of the NdeI/XbaI restriction fragment from the original template vector, this construct contained an approximately 1,000 bp long stretch of the original agrin 3' UTR sequence. As the insert size for functional virus assembly is limited to 8 kb, the construct was subsequently shortened by performing a partial restriction digest with NheI and XbaI enzymes to remove approximately 600 bp of the 3'UTR sequence of agrin.

Mutant SN-agrin (SN-agrin-mutant): Distinct mutant variants of the SN-agrin-x12, y4, z8 isoform, uncleavable for neurotrypsin at either the α or the β site (the P1 cleavage positions mutated to alanine, respectively; (Reif et al., 2007)) were generated in our lab. To yield a completely uncleavable agrin variant for pCDNA3.1(+) based as well as adenovirus based expression, the different fragments of these mutated variants were assembled. For this, an EcoRV/HindIII fragment of an agrin variant mutated at the β site was subcloned into the previously cloned pCDNA3.1(+) wild-type SN-agrin variant described above. The mutation at the α-site was subsequently inserted by ligation of a NdeI/EcoRV-fragment from a mutant clone into the aforementioned wild-type SN-agrin clone, already carrying the mutation at the

β site. For adenovirus production, this final construct was subcloned via NotI and XbaI restriction sites into the pCMVtransfer vector to generate pCMVtransfer SN-agrin-mutant.
SN-agrin-mutant-mRFP: A HindIII fragment, containing the whole 5' agrin sequence including the mutated β site sequence from the SN-agrin-mutant clone, was ligated into the SN-agrin-mRFP vectors, lacking the original region flanked by HindIII restriction sites.
mRFP-SN-agrin-mutant: A SalI fragment of mRFP-SN-agrin, containing the mRFP sequence as well as approximately the first 1,000 bp of the 5' region of SN-agrin, was ligated into the previously generated SN-agrin-mutant vectors.
LN-agrin: The cDNA encoding the N-terminal domain (NtA; *mus musculus*) of the secreted isoform of agrin was cloned by A. Zurlinden in our lab. This cDNA was subcloned into the SN-agrin construct (*rattus norvegicus*) via a SmaI restriction site, leading to a secreted variant of wild-type agrin-x12, y4, z8 carrying the coding information for the LN domain instead of the SN domain. This construct was exclusively generated in the pCDNA3.1(+) expression vector.

For all agrin PCR reactions the following reaction mix was prepared, using the PfuUltra hot start DNA Polymerase (Stratagene, La Jolla, CA, USA) to yield long transcripts with very low error rates: 10 ng template DNA, 1x PCR-buffer, 0.25 mM dNTPs, 0.5 µM forward primer, 0.5 µM reverse primer and 2.5 U polymerase. For all mRFP PCR reactions the following reaction mix was prepared, using the 'expand high fidelity PCR system' (Roche Diagnostics (Schweiz) AG, Rotkreuz, Switzerland): 10 ng template DNA, 1x PCR-buffer, 0.25 mM dNTPs, 0.5 µM forward primer, 0.5 µM reverse primer and 2.5 U polymerase. The primer sequences and the PCR program used for each reaction are indicated below. Corresponding restriction enzyme recognition sites within the primer are indicated in green and mutations introduced into the agrin coding sequence are marked in red. All reactions were performed in a Thermocycler T3 (Biometra biomedizinische Analytik GmbH, Göttingen, Germany):

SN-agrin-mRFP generation:
agrin-PCR
5p-Agrin-NotI 5'-AAG CGG CCG CTG TAT GTA TCA TGC CTC-3'
3p-mid-Agrin-NdeI 5'-TGC CAT ATG TCA CAC CGT C-3'
5p-mid-Agrin-NdeI 5'-TGA CAT ATG GCA ATG AAT GC-3'
3p-mut-Agrin-BglII 5'-TTA GAT CTG TGG CAG CTA AGG GAG TG-3'
PCR program: 1x (2', 95 °C), 30x (30'', 95 °C; 30'' 51 °C; 3.5', 72 °C), 1x (10' 72 °C)

mRFP-PCR
5p-mRFP-pRSETB-BglII 5'-AAA GAT CTG GTC CGA TTG CCT CCT CC-3'
3p-mRFP-pRSETB-XbaI 5'-AAT CTA GAT TGT TAG CAG CCG GAT CAA GC-3'
PCR program: 1x (3', 95 °C), 20x (30'', 94 °C; 30'' 56 °C; 60'', 72 °C), 1x (7' 72 °C)

5' of wild-type SN-agrin generation:
agrin-PCR
5p-Agrin-NotI 5'-AAG CGG CCG CTG TAT GTA TCA TGC CTC-3'
3p-mid-Agrin-NdeI 5'-TGC CAT ATG TCA CAC CGT C-3'
PCR program: 1x (2', 95 °C), 30x (30'', 95 °C; 30'' 51 °C; 3.5', 72 °C), 1x (10' 72 °C)

mRFP-SN-agrin generation:
agrin-PCR
5p-mut-Agrin -NotI 5'-AAG CGG CCG CTG TAT CTA TCT TGC CTC-3'
3p-mid-Agrin-NdeI 5'-TGC CAT ATG TCA CAC CGT C-3'
PCR program: 1x (2', 95 °C), 30x (30'', 95 °C; 30'' 51 °C; 3.5', 72 °C), 1x (10' 72 °C)
mRFP-PCR
5p-mRFP-pRSETB-NotI 5'-AAG CGG CCG CTG TAT CTA TCT TGC CTC-3'
3p-w/o-stop-mRFP-pRSETB-NotI 5'-TTG CGG CCG CTG CTG AGG CGC CGG TGG AG-3'
PCR program: 1x (3', 95 °C), 20x (30'', 94 °C; 30'' 56 °C; 60'', 72 °C), 1x (7' 72 °C)

Subsequent to the PCR reaction, samples were constituted with 6x loading buffer (10 mM Tris/HCl pH 7.5, 30% glycerol, 0.1 % Xilene cyanol, 0.1 % bromphenol blue) and analysed by agarose gel electrophoresis (0.8-2 % agarose in TAE buffer (40 mM Tris-acetate, 2 mM Na_2EDTA, pH 8.5), containing 1 µg/ml ethidium bromide). Positive bands were excised from the gel and purified as stated in section 2.2.5. Eluted PCR fragments were subsequently prepared for ligation by digesting with the appropriate restriction enzymes indicated in the text, according to manufacturers protocols (section 2.2.5).

2.2.10 Detection of endogenously expressed agrin and neurotrypsin transcripts in cultured cells. To confirm the endogenous neuronal expression of neurotrypsin and agrin variants *in vitro*, messenger RNA (mRNA) was isolated from either cultured neurons (see section 2.4.1) or from cultured cortical astrocytes (see section 2.4.3), used as feeder cells for neuronal cultures (section 2.2.10.1). Isolated mRNA was then re-transcribed into complementary DNA (cDNA; section 2.2.10.2) and finally analysed by PCR for neurotrypsin and agrin transcripts detection (section 2.2.10.3).

2.2.10.1 RNA isolation from cultured hippocampal neurons and cortical astrocytes. Cultured hippocampal neurons (section 2.4.1) were grown in high density (400,000 cells/dish) on poly L-lysine coated (0.1 mg/ml) 35 mm plates (Corning B.V. Life Sciences, Schiphol-Rijk, The Netherlands) in the presence of Cytosine arabinoside (ARA-C, 15 µM, Sigma Aldrich Co., Saint Louis, MO, USA) to suppress glia cell growth. Alternatively, cortical astrocytes (section 2.4.3), usually employed as glia-feeder cells for hippocampal neuron cultures (section 2.4.1), were grown in 35 mm dishes (Corning B.V. Life Sciences, Schiphol-Rijk, The Netherlands). Total mRNA was isolated using TRI-reagent (Sigma Aldrich Co., Saint Louis, MO, USA) according to standard manufacturers protocol. Briefly, cells were washed twice with ice-cold PBS (137 mM NaCl, 2.7 mM KCl, 8 mM Na_2HPO_4, 1.5 mM

KH_2PO_4, pH 7.4) and lysed in 130 µl/well TRI-reagent. Homogenous lysate was incubated for 5 min at room temperature, 25 µl chloroform were added and the sample was shaken vigorously for 15 sec. The mixture was incubated for further 2 to 15 min at room temperature and finally centrifuged at 12,000 g for 15 min at 4 °C to produce a red organic phase (proteins), the DNA-containing interphase and the upper aqueous phase containing RNAs. The RNA-containing aqueous phase was mixed in a new tube with 62.5 µl isopropanol, incubated for 5-10 min at room temperature and centrifuged at 12,000 g for 10 min at 4 °C. The resulting RNA-containing pellet was washed with 75 % ethanol (7,500 g, 5 min, 4 °C). The RNA pellet was subsequently dried for 5-10 min at room temperature and resuspended in 15 µl diethylpyrocarbonate-treated H_2O (DEPC-H_2O) at 55 °C for 10 min with a micropipette

2.2.10.2 cDNA synthesis from isolated RNA. The isolated RNA (section 2.2.10.1) was re-transcribed into cDNA using the ThermoScript™ RT-PCR System (Invitrogen AG, Basel, Switzerland) according to manufacturers protocols. Briefly, 1 µg isolated RNA was supplemented with 2.5 µM oligo-dT-primer (neurotrypsin detection) or 2.5 µM hexanucleotide-primer (agrin detection) and 2 mM dNTPs in a 0.2 ml PCR tube (Eppendorf AG, Hamburg, Germany) and denatured for 5 min at 65 °C. The master reaction mix (1x cDNA-synthesis buffer, 5mM DTT, 40 U RNase OUT™, 15 U ThermoScript™ in DEPC-H_2O) was subsequently added. Only samples containing hexanucleotid-primer were incubated for 10 min at 25 °C prior to cDNA synthesis, all other samples were kept on ice. Then, cDNA synthesis was performed by incubating the samples for 50 min at 51 °C. The synthesis reaction was terminated by incubation of the samples for 5 min at 85 °C and template RNA was finally digested with 2 U RNAse H for 20 min at 37 °C. Samples were stored at -20 °C.

2.2.10.3 PCR detection of neurotrypsin and agrin transcripts. Finally, isolated cDNA (section 2.2.10.2) was analysed by PCR using the 'expand high fidelity PCR system' (Roche Diagnostics (Schweiz) AG, Rotkreuz, Switzerland) with neurotrypsin and agrin-transcript specific primers. For all PCR reactions the following reaction mix was prepared: 2 µl cDNA-sample (section 2.2.10.2; or 10 ng vector DNA in neurotrypsin and agrin control reactions), 1x PCR-buffer, 1 mM dNTPs, 0.5 µM forward primer, 0.5 µM reverse primer, 5 µl DMSO and 2.5 U polymerase mix. The primer sequences and the PCR program used for each mouse line are indicated below (for all analyses, GAPDH was used as a positive control for PCR amplification). All reactions were performed as hot start PCR in a Thermocycler T3 (Biometra biomedizinische Analytik GmbH, Göttingen, Germany):

Neurotrypsin (*mus musculus*) transcript detection:
Kringle-Fw 5'-CCG ACG ATT CCA CGC CGC-3'
BI 5'-CTG TGG TAG ACA ATC TCC-3'
GAPDH-Fw 5'-TGC CAT CAA CGA CCC CTTC-3'
GAPDH-back 5'-GGA TGA TGT TCT GGG CTG C-3'

PCR program: 1x (3', 95 °C), 35x (30'', 94 °C; 30'' 51 °C; 60'', 72 °C), 1x (7' 72 °C)

Transmembrane agrin (*mus musculus*) isoform transcript detection:
5pAgrin-SN-N-term 5'-TGC AAC ATC TGC TTG ATC C-3'
3pAgrinRT-N-term 5'-TGT AGC TCA CAC TCG TTG C-3'
GAPDH-Fw 5'-TGC CAT CAA CGA CCC CTTC-3'
GAPDH-back 5'-GGA TGA TGT TCT GGG CTG C-3'
PCR program: 1x (3', 95 °C), 35x (30'', 94 °C; 30'' 51 °C; 60'', 72 °C), 1x (7' 72 °C)

Secreted agrin (*mus musculus*) isoform transcript detection:
5pAgrin-LN-N-term 5'-AGA TCC TCA ACG TGG ACC-3'
3pAgrinRT-N-term 5'-TGT AGC TCA CAC TCG TTG-3'
GAPDH-Fw 5'-TGC CAT CAA CGA CCC CTTC-3'
GAPDH-back 5'-GGA TGA TGT TCT GGG CTG C-3'
PCR program: 1x (3', 95 °C), 35x (30'', 94 °C; 30'' 51 °C; 60'', 72 °C), 1x (7' 72 °C)

Subsequent to the PCR reaction, samples were constituted with 6x loading buffer (10 mM Tris/HCl pH 7.5, 30% glycerol, 0.1 % Xilene cyanol, 0.1 % bromphenol blue) and analysed by agarose gel electrophoresis (2 % agarose in TAE buffer (40 mM Tris-acetate, 2 mM Na_2EDTA, pH 8.5), containing 1 μg/ml ethidium bromide).

2.2.11 PCR genotyping. Genomic DNA was isolated by alkaline lysis from tail biopsies of embryos or postnatal animals. For this, a 0.5 cm tail biopsy was incubated for 45 min at 96 °C in 300 μl alkaline lysis reagent (25 mM NaOH; 0.2 mM Na-EDTA, pH 12.0). The reaction was stopped by adding 300 μl neutralising reagent (400 mM Tris-HCl, pH 5.0). Genotyping was performed with Taq polymerase (Sigma Aldrich Co., Saint Louis, MO, USA) according to the standard manufacturers protocol. For all PCR reactions the following reaction mix was prepared: 100 ng extracted DNA-sample, 1x PCR-buffer, 0.25 mM dNTPs, 1.5 mM $MgCl_2$, 0.5 μM forward primer, 0.5 μM reverse primer and 0.5 U Taq-Polymerase. The primer sequences and the PCR program used for each mouse line are indicated below (for all but neurotrypsin-deficient and agrin-deficient animals, TAG was used as a positive control for PCR amplification). All reactions were performed as hot start PCR in a Thermocycler T3 (Biometra biomedizinische Analytik GmbH, Göttingen, Germany):

Neurotrypsin (homo sapiens) overexpressing mice:
hNTSIIfor 5'-GCA ATG TGC CAG ATT CAG CAG-3'
Thy1back 5'-CCC ATG TTC TGA GAT ATT GGA AG-3'
TAG-83for 5'-GGA GGA GAG AGA CCC CGT GAA A-3'
TAG-82back 5'-ACA CGA AGT GAC GCC CAA TCC GT-3'
PCR program: 1x (3', 95 °C), 40x (45'', 95 °C; 45'' 63 °C; 60'', 72 °C), 1x (5' 72 °C)

Neurotrypsin (*mus musculus*) overexpressing mice:

THY1-300 5’-AGT GCT GGA ATC AAA GGT GTG AGC-3’
mNTbegR 5’-AGG TCG AGG GAC CTA ATA ACT TCG-3’
mNTIIfor 5’-CAA TGT GCC AGA CTA AGC ACC-3’
THY1-back 5’-CCC ATG TTC TGA GAT ATT GGA AG-3’
TAG-83for 5’-GGA GGA GAG AGA CCC CGT GAA A-3’
TAG-82back 5’-ACA CGA AGT GAC GCC CAA TCC GT-3’
PCR program: 1x (3’, 95 °C), 40x (45’’, 95 °C; 45’’ 56 °C; 60’’, 72 °C), 1x (5’ 72 °C)

Mice overexpressing a catalytically inactive variant of neurotrypsin (*mus musculus*):
mNTIIfor 5’-CAA TGT GCC AGA CTA AGC ACC-3’
Thy1back 5’-CCC ATG TTC TGA GAT ATT GGA AG-3’
TAG-83for 5’-GGA GGA GAG AGA CCC CGT GAA A-3’
TAG-82back 5’-ACA CGA AGT GAC GCC CAA TCC GT-3’
PCR program: 1x (3’, 95 °C), 40x (45’’, 95 °C; 45’’ 56 °C; 60’’, 72 °C), 1x (5’ 72 °C)

Neurotrypsin-deficient mice:
NTKOF01 5’-CAG AGC TCC TGG CGC TCA TC-3’
NTKOR02 5’-GGA AGA CAA TAG CAG GCA TGC TG-3’
NTKOR03 5’-CTC GCA GCT CAG CCC AAC TG-3’
PCR products of NTKOF01 and NTKOR02 indicated a neurotrypsin-deficient genotype and products of NTKOF01 and NTKOR03 indicated the wild-type allele.
PCR program: 1x (3’, 95 °C), 40x (45’’, 95 °C; 45’’ 62 °C; 60’’, 72 °C), 1x (5’ 72 °C)

Agrin-deficient mice:
PGK-Neo (77730) 5- TCG CAA GTT CTA ATT CCA-3’
AS Int-33 (30234) 5-GGG CAG GGC TAA CAC CAA-3’
Ex31fw 5-CAG GGG ATA GTT GAG AAG-3’
Ex32rev 5-GCT GGG ATC TCA TTG GTC-3’
PCR products of 77730 and 30234 indicated the mutant allele and products of Ex31fw and Ex32rev indicated the wild-type allele.
PCR program: 1x (3’, 95 °C), 40x (45’’, 95 °C; 45’’ 56 °C; 45’’, 72 °C), 1x (5’ 72 °C)

Subsequent to the PCR reaction, samples were constituted with 6x loading buffer (10 mM Tris/HCl pH 7.5, 30% glycerol, 0.1 % Xilene cyanol, 0.1 % bromphenol blue) and analysed by agarose gel electrophoresis (2 % agarose in TAE buffer (40 mM Tris-acetate, 2 mM Na_2EDTA, pH 8.5), containing 1 μg/ml ethidium bromide).

2.3 Adenovirus production and application

To achieve efficient ectopic expression of neurotrypsin and agrin variants in cultured hippocampal neurons, recombinant adenoviruses were generated. Cultured neurons are difficult to transfect and transfection methods commonly applied for ectopic expression of

recombinant proteins in cultured cells, including calcium phosphate precipitation or lipid-mediated transfection using, e.g., lipofectamine (Invitrogen AG, Basel, Switzerland), result in very low transfection levels of neurons. In contrast, high transfection rates of neurons may be achieved by using recombinant viral systems (Washbourne and McAllister, 2002). The main advantages of the use of recombinant adenoviruses for ectopic expression analyses in cultured neurons, when compared to most other viral vector systems, is their low toxicity, their comparably easy construction and the potential insert size of DNA fragments of up to 8 kb. Adenoviruses do not integrate into the genome and, therefore, they do not cause any gene inactivation or misregulation of oncogenes. In addition, adenoviruses have the potential to also infect post-mitotic cells. Though, the usage of the adenoviral system has some potential drawbacks. Neurons are not natural hosts for the adenovirus and, therefore, very high multiplicities of infection (MOI, viral titers; such as MOIs of 10 to 100) are required for effective infection of a large number of cells. In contrast, e.g., herpes simplex viruses efficiently infect neurons with low MOIs (MOI as low as 1). However, recombinant adenoviruses have been successfully used for infection of neurons in dissociated cultures, slice cultures and *in vivo* (Akli et al., 1993; Wilkemeyer et al., 1996; Giger et al., 1997) as the usage even of MOI up to 100 did not cause toxic effects. The main limitation of the adenoviral system is that glial cells are much more efficiently infected than neurons. This can lead to difficulties when neurons in mixed neuronal cultures need to be targeted.

The adenoviral expression vectors used in this work were derived from the human adenovirus 5 (Acc. Nr. M73260). These vectors lack the ER1 (base pairs 343-3532) and ER3 (base pairs 28140- 30821) regions of the viral genome, both to decrease the biohazard potential of the otherwise highly infective virions and to enable integration of up to 8 kb foreign DNA, e.g., an expression construct. ER1 codes for viral transactivators, which are necessary for initiation of viral DNA replication and the expression of remaining viral proteins. These adenoviruses are therefore incapable of replication in conventional cells. However, these viruses can be amplified in cell lines that express the ER1 gene products such as HEK293 cells (section 2.3.1). ER3 codes for several gene products that interfere with the human immune answer. It also codes for the adenovirus death protein (ADP), which is required for the efficient cell lysis and release of virus from infected cells (Tollefson et al., 1996). The infection potential of ER3 virus mutants of cultured cells is indistinguishably from wild-type virus variants and therefore, in combination with the E1 deletion, enables the production of recombinant viruses with low biohazard potential. However, virus producing HEK293 cells lyse more slowly. Yet, this has no influence on virus amplification in HEK293 cells since the commonly used protocols recommend to release amplified virus from infected cells by employing freezing and thawing or sonication methods (section 2.3.1).

2.3.1 Generation and production of recombinant adenoviruses expressing agrin and membrane targeted eGFP constructs. A previously described adenoviral expression system

(Mohanty et al., 2005), utilising type 5, E1/E3-deficient adenoviruses, was used to enable convenient and efficient ectopic expression of neurotrypsin variants, eGFP, membrane-targeted eGFP (MARCKS-eGFP) and agrin variants in cultured neurons. The necessary tools for virus production, including the transfer vector as well as the receiver vector carrying most of the adenoviral genome (Fig. 18A) were kindly provided by T. Trüb (University of Zurich, Zurich, Switzerland). The mouse neurotrypsin(-eGFP) and eGFP expression constructs were generated in our lab as described before ((Frischknecht et al., 2008) and section 2.2.8). To analyse the neurotrypsin-agrin interaction in cultured neurons in detail, I generated the following adenoviruses (AV) also expressing the respective construct under the control of the CMV promoter (Fig. 18A): AV-rat transmembrane agrin-x12, y4, z8 (AV-SN-agrin), AV-mRFP-SN-agrin ((Campbell et al., 2002), fused in-frame to the 5'-end of SN-agrin-x12, y4, z8), AV-SN-agrin-mRFP (mRFP fused in-frame to the 3'-end of SN-agrin-x12, y4, z8), AV-SN-agrin-mutant (the corresponding amino acids in the P1 positions of the respective alpha and beta cleavage sites of neurotrypsin (Reif et al., 2007) within SN-agrin-x12, y4, z8 were mutated to alanine, section 2.2.9), AV-mRFP-SN-agrin-mutant (mRFP fused in-frame to the 5'-end of SN-agrin-mutant), AV-SN-agrin-mutant-mRFP (mRFP fused in-frame to the 3'-end of SN-agrin-mutant) and AV-MARCKS-eGFP (eGFP fused in frame to the 3'-end of amino acids 1-41 of the MARCKS protein ((De Paola et al., 2003), section 2.2.8).

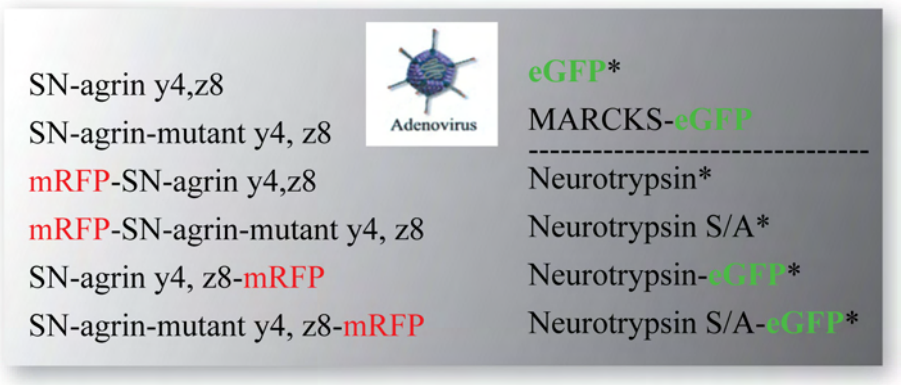

Figure 17: Overview of produced adenoviruses. The following recombinant adenoviruses were generated (section 2.3.1): Adenoviruses expressing wild-type transmembrane (SN)-agrin-x12, y4, z8 (*rattus norvegicus*). An untagged variant as well as variants, carrying mRFP either at agrin's N- or its C-terminus were produced. Alternatively, the same constructs were generated with a mutant variant of SN-agrin, not cleavable by neurotrypsin (SN-agrin-mutant y4, z8). Adenoviruses expressing eGFP alone, or expressing a myristoylated alanine-rich C-kinase substrate (*homo sapiens*; MARCKS)-eGFP fusion protein that targets eGFP to the cellular membranes. Adenoviruses expressing neurotrypsin (*mus musculus*) or a catalytically inactive variant of neurotrypsin (neurotrypsin S/A; *mus musculus*). Again, untagged or C-terminally eGFP-tagged variants of neurotrypsin were generated. * produced by Miriam Viesti and Anna Fejtova

Recombinant adenoviruses were generated as previously described (Mohanty et al., 2005). Briefly, the expression cassettes for each construct were inserted in-frame behind the CMV promoter cassette of the corresponding transfer vector (pCMVtransfer, Fig. 18A) as

described in sections 2.2.8-9. Cre-mediated recombination (Sternberg and Hamilton, 1981) of the pCMVtransfer-expression construct with a vector that contained the main part of the adenovirus genome (pAd) was then performed in the *E. coli* strain BM25.8 to obtain finally assembled virus expression construct DNA (Fig. 18A). These finally assembled constructs were retransformed (section 2.2.1) into the *E. coli* DH5α strain and subsequently amplified by mini-preparation analysis according to the manufacturers standard protocol (section 2.2.4). Positive clones, identified by restriction digest analysis, were linearised by PacI digestion for final transfection into the HEK293 helper cell line to produce virus particles (Fig. 18A).

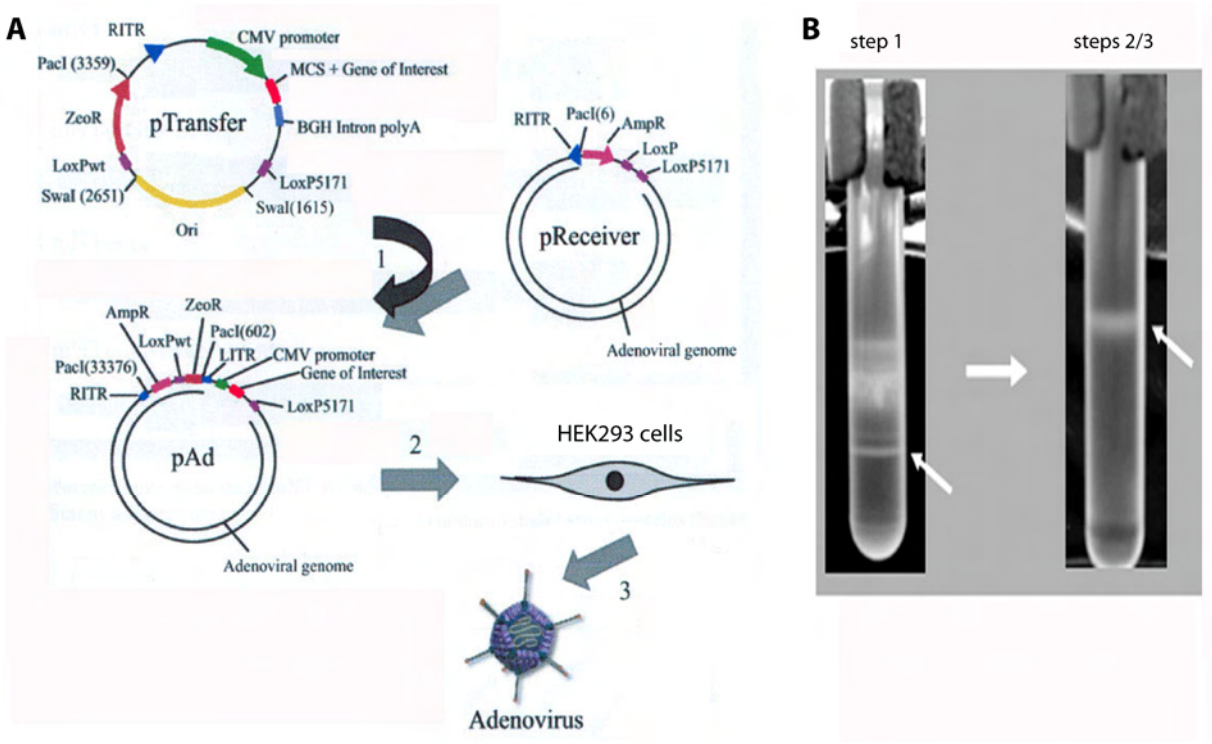

Figure 18: Production and purification of recombinant adenoviruses. ***A,*** Schematic overview of the protocol applied for adenovirus vector production. The cDNA of the expression-construct was cloned into the multiple cloning site 3' of the CMV-promoter cassette of the pTransfer (pCMVtransfer) vector. Co-transformation of *E. coli* BM25.8 bacteria with the pCMVtransfer vector construct and the pReceiver vector, carrying the main part of the virus genome, resulted in Cre-LoxP mediated generation of the final E1, E3-deficient recombinant adenovirus vector (pAd). Due to the endogenous expression of the adenoviral E1 genes, essential for virus amplification, HEK293 cells were employed for the production of the E1, E3-deficient adenoviruses. Initial virus particles were produced by transfection of HEK293 cells with the linearised pAd vector. High titer adenovirus stocks were generated by subsequent rounds of HEK293 cell infection with freshly generated virions. ***B,*** Purification of high titer virus particles. Several rounds of CsCl density gradient centrifugation (steps1-3) resulted in the concentration and purification of adenovirus particles (arrows).

Line 293 of human embryonic kidney cells (HEK293) is characterised as a constantly dividing cell-line expressing the E1 genes of the adenovirus genome, responsible for virus amplification and cell lysis (Graham et al., 1977). This cell-line was therefore used for the production of the E1/E3-deficient adenoviruses. HEK293 cells growing on 6-well cell culture

plates (Nunc GmbH & Co. KG, Wiesbaden, Germany) were transfected with a PacI-linearised adenoviral vectors (pAd, Fig. 18A), using Lipofectamine 2000 according to the manufacturers standard protocol (Invitrogen, Basel, Switzerland; see below). Successfully transfected cells produced infectious viruses that were expanded by subsequent infection of fresh cells. For large-scale virus production, overinfected cells were collected and resuspended in collection buffer (10 mM Tris-HCl, pH 8.1, containing 150 mM NaCl and 1 mM $MgCl_2$). The viral particles were released by three cycles of freezing and thawing and 5 min sonication on ice. Finally, the viruses were purified by several rounds of CsCl density gradient centrifugation, using one CsCl step gradient and two continuous CsCl gradients. The CsCl step gradient contained from bottom to top 2 ml 534.66 g/l (1.40 g/cm^3) CsCl in TD buffer (137 mM NaCl, 6 mM KCl, 0.7 mM Na_2HPO_4, 25 mM Tris-HCl, pH 7.5), 2 ml 331.7 g/l (1.25 g/cm^3) CsCl in TD buffer, and 6 ml of virus containing cell lysate. The banded virus from the step gradient (Fig. 18B, step 1) was isolated with an 20 g injection needle and mixed with 466.67 g/l (1.35 g/cm^3) CsCl in TD buffer and centrifuged in a Beckman SW41 rotor (Beckmann Coulter Intl. SA, Nyon, Switzerland) at 30,000 rpm for 16 hours (Fig. 18B, step 2). The virus was collected and once more purified on the continuous gradient (Fig. 18B, step 3). After purification the virus was dialysed in Slide-A-Lyzer dialysis cassettes (0.5-3ml, 10,000 MWCO; Pierce, Rockford, IL, USA) against TD buffer, transferred to Cryo tubes (Nunc GmbH & Co. KG, Wiesbaden, Germany), subsequently frozen in liquid nitrogen and stored at -80 °C. Virus titers were determined by plaque assays on HEK293 cells (Payment and Trudel, 1993) or by cytopathic effect assays on HEK293. Titers were calculated according to the Spearman-Kärber formula (Spearman, 1908; Kärber, 1931; Miller, 1973).

2.3.2 Infection of cultured cells. The infection potential and construct expression of purified virus was first tested with cos7 cells. Therefore, purified virus was added in varying concentrations to the cell-culture medium and cos7 cells were analysed 24-36 hours post-infection by Western blotting (section 2.4.8) and immunocytochemistry (section 2.4.10). All constructed adenoviruses successfully infected cos7 cells, even viruses from low titer virus preparations. Cultured neurons growing on poly-L-lysine coated coverslips (section 2.4.1) were infected at varying stages of development. Therefore, purified virus was added in varying concentrations to the culture medium and virus-mediated ectopic expression in cultured neurons was analysed 3-5 days post-infection by immunocytochemistry (section 2.4.10). Usually, 1-5 µl of virus preparations with a titer around 5 $LogTCID_{50}$/ml, determined by cytopathic effect assays on HEK293 cells (section 2.3.1), were sufficient to efficiently infect cultured neurons at varying developmental stages.

2.4 Cell culture techniques

2.4.1 Preparation of dissociated hippocampal neuron cultures. Primary dissociated hippocampal cultures were prepared from embryonic day 18 NMRI mice as previously described (Banker, 1980; Goslin, 1998; Kaech and Banker, 2006). Briefly, cell suspensions, obtained after trypsin treatment and careful trituration of excised hippocampal tissue, were plated onto round glass coverslips (diameter 18 mm; corrected thickness (0.17 mm ± 0.1 mm), Menzel-Glaeser, Braunschweig, Germany) coated with 0.5 mg/ml poly-L-lysine (Sigma, Saint Louis, MO, USA). After 1-2 hours at 37 °C, the coverslips were transferred into 12-well plates (Nunc GmbH & Co. KG, Wiesbaden, Germany) containing a 70-80 % confluent monolayer of astrocytes (section 2.4.3) and 1 ml DMEM supplemented with B27, 5 mM glutamine, 1 mM sodium pyruvate, 0.5 mg/ml Albumax and 1/100 antibiotic/antimycotic solution (100x). Cultures were maintained at 37 °C in a humidified incubator with an atmosphere of 95 % air and 5 % CO_2. All chemicals used for neuronal cultures were obtained from Invitrogen AG (Basel, Switzerland), unless otherwise indicated.

2.4.2 Preparation of cultured hippocampal neurons from transgenic animals overexpressing active mouse neurotrypsin. As an attempt to establish a neuronal culture system with endogenous overexpression of active neurotrypsin, hippocampal neuron cultures were prepared from heterozygous transgenic animals constitutively overexpressing active mouse neurotrypsin (line *Tg(Prss12)*533.1Zbz). Prior to culture preparation, E18-mouse embryos were removed from a pregnant transgenic mother, decapitated and the corresponding heads were kept in HBSS solution (Invitrogen AG, Basel, Switzerland) on ice while the respective embryos were genotyped to identify transgene-positive animals (section 2.2.11). Finally, primary dissociated hippocampal cultures were prepared from transgene positive embryonic brains as described in section 2.4.1. Unfortunately, neuronal cultures generated from transgenic animals did not overexpress neurotrypsin and were therefore not further analysed. Most likely, Thy1-promoter mediated expression of the transgene (section 2.1.1), starting around postnatal day 5 *in vivo* (Radrizzani et al., 1995), is not activated in neuronal cultures prepared from prenatal brains (confirmed by internal communication with P. Caroni, FMI Basel, Switzerland).

2.4.3 Preparation of glia-feeder cultures. Cortical astrocytes were isolated from postnatal day 2 NMRI mice and expanded in culture as previously described (Banker, 1980; Goslin, 1998). In brief, a cell suspension obtained after trypsin treatment and trituration of excised cortical tissue was plated onto 10 cm culture dishes (Corning B.V. Life Sciences, Schiphol-Rijk, The Netherlands) and cultured in DMEM supplemented with 10 % FCS and 1/100 antibiotic/antimycotic solution (1/100). The culture-medium was replaced one day after the preparation and cells were grown till 90 % confluency and then splitted to 4 x 10 cm culture

dishes for further expansion. Cultures were maintained at 37 °C in a humidified incubator with an atmosphere of 95 % air and 5 % CO_2. All chemicals used for glia cultures were obtained from Invitrogen AG (Basel, Switzerland), unless otherwise indicated.

2.4.4 Preparation of glia-feeder cultures from agrin-deficient animals. In the central nervous system, agrin is expressed by neurons as well as glial cells. Glial cells are known to express secreted agrin isoforms that may be deposited along neurons in a neuron-glia co-culture system. To exclusively detect neuronal expressed agrin in neuronal cultures, glia-feeder cultures were generated from agrin-deficient animals (Lin et al., 2001). Agrin-deficient animals die at birth due to respiratory failure and agrin-deficient glia were therefore isolated from cortices of E19 embryos. Prior to astrocyte preparation, E19 mouse embryos were removed from a pregnant mother, heterozygous for the agrin null-allele and mated with a heterozygous male. The embryos were decapitated and the corresponding heads were kept in HBSS solution (Invitrogen AG, Basel, Switzerland) on ice while the respective embryos were genotyped to identify agrin-deficient animals (section 2.2.11). Finally, cortical glia cultures were prepared from agrin-deficient embryonic brains as described in section 2.4.3.

2.4.5 Culturing cos7 and HEK293 cells. Cos7 is a continuously dividing cell-line, derived from kidney cells of the African green monkey (*Chlorocebus aethiops*), because of expression of the SV40 T-antigen of the SV40 virus. Cos7 cells are conventionally used for a wide range of cell culture applications and especially suitable for microscopic analyses of (ectopically) expressed proteins due to their flat and sprawled adherent growth on plastic or glass surfaces. Line 293 of human embryonic kidney cells (HEK293) is characterised as a constantly dividing cell-line expressing the adenoviral E1 genes (Graham et al., 1977) and was used in this study for adenovirus production (section 2.3). Cos7 as well as HEK293 cells were generally grown in 10 cm culture dishes (Corning B.V. Life Sciences, Schiphol-Rijk, The Netherlands) in DMEM supplemented with 10 % fetal calf serum (FCS) at 37 °C in a humidified incubator with an atmosphere of 95 % air and 5-10 % CO_2. Cells were regularly passaged when grown confluent. Briefly, cells were washed once with HBSS (Invitrogen AG, Basel, Switzerland) and detached with trypsin solution (Invitrogen AG, Basel, Switzerland) diluted 1/10 in HBSS (without Mg^{2+} and Ca^{2+}, Invitrogen AG, Basel, Switzerland). Usually, 1/10 of cells were transferred to new 10 cm dishes and further incubated with DMEM/10 % FCS at 37 °C in a humidified incubator with an atmosphere of 95 % air and 5-10 % CO_2. For storage purposes, cells were frozen in DMEM/10 % FCS containing 10 % DMSO (Sigma Aldrich Co., Saint Louis, MO, USA) and stored at -80 °C.

2.4.6 Transient transfection of cos7 cells on glass coverslips. Cos7 cells were grown to 30-40 % confluency on poly-L-lysin (0.1 mg/ml, P-1524, Sigma Aldrich Co., Saint Louis, MO, USA) coated glass coverslips (diameter 18 mm; corrected thickness of 0.17 mm ± 0.1 mm,

Menzel-Glaeser, Braunschweig, Germany) in 12-well culture plates (Nunc GmbH & Co. KG, Wiesbaden, Germany) containing 1 ml/well DMEM/10 % FCS. Transfection of cells in one well was performed by mixing solution A (2 µl Lipofectamine 2000 in 100 µl OptiMEM I (both Invitrogen AG, Basel, Switzerland)) after 5 min with solution B (total 1 µg vector DNA for single transfections or total 1.5 µg vector DNA for double transfections in 100 µl OptiMEM I). The transfection mix was then incubated at room temperature for 20-30 min. During the incubation period, cell culture-medium was replaced with fresh DMEM/10 % FCS. Finally, the transfection-mix was added drop-wise to the well and cells were further incubated for 24 hours at 37 °C in a humidified incubator with an atmosphere of 95 % air and 5-10 % CO_2.

2.4.7 Transient transfection of cos7 and HEK293 cells in 35 mm dishes or on 6-well plates. Cos7 cells were grown to 80 % confluency in 35 mm dishes (Corning B.V. Life Sciences, Schiphol-Rijk, The Netherlands) or on 6-well culture plates (Nunc GmbH & Co. KG, Wiesbaden, Germany) containing 2 ml/well DMEM/10 % FCS. Transfection of cells in one well was performed by mixing solution A (6 µl Lipofectamine 2000 in 250 µl OptiMEM I (both Invitrogen AG, Basel, Switzerland)) after 5 min with solution B (total 2 µg vector DNA for single transfections or total 3 µg vector DNA for double transfections in 250 µl OptiMEM I). The transfection mix was then incubated at room temperature for 20-30 min. During the incubation period, cell culture-medium was replaced with fresh DMEM/10 % FCS. Finally, the transfection-mix was added drop-wise to the well and cells were further incubated for a minimum of 36 hours at 37 °C in a humidified incubator with an atmosphere of 95 % air and 5-10 % CO_2.

2.4.8 Processing of cultured cells for Western blotting. Supernatants (cell-culture medium) of untransfected or transiently transfected cos7 cells, growing in 6-well plates (Nunc GmbH & Co. KG, Wiesbaden, Germany), were transferred to a 2 ml tube (Eppendorf AG, Hamburg, Germany), containing protease inhibitors (1/100 dilution, P-8340, Sigma Aldrich Co., Saint Louis, MO, USA). Cell debris was removed by centrifugation in a tabletop centrifuge for 10 min, 14,000 rpm, 4 °C and resulting supernatants were transferred to fresh tubes, frozen in liquid nitrogen and stored at -80 °C. Cells adhering to the culture dish were washed once in ice-cold PBS (137 mM NaCl, 2.7 mM KCl, 8 mM Na_2HPO_4, 1.5 mM KH_2PO_4, pH 7.4), scraped off in 300 µl lysis buffer (20 mM Tris/HCl, pH7.5; 150 mM NaCl, 5 mM EDTA, 1 % (w/v) CHAPS and 0.1 % (w/v) SDS), transferred to 1.5 ml tubes (Eppendorf AG, Hamburg, Germany) and incubated for a minimum of 30 min on ice before frozen in liquid nitrogen and stored at -80 °C. SDS-PAGE/Western blot analyses were performed as described in section 2.1.4.

2.4.9 Functional analyses of filopodia induction by agrin on cos7 cells. The overexpression of transmembrane agrin causes filopodia-like membrane extensions in a variety of different cell types, including neurons and cos7 cells. To analyse a possible impact of neurotrypsin-activity on this function of agrin, I performed immunofluorescence analyses of transiently transfected cos7 cells, transfected with plasmids expressing either agrin and/or neurotrypsin variants. Fixed and permeabilised cells were stained with specific primary antibodies against agrin or neurotrypsin and fluorescently-labeled secondary antibodies (section 2.4.10). Additionally, filamentous actin (F-actin) structures within the cell and within motile surface elements, like filopodia, were specifically visualised with fluorescently labelled Phalloidin (Molecular Probes, Invitrogen AG, Basel, Switzerland). Alternatively, membrane structures were visualised by (co-)transfection of cells with MARCKS-eGFP (section 2.2.8). Quantification of the effect of neurotrypsin on agrin's ability to cause filopodia was performed by a rough estimation of filopodia positive and negative cells for each set of transfections. The appearance of an excess of filopodia-like structures at multiple sites of the cellular surface identified cos7 cells as filopodia-positive. In contrast, filopodia-negative cells had a similar appearance as the average control cell with little or no filopodia.

2.4.10 Immunocytochemistry. Cells growing on poly-L-lysine coated coverslips (see sections 2.4.1, 2.4.2 and 2.4.6) were washed in HBSS (Invitrogen AG, Basel, Switzerland) for 5 min at room temperature and fixed in fixation solution (4 % paraformaldehyde in PBS, 137 mM NaCl, 2.7 mM KCl, 8 mM Na_2HPO_4, 1.5 mM KH_2PO_4, pH 7.4) for 5-10 min at room temperature. Samples were subsequently blocked with blocking solution (10 % FCS/PBS, 0.1 % glycine and 0.05 % NaN_3) either for at least 1 hour at room temperature or for at least 12 hours at 4 °C. Protein detection was performed by incubation of the cells in primary antibody incubation solution (3 % FCS/PBS), containing primary antibodies. This step was performed on Parafilm M (Brand GmbH & Co. KG, Wertheim, Germany) in a wet chamber, preferably overnight at 4 °C or alternatively for 2 hours at room temperature. Cells were washed 3 times 10 min with PBS and incubated on Parafilm M in a wet chamber with secondary antibody incubation solution, containing fluorescence-labelled secondary antibodies, detecting the primary antibodies. If necessary, fluorescence-labeled Phalloidin (1:25; Molecular probes, Invitrogen AG, Basel Switzerland) was included in the secondary antibody incubation solution to visualise the actin-cytoskeleton, including motile cell-surface elements like filopodia. In general, for detection of intracellular epitopes, 0.5 % Saponin was included in any antibody incubation solution to permeabilise cells. Cells were finally washed with PBS for at least 3 times 10 min and mounted with Vectashield (Vector Laboratories, Burligame, CA, USA). Mounted samples were sealed with conventional nail polish and stored at 4 °C in the darkness. Cells were analysed using a Leica SP2 confocal microscope and Leica LCS software (Leica Mikrosysteme Vertrieb GmbH, Wetzlar, Germany). Recorded images were carefully processed using Photoshop CS2 (Adobe Systems Inc., San Jose, CA, USA).

3. Results

3.1 Analysis of the neurotrypsin-agrin interaction in the murine brain.

3.1.1 Agrin is a substrate of neurotrypsin in the murine CNS.

Agrin is a substrate of neurotrypsin *in vitro* (Reif et al., 2007) and neurotrypsin-dependent cleavage of agrin was observed at the NMJ *in vivo* (Bolliger, M. *et al.,* unpublished observations). To confirm that agrin is a substrate of neurotrypsin also in the CNS, I analysed mouse brain homogenates of neurotrypsin-deficient mice (Ntd), agrin-deficient mice and their corresponding wild-type littermates by Western blotting. So far, analyses of neurotrypsin-deficient mice did not reveal an apparent phenotype and corresponding brain homogenates from postnatal day 4 (P4) pups were analysed. In contrast, agrin-deficient mice die at birth due to respiratory failure and, thus, brain homogenates of 19 days old embryos (E19) were analysed. Both 90-kDa and 22-kDa agrin cleavage fragments were indeed detected in brain homogenates of wild-type mice but did not appear in samples of Ntd animals when analysed with each two different polyclonal antibodies directed against the 90-kDa or the C-terminal 22-kDa fragment, respectively (Fig. 19B). The week signals detected with the anti-C-22-agrin antibodies in between 20 and 25 kDa in samples of Ntd animals represented unspecific signals, as signals of similar intensity also appeared in tissue from corresponding agrin-deficient animals (Fig. 19C). Confirming the better quality and higher affinity of the anti-C-90-agrin antibodies, no signals for the 90-kDa fragment were detected in brain homogenates of agrin-deficient mice. Therefore, these data confirmed that the C-terminal 90-kDa and 22-kDa agrin fragments are generated in the murine brain and that their appearance is exclusively dependent on neurotrypsin activity. Furthermore, this SDS-PAGE analysis, based on a Bis-Tris buffer adjusted to neutral pH and gradient gels, enabled the detection of full-length agrin as three distinct groups of bands between 220 and 500 kDa. We termed these three distinct groups of bands upper, middle and lower full-length agrin variants. Both the anti-C-90 and the anti-C-22 antibodies detected these variants of full-length agrin in an identical band pattern. The slight differences in the relative intensity of the upper, middle, and lower variants obtained with the anti-C-22, compared to the anti-C-90 antibodies, most likely reflected a differential preference of the antibodies for distinct variants of agrin rather than contributions from neurotrypsin-dependent cleavage fragments (see material and methods, section 2.1.2). All three full-length agrin bands appeared in brain homogenate of wild-type as well as Ntd mice. However, in particular the upper and middle full-length bands appeared stronger in tissue from Ntd mice (Fig. 19B). The increase of full-length agrin signals most likely reflects the lack of neurotrypsin-dependent cleavage of agrin and therefore an accumulation of unprocessed agrin variants in the brains of Ntd mice (see section 3.1.3). The identity of the three distinct groups of bands as variants of agrin was confirmed by Western blot analyses of brain homogenates from agrin-deficient mice, compared to brain homogenates from their wild-type littermates (Fig. 19C). All three groups of full-length agrin bands were exclusively

present in wild-type tissue when detected with the high affine anti-C-90-agrin antibodies. Similar results were obtained with the anti-C-22-agrin antibodies. However, these less affine antibodies also detected a weaker and unspecific band at the level of the bottom full-length agrin variants in tissue from agrin-deficient mice.

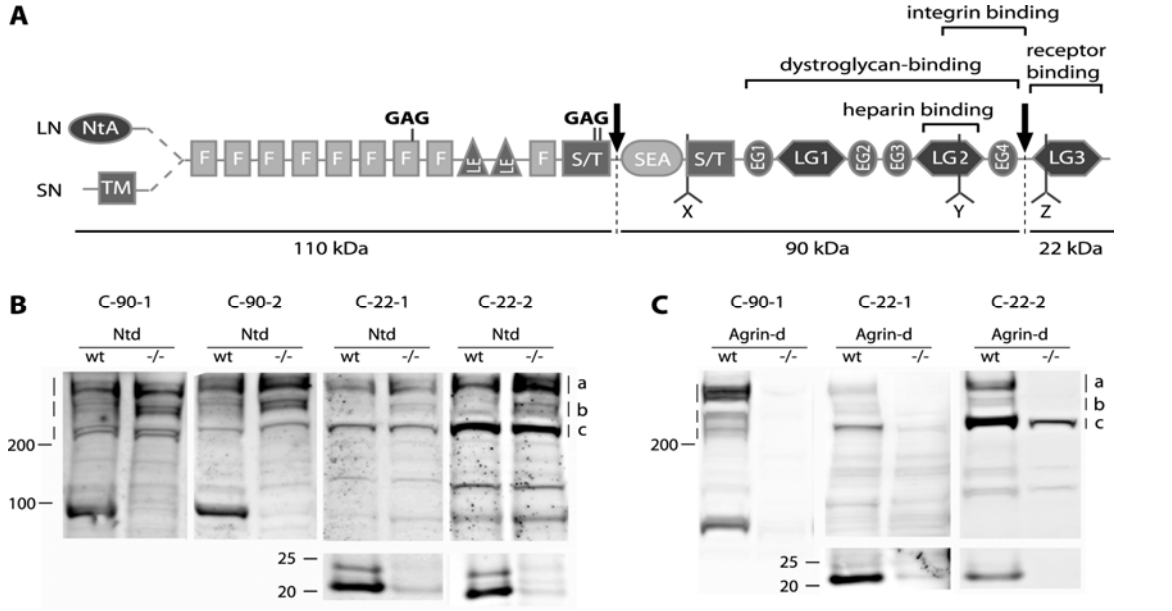

Figure 19. The C-90 and C-22 agrin fragments are exclusively generated by neurotrypsin in the mouse CNS. ***A,*** Schematic overview of agrin's protein structure (modified from (Hoch et al., 1993; Bezakova and Ruegg, 2003)). Alternative splicing leads to the expression of a variety of transmembrane (SN) or secreted (LN) agrin variants, containing variable inserts of several amino acids at the x, y, and z splice sites. Binding sites within the C-terminal moiety of agrin are indicated. Neurotrypsin-dependent cleavage of agrin (indicated by arrows) generates two C-terminal fragments of 90 kDa and 22kDa. NtA - N-terminal agrin domain; TM - transmembrane domain; F - follistatin-like domains; GAG - glycosaminoglycan side chains; LE - laminin-epidermal growth factor (EGF)-like domains; S/T - serine-threonine-rich region; SEA - sperm protein, enterokinase and agrin domain; EG - EGF-like domains; LG - laminin-globular domains. ***B,*** Comparison of different polyclonal antibodies generated against the respective neurotrypsin cleavage fragments of agrin. Western Blot analyses of P4 mouse brain homogenates from neurotrypsin deficient (Ntd) animals compared to brain homogenates obtained from their wildtype (wt) littermates. Molecular mass references are indicated in kDa. Both antibodies directed against the C-90 agrin fragment (C-90-1; C-90-2) detected a double band at 90 kDa in wildtype tissue but not in tissue from Ntd animals. Similarly, the antibodies directed against the C-22 agrin fragment (C-22-1; C-22-2) detected a specific double band at around 22 and 24 kDa in wildtype tissue on top of unspecific bands visible in neurotrypsin-deficient samples (compare to ***C***). These findings indicated that the C-90 and C-22 agrin fragments were exclusively generated by neurotrypsin activity. In addition to the detection of their respective cleaved antigens, all antibodies similarly detected three distinct groups of bands above 200 kDa, most likely indicating differentially glycanated variants of full-length agrin. These groups of bands were termed upper (a), middle (b) and lower (c) variants of full-length agrin. ***C,*** Confirmation of the specificity of the different polyclonal antibodies generated against the respective neurotrypsin cleavage fragments of agrin. Western Blot analyses of E19 mouse brain homogenates from agrin-deficient (Agrin-d) animals or their wildtype littermates (wt). The three groups of bands above 200 kDa as well as the bands at around 90 kDa (C-90-1) and 22-kDa (C-22-1; C-22-2) indeed correspond to agrin as these bands appear in wildtype but not in Agrin-d tissue. The C-90-1 antibody was by far the most specific and strongest antibody tested as it detected strong bands only in wt but not in Agrin-d tissue. Both the C-22 antibodies were comparably less affine and also detected unspecific signals, mainly at the level of the lower full-length agrin variants but also faintly at the level for both 22-kDa fragment bands.

On Western blots made from standard SDS-PAGE gels, the variant forms of agrin were not resolved, but appeared as a broad smear ranging from 220 to 500 kDa. This feature was suggested to reflect the existence of differently glycanated agrin variants (Bezakova and Ruegg, 2003). Differential glycanation as the molecular basis underlying all of these resolved agrin variants was indeed confirmed by heparitinase digestion of brain homogenates, which resulted in a shift of all upper and middle bands to the level of the lower bands (Fig. 20B). Based on these results we concluded that the lower group of bands reflected agrin variants without or with little glycanation, while the middle and upper groups were composed of variants with intermediate and strong glycanation.

3.1.2 Expression of neurotrypsin and agrin, as well as neurotrypsin-dependent agrin cleavage predominate during neural development.

To obtain a detailed view of neurotrypsin-dependent processing of agrin, I analysed the expression pattern of neurotrypsin together with full-length agrin and the neurotrypsin-dependent fragments of agrin by Western blotting of brain homogenates from mice of various developmental and adult stages. The analysis of samples from E14 through P730 demonstrated that neurotrypsin protein expression was developmentally regulated with peak expression between E18 and P10 (Fig. 20A). This is in accordance with previously reported mRNA expression profiles, indicating that neurotrypsin expression is strongest around the first postnatal week in a variety of CNS regions ((Wolfer et al., 2001); Fig. 12). The expression of full-length agrin was similarly developmentally regulated, also with maximal expression between E18 and P10 (Fig. 20A). Subsequently, expression declined until P30, but persisted at a low level throughout adult life. Similar overall expression profiles of agrin mRNA have been reported previously (Cohen et al., 1997; Li et al., 1997). The analysis allowing resolution of the glycanation-dependent variants of agrin (section 3.1.1) revealed that the stage-dependent regulation of agrin expression was most pronounced for the upper group of variants, representing the most heavily glycanated forms of agrin. These variants exhibited the most pronounced developmental rise as well as a stronger decline during adulthood. In contrast, the expression of the middle and lower groups of agrin variants was only slightly enhanced during development and less reduced during adulthood.

The abundance of the neurotrypsin-dependent agrin fragments roughly reflected the temporal expression pattern of full-length agrin and neurotrypsin. Both neurotrypsin-dependent fragments of agrin were detected as double bands (Fig. 20A). The two bands of the 90-kDa fragment showed a differential regulation between E14 and P15. The upper 90-kDa band was strongest in the samples from E14 brain and its intensity declined in the first postnatal days. In contrast, the lower 90-kDa band was strongest between E18 and P15. Beyond P15, both bands persisted throughout adult life at equal but weak levels. To confirm their identity, I purified both 90-kDa bands by immunoaffinity isolation from mouse brain homogenates, subjected them to tryptic digestion, and analysed the peptides by mass spectrometry. Several sequences of agrin-derived peptides, covering the 90-kDa fragment,

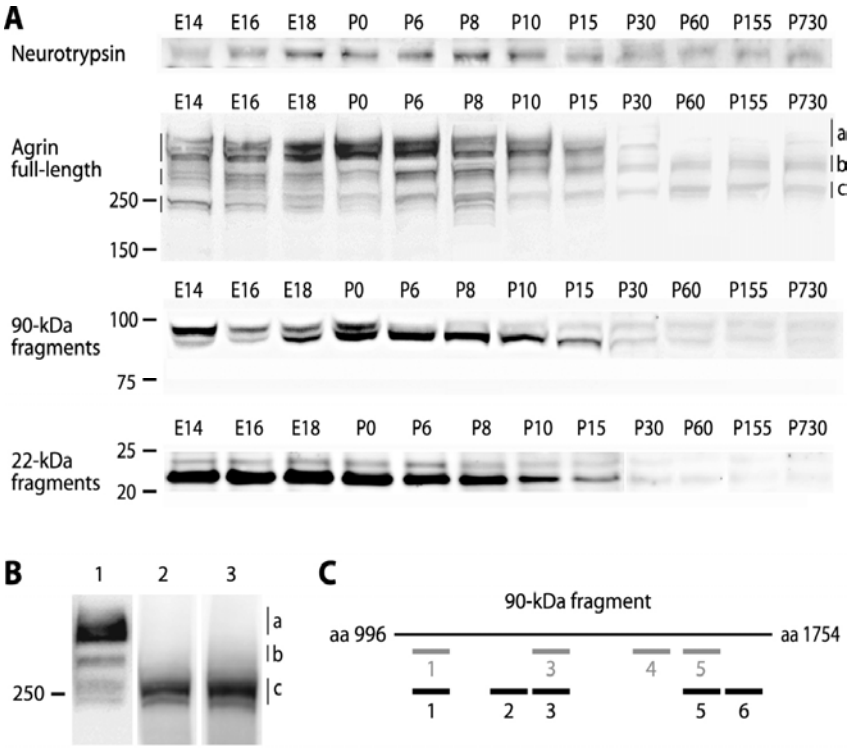

Figure 20. Expression of neurotrypsin and agrin, as well as neurotrypsin-dependent agrin cleavage are developmentally regulated. ***A,*** Western blot analyses of mouse brain homogenates obtained from animals of E14 to P730. Peak expression of neurotrypsin and agrin was found during the first postnatal week. The protein bands above 220 kDa, detected with the anti-C-90 agrin antibody, represent differentially glycosylated variants of full-length agrin. They can be categorised into three distinct groups, termed upper (a), middle (b) and lower (c) variants of agrin. Neuro-trypsin-dependent cleavage of agrin also appeared strongest around the first postnatal week. Both cleavage products of agrin appeared as double bands. Molecular mass references are indicated in kDa. ***B,*** Heparitinase digestion of P6 mouse brain homogenates. In control samples, full-length agrin was detected as three distinct groups of bands, running above 220 kDa (1: control). Digestion with heparitinase III resulted in the disappearance of the upper and middle variants, characterising them as glycanated variants of agrin (2: 2 h digestion, 3: 5 h digestion). ***C,*** Mass spectrometric analysis of the purified 90-kDa fragments from brains of P25-P50 mice overexpressing active neurotrypsin confirmed that both bands correspond to the C-terminal region of agrin. The detected tryptic peptides of the isolated protein bands (grey: upper 90 kDa band; black: lower 90-kDa band) were aligned within the designated C-terminal region of agrin ranging from amino acid (aa) 996 to aa 1754 (NCBI protein accession no. AAA40703.1). The identified peptides were: 1-SIESTLDDLFR (pos. 1061-1071), 2-ALETEGLLLYNGNAR (pos. 1293-1307), 3-FDTGSGPAVLTSLVPVEPGR (pos. 1325-1344), 4-GPSGLLLYNGQK (pos. 1563-1574), 5-EPLYVGGAPDFSK (pos. 1656-1668), 6-GHQLLTQEHVLR (pos 1690-1701).

were found in both bands (Fig. 20C). The two bands of the 22-kDa fragment, detected with the C-22-1 antibody exhibiting higher affinity compared to the C-22-2 antibody used in our previously published study ((Reif et al., 2007), were of equal relative intensity at all time points with much stronger signals for the lower band (Fig. 20A). Highest levels of the 22-kDa fragment were found between E14 and P8. The decline in the intensity of the 22-kDa fragment between P8 and P15 correlated well with a drop in expression of both full-length agrin and neurotrypsin. Similar to the 90-kDa fragment, the 22-kDa fragment remained detectable throughout adult life. In contrast, the high levels of the 22-kDa fragment detected already at E14 do not correlate well with the relatively low expression levels of neurotrypsin. This discrepancy could be due to particularities in the spatial locations of agrin and neurotrypsin at early developmental stages, which are not reflected in the results of Western blot analyses based on homogenates of whole brains. The molecular basis underlying the differential electrophoretic mobility of the two variants of the 90-kDa and the 22-kDa

fragments of agrin is currently not clear. Based on the highly specific nature of the proteolytic activity of neurotrypsin (Reif et al., 2007), differential proteolytic cleavage is unlikely. Rather, the variants of the two agrin fragments may reflect different splice variants of agrin or differential post-translational modifications (Bezakova and Ruegg, 2003), such as potential O-linked glycosylation as predicted for the region of agrin giving rise to the 90-kDa fragment (Parkhomovskiy et al., 2000; Xia and Martin, 2002).

3.1.3 The glycanated variants of CNS agrin are preferred substrates of neurotrypsin.

To analyse the neurotrypsin-dependent cleavage of agrin in detail, I performed quantitative densitometry of Western blots of mouse brain homogenates. Brain samples were prepared at P9 from neurotrypsin-deficient (Ntd) mice, mice overexpressing catalytically active (Nto-act) or a catalytically inactive (Nto-inact) neurotrypsin and compared with brain samples from their wild-type littermates. The analyses of Nto-inact mice were included as a control to confirm that the catalytic activity of neurotrypsin is strictly required for neurotrypsin-dependent cleavage of agrin (see below). Representative Western blots of neurotrypsin, and full-length agrin, detected with the anti-C-22 antibody, as well as its 90-kDa and 22-kDa fragments are shown in Figure 21A-D. Western blotting of neurotrypsin confirmed its absence in Ntd mice and its excess in neurotrypsin-overexpressing mice (Fig. 21A). Neither the 90-kDa nor the 22-kDa fragment of agrin was found in samples from Ntd mice, confirming their origin from neurotrypsin-dependent cleavage of agrin (Fig. 21C-F). Accordingly, both fragments were increased in samples from Nto-act mice (Fig. 21C-F). Densitometry revealed that overexpression of active neurotrypsin resulted in a significant four-fold increase of the 90-kDa fragment (392.0 ± 44.1 % (mean ± S.E.M.) of wild type; Fig. 21E). In contrast, the 22-kDa fragments showed an increment of only 1.5-fold (148.4 ± 7.9 % of wild type; Fig. 21F). This discrepancy may be explained by higher diffusive properties of the 22-kDa fragments or different stabilities of the respective fragments. In samples from transgenic Nto-inact mice the signal intensities of both agrin fragments did not significantly differ from those of wild-type mice (92.6 ± 5.0 % of wild type for the 90-kDa fragment and 111.7 ± 7.2 % of wild type for the 22-kDa fragment; Fig. 21E, F. The neurotrypsin-dependent increase of the agrin fragments in samples from Nto-act mice coincided with a decrease of full-length agrin (Fig. 21G-I). I measured the signal intensities of the upper, middle and lower groups of full-length agrin in samples from Nto-act, Nto-inact, and Ntd mice using an antibody against the 22-kDa fragment and normalised the results to the corresponding signals of wild-type littermates. The results indicated that the protein levels for upper and middle full-length agrin were significantly decreased in the brain of Nto-act mice (59.1 ± 4.4 % and 75.2 ± 8.7 % of wild-type, respectively; Fig. 21G), unaltered in Nto-inact mouse brains (103.6 ± 2.7 % and 103.7 ± 0.3 % of wild type, respectively; Fig. 21H), and increased in the brain of Ntd mice (216.4 ± 23.2 % and 156.4 ± 14.0 % of wild type, respectively; Fig. 21I). In contrast, no alterations of the lower group of full-length agrin were measured in all analysed

tissues (Nto-act 99.0 ± 6.2 %, Nto-inact 97.9 ± 2.2 %, and Ntd 99.4 ± 10.2 % of wild type; Fig. 21G-I).

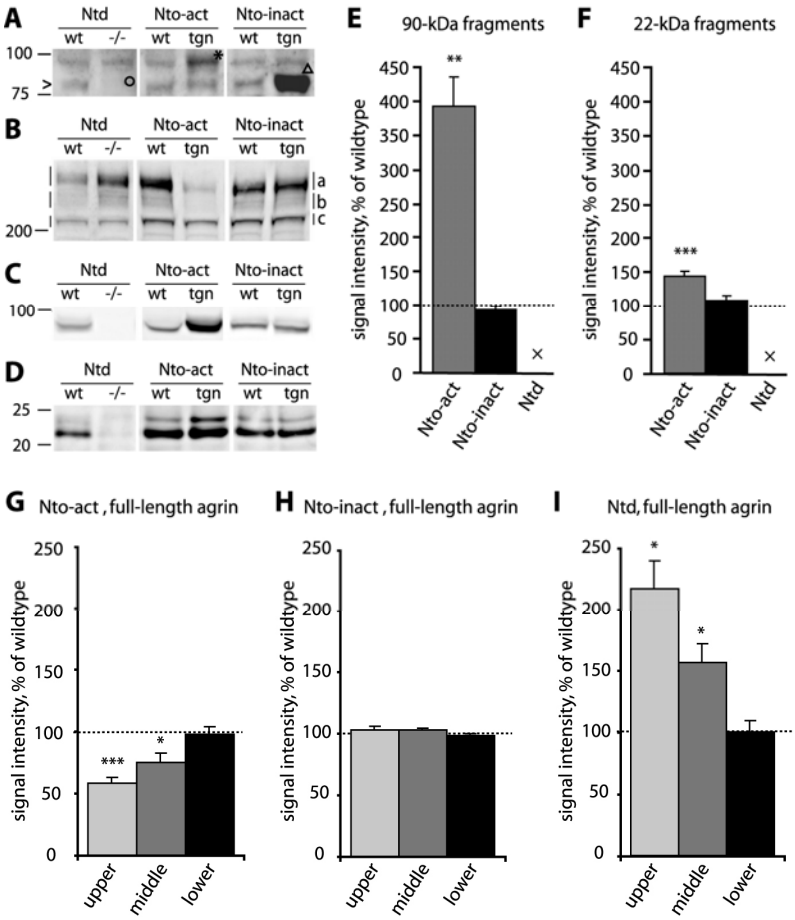

Figure 21. Neurotrypsin exclusively cleaves glycanated agrin variants in the mouse brain, generating the 90-kDa and 22-kDa fragments ***A-D,*** Representative images of Western blots from P9 mice confirm that agrin is a substrate of neurotrypsin. Brain homogenates from neurotrypsin-deficient (Ntd), human neurotrypsin-overexpressing (Nto-act) mice or from mice that overexpress a catalytically inactive variant of mouse neurotrypsin (Nto-inact) were compared to brain homogenates from their wildtype (wt) littermates. Molecular mass references are indicated in kDa. ***A,*** Neurotrypsin detected in samples of Ntd, Nto-act, and Nto-inact brain homogenates. Endogenous neurotrypsin was detected as a single band at 85 kDa (arrowhead) in samples of all genotypes except Ntd (circle). In contrast to mouse neurotrypsin, human neurotrypsin contains an additional SRCR domain, resulting in an approximate Mr of 95 kDa. Transgenic human neurotrypsin was detected in samples of Nto-act mice as a double band at around 95 kDa (asterisk) with a much stronger signal for the upper band. This human neurotrypsin-specific double band was situated on top of a weak unspecific band visible in samples of all genotypes, including Ntd. Transgenic inactive mouse neurotrypsin was detected at 85 kDa, superimposed over endogenous neurotrypsin (triangle). ***B-D,*** Cleavage of the variants of full-length agrin (upper (a), middle (b) and lower (c) full-length agrin variants, C-22 antibody) as well as the appearance of the 90-kDa and the 22-kDa fragments, detected in brain homogenates of Ntd, Nto-act, and Nto-inact mice. ***E, F,*** Quantitative densitometric Western blot analyses of the appearance of the 90-kDa and the 22-kDa fragments, respectively, revealed that these fragments were only generated by active neurotrypsin. ***G-I,*** Quantitative analyses of full-length agrin signals, detected with the C-22 antibody, confirmed that neurotrypsin exclusively cleaved the upper and middle variants of agrin, with preference for the most heavily glycanated upper variants. Signal intensities of the upper, middle and lower agrin variants in samples from Nto-act ***(G)***, Nto-inact ***(H)*** and Ntd ***(I)*** mice. Signal intensities of Ntd, Nto-act or Nto-inact samples, normalised to signals of the corresponding wildtype littermate controls (wildtype values set to 100 %), are shown. Data represent mean values ± S.E.M. For each genotype, two Western blots with samples of at least three different animals per genotype were analysed ($n \geq 6$). × = no signal detected; * = $P<0.05$; ** = $P<0.01$; *** = $P<0.001$.

I also measured the signal intensities of the upper, middle and lower groups of full-length agrin in samples from Nto-act, Nto-inact and Ntd mice using the anti-C-90 antibodies. Again, results obtained by quantitative densitometry of Western blots were normalised to the corresponding signals of wild-type littermates (Fig. 22). A representative Western blot of full-

length agrin, detected with the anti-C-90-1 antibody, is depicted in Figure 22A. The data obtained with the anti-C-90-agrin antibodies mainly supported the results obtained with the anti-C-22 antibody (see above) and confirmed that the protein levels for upper and middle full-length agrin were significantly decreased in the brain of Nto-act mice (68.3 ± 2.2 % and 71.2 ± 5.8 % of wild type, respectively; Fig. 22B, anti-C-90-1 antibody) and unaltered in Nto-inact mouse brains (104.1 ± 4.1 % and 105.2 ± 4.2 % of wild type, respectively; Fig. 22C, anti-C-90-1 antibody). Furthermore, no alterations of the lower group of full-length agrin were measured in the analysed tissues of Nto-act (99.7 ± 1.6 %, Fig. 22B, anti-C-90-1 antibody) and Nto-inact (104.9 ± 3.2 %, Fig. 22C, anti-C-90-1 antibody) animals. However, slight differences were observed with brain homogenates of Ntd mice when results obtained with the anti-C-90 antibodies (Fig. 22D, E) were compared to the data presented with the anti-C-22 antibody (Fig. 21I). When detected with the respective C-90 antibodies, bottom full-length agrin levels were reduced in brain homogenates of Ntd mice to 83.0 ± 2.8 % (C-90-1 antibody, Fig. 22D) or 65.5 ± 12.9 % (C-90-2 antibody, Fig. 22E) of wild-type levels. This was in strong contrast to experiments performed with the anti-C-22 antibody (Fig. 21I), where no differences of bottom full-length agrin levels were detected between samples of Ntd and wild-type animals. Also, the increase of upper and middle full-length agrin signals in brain homogenates of Ntd mice, detected with the anti-C-90 antibodies, was less prominent when compared to results obtained with the C-22 antibody. The levels for the upper variants were slightly increased in samples of Ntd mice (anti-C-90-1 antibody, 110.4 ± 1.0 %; anti-C-90-2 antibody, 129.2 ± 9.4 % of wild type, respectively; Fig. 22D, E) and changes concerning the middle variants were even less pronounced (anti-C-90-1 antibody, 102.7 ± 2.2 %; anti-C-90-2 antibody, 111.7 ± 1.7 % of wild type, respectively; Fig. 22D, E). Differences in signal detection between the anti-C-22 and the anti-C-90 antibodies were apparent in Ntd samples only. Interestingly, utilisation of different anti-C-90-agrin antibody concentrations resulted in the measurement of varying full-length agrin signal intensities (data not shown). It is currently inexplicable why these variations were only measured with samples of Ntd animals. These findings suggest that difficulties with anti-C-90 antibody detection in Ntd samples led to the determination of different results. However, if levels for bottom full-length agrin signals in samples of Ntd mice, detected with the anti-C-90 antibodies, are adjusted to wild-type levels, the corresponding increase of upper and middle full-length agrin signals would closely resemble the anti-C-22 antibody data. Thus, the data obtained with the anti-C-90 antibodies mainly supported the results determined with the anti-C-22 antibody.

Taken together, these results demonstrated that only the glycanated variants of full-length agrin are cleaved by neurotrypsin. Furthermore, I registered a tendency for preferential cleavage of the variants of the upper group, as their increase in Ntd and decrease in Nto-act mice was stronger compared to the variants of the middle group. However, the differences were not statistically significant.

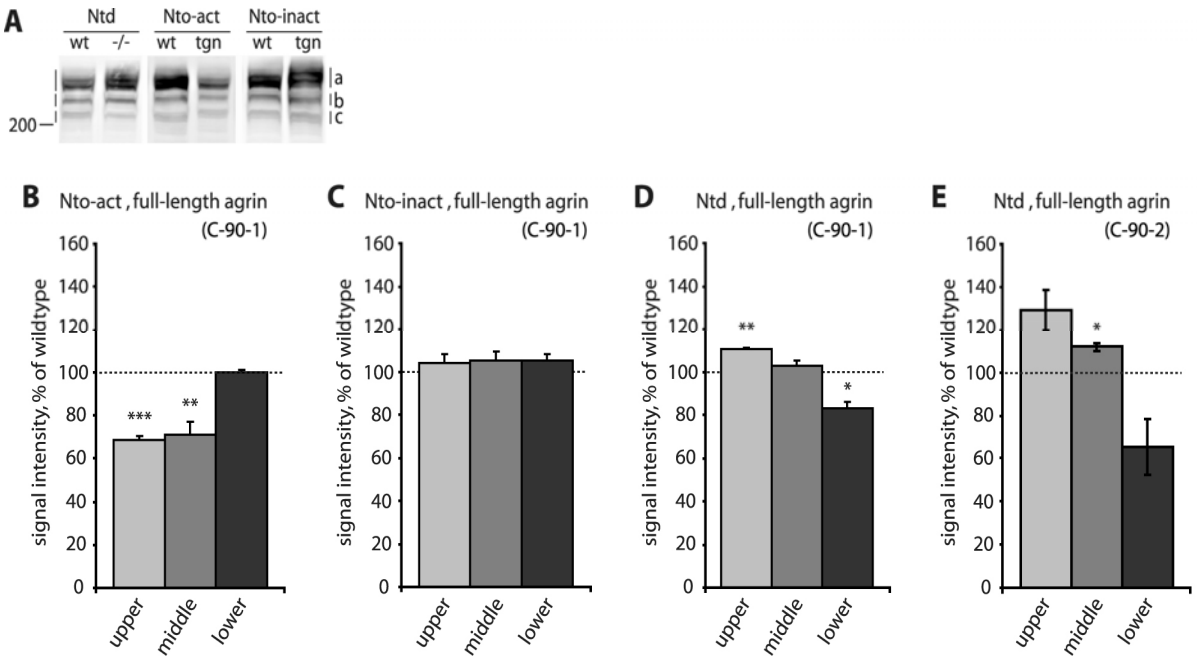

Figure 22. Neurotrypsin exclusively cleaves glycanated agrin variants in the mouse brain, generating the 90-kDa and 22-kDa fragments. ***A,*** Representative image of a Western blot from P9 mice, developed with the antibody directed against the C-90 agrin fragment, detecting full-length agrin (upper (a), middle (b) and lower (c) full-length agrin variants). Brain homogenates from neurotrypsin-deficient (Ntd), human neurotrypsin-over-expressing (Nto-act) mice or from mice that overexpress a catalytically inactive variant of mouse neurotrypsin (Nto-inact) were compared to brain homogenates from their wildtype (wt) littermates. Molecular mass references are indicated in kDa. ***B-E,*** Also the quantitative analysis of full-length agrin signals, detected with the anti-C-90-agrin antibodies (C-90-1; C-90-2), confirms that neurotrypsin exclusively cleaves the glycanated variants of agrin (compare to Fig. 21). However, slight differences between C-90 and C-22 antibodies were detected with Ntd samples (see main text). Signal intensities of the upper, middle and lower agrin variants in samples from Nto-act (***B,*** C-90-1), Nto-inact (***C,*** C-90-1) and Ntd (***D,*** C-90-1; ***E,*** C-90-2 antibody) mice are shown, normalised to signals of the corresponding wildtype littermate controls (wildtype values set to 100 %). Data represent mean values ± S.E.M. For each genotype, two Western blots with samples of at least three different animals per genotype were analysed ($n \geq 6$). × = no signal detected; * = $P<0.05$; ** = $P<0.01$; *** = $P<0.001$.

3.1.4 The most heavily glycanated variants of agrin are enriched in synaptosomes.

Neurotrypsin localises to presynaptic terminals *in vivo* (Molinari et al., 2002; Stephan et al., 2008) and results obtained with cultured hippocampal neurons indicated its activity-dependent release from synaptic terminals (Frischknecht et al., 2008). Experiments with fluorescently tagged neurotrypsin indicated that neurotrypsin lingered in the synaptic extracellular space after activity-dependent externalisation from presynaptic intracellular stores. Therefore, we speculated about a local proteolytic role of neurotrypsin in the synaptic or perisynaptic region. To test this hypothesis, I prepared synaptosomes from brains of wild-type mice (P12 to P15) and their content of neurotrypsin, agrin, and neurotrypsin-dependent agrin fragments was visualised by SDS-PAGE and Western blotting (Fig. 23A, C). The quality of the synaptosomal preparations was evaluated by electron microscopy and Western blotting. The morphological analysis confirmed the integrity of the synaptosomal fraction that was strongly enriched in synaptic structures, mainly consistent of resealed presynaptic

membranes associated with post- and perisynaptic structures (Fig. 23B). Western blotting of the initial brain homogenate (S1), the soluble fraction (S2), and the synaptosomal fraction (SS, Fig. 23A), using an antibody against the postsynaptic density protein PSD-95 as a synaptic marker, also demonstrated the synaptic enrichment of these synaptosomal preparations (Fig. 23C, 24A, 25A). Endogenous neurotrypsin was found in the synaptosomal as well as in the other fractions of the preparation (Fig. 23C, 24A, 25A). This observation is in accordance with our immunohistological localisation studies of neurotrypsin, as well as with our live imaging studies of intracellular trafficking of neurotrypsin. Both studies indicated that, besides its synaptic localisation, a fraction of neurotrypsin is localised to intracellular compartments ranging from the rough endoplasmatic reticulum through the Golgi apparatus to

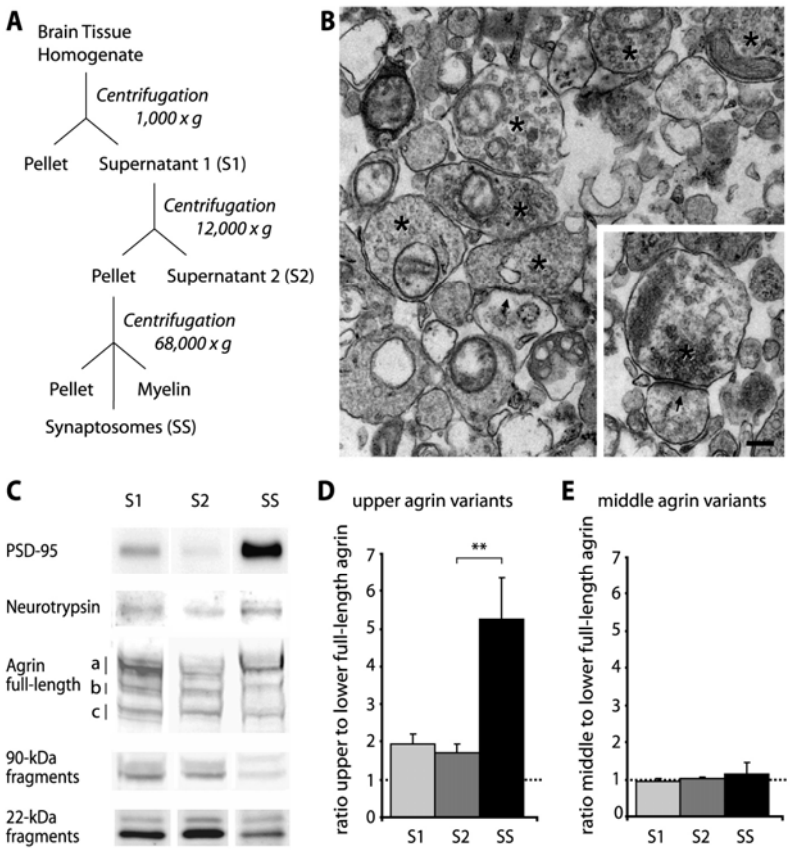

Figure 23. The upper variants are the predominant isoforms of agrin in synaptosomes. ***A,*** Schematic representation of the fractionation protocol used to prepare synaptosomes. ***B,*** Electron micrographs of a representative synaptosomal sample confirmed the integrity of the preparations. Presynaptic structures were prominent (asterisk) and in many cases attached postsynaptic structures were found (arrow). Scale bars: 0.2 µm. ***C,*** Representative Western blots of a synaptosomal preparation from brains of 12- to15-days-old wildtype mice. Post-synaptic-density protein 95 (PSD-95) was strongly enriched in the synaptosomal fraction (SS) and served as a control for the quality of the preparation. Endogenous neurotrypsin was found in the synaptosomal as well as in the other fractions of the preparation (soluble fraction 1 of the brain homogenate (S1), soluble fraction 2 (S2)). Mainly the upper agrin variants were detected in synaptosomes, whereas all three groups of agrin variants were detected with similar intensities in the other fractions of the preparation (upper (a), middle (b) and lower (c) variants). ***D, E,*** Quantitative densitometric Western blot analyses of synaptosomal preparations confirmed upper variants as the predominant isoforms of agrin in synaptosomes. Based on normalisation to lower full-length agrin, only the upper ***(D)*** but not the middle variants ***(E)*** were found enriched in the synaptosomal fraction of wildtype mice. Data represent mean values ± S.E.M (n = 5). ** = P<0.01.

axonal transport vesicles. However, the synaptosomal preparation protocol utilises homogenisation and therefore tissue disruption to yield a fraction enriched in synaptosomes. The intermediate fractions of the preparation therefore partially contain synaptic material. Hence, neurotrypsin detected in the soluble fraction (S2) represents a heterogenous pool of

non-synaptic as well as synaptic origin. Likewise, all three groups of full-length agrin were detected in all fractions (Fig. 23C). However, their relative amounts varied between the distinct fractions. As the distribution of all three groups of full-length agrin appeared to be different in the distinct fractions, I quantified the full-length variants of agrin in each fraction by densitometry of the Western blots and normalised the upper and middle group of variants to the lower group. These analyses revealed that the upper group was the predominant form of full-length agrin in all analysed fractions. I measured in homogenate (S1) and in the soluble fraction (S2) approximately two times more upper than lower full-length agrin (ratios to lower group of 1.95 ± 0.25 and 1.70 ± 0.25 (mean ± S.E.M.), respectively; Fig. 23D). In synaptosomes, the upper variant was more than five-fold enriched (ratio to lower group of 5.25 ± 1.11; Fig. 23D). In contrast, the relative amounts of the middle group were nearly identical with those of the lower group of variants in all fractions (Fig. 23E, ratio for S1 = 0.96 ± 0.05, for S2 = 1.01 ± 0.05, for SS = 1.16 ± 0.27). These results indicated that the upper group of agrin variants is the predominant agrin variant in synaptosomes. In addition, both neurotrypsin-dependent cleavage fragments of agrin appeared in all analysed fractions, including synaptosomes (Fig. 23C).

3.1.5 Neurotrypsin-mediated cleavage of agrin is localised at synapses.

The synaptic localisation of neurotrypsin (Molinari et al., 2002; Stephan et al., 2008), its activity-dependent externalisation from presynaptic terminals (Frischknecht et al., 2008), and the appearance of the neurotrypsin-dependent agrin fragments in synaptosomes (Fig. 23) suggested a local proteolytic activity of neurotrypsin at synapses. To test this hypothesis, I compared the extent of neurotrypsin-dependent cleavage of agrin in synaptosomes and other subcellular brain fractions of neurotrypsin-overexpressing mice (Nto-act) and their wild-type littermates (P12 to P15; Fig. 24A). Evaluation by electron microscopy revealed no morphological differences between synaptosomes from wild-type littermates and Nto-act mice (data not shown). In addition, Western blotting confirmed the overexpression of human neurotrypsin in Nto-act mouse brains with a distribution similar to endogenous neurotrypsin (Fig. 24A).

The comparison of full-length agrin signals in synaptosomes and the other subcellular fractions from wild-type and Nto-act mice revealed both the predominant cleavage of agrin in the synaptosomal fraction and the preferred cleavage of the upper group of full-length agrin (Fig. 24A, arrow). The synaptosomal upper group of full-length agrin was identified as the predominant target for neurotrypsin at synapses, because its levels were reduced to 40.1 ± 4.7 % in samples of Nto-act mice (Fig. 24B), while its reduction was only to 64.5 ± 3.3 % in the soluble fraction and to 62.2 ± 4.7 % in the homogenate of neurotrypsin-overexpressing mice. Neurotrypsin-dependent cleavage of full-length agrin was not as strong for the middle group as found for the upper group of bands, but the tendency was conserved (Fig. 24C). Signals for the middle variants of agrin signals were reduced to approximately 80 % of wild-type levels (79.3 ± 5.8 % and 79.8 ± 6.1 %) in the homogenate and soluble fraction, respectively, and to

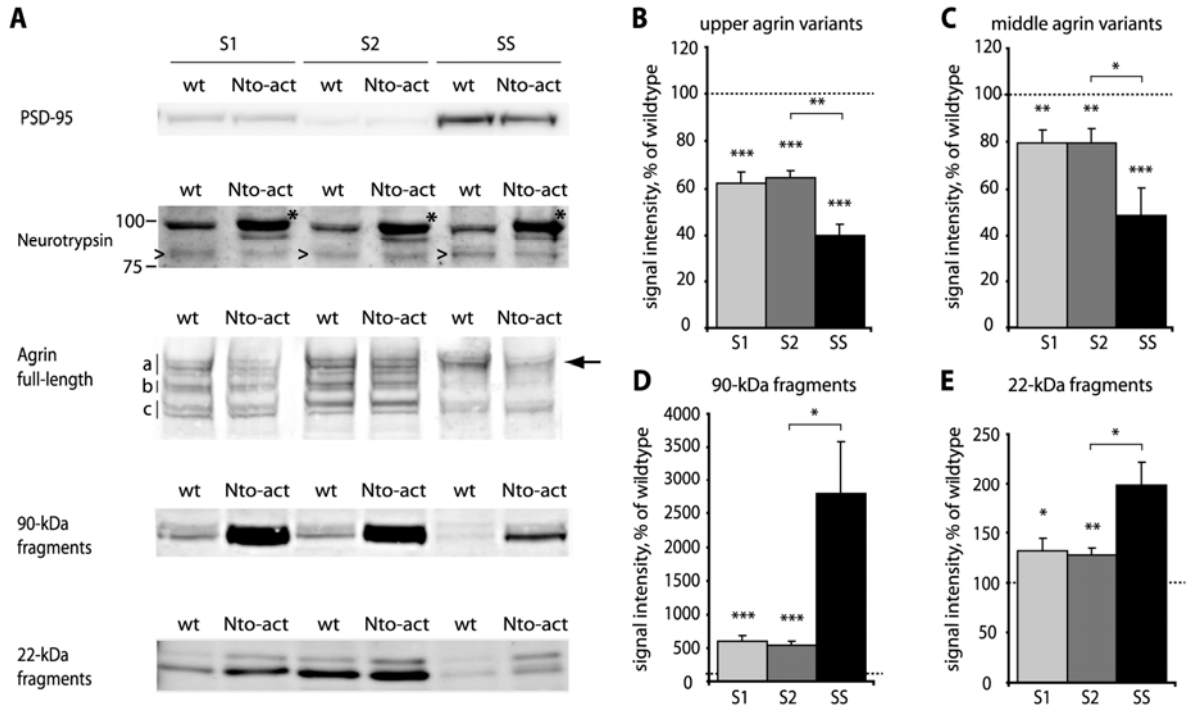

Figure 24. Neurotrypsin preferentially cleaves synaptic agrin. ***A,*** Western blot analysis of a representative synaptosomal preparation from brains of 12- to 15-days-old mice overexpressing active human neurotrypsin (Nto-act) compared to their wildtype (wt) littermate samples. Postsynaptic-density protein 95 (PSD-95) was strongly enriched in the synaptosomal fraction (SS) and served as a control for the quality of the preparation. Endogenous (murine) neurotrypsin (arrowhead) as well as overexpressed human neurotrypsin (asterisk) were found in the synaptosomal (SS) fraction, but as expected they were also detected in the other fractions of the preparation (soluble fraction 1 of the brain homogenate (S1), soluble fraction 2 (S2)). Human neurotrypsin was detected as a double band of approximately 100 kDa on top of an unspecific band that was also visible in the wildtype samples. The overexpression of neurotrypsin led to a major decline of upper full-length agrin, especially in synaptosomes (arrow; upper (a), middle (b) and lower (c) full-length agrin variants) and a corresponding increase of the 90-kDa and the 22-kDa fragments in all fractions. Molecular mass references are indicated in kDa. ***B-E,*** Quantitative Western blot analyses of synaptosomal preparations from postnatal day 12 to 15 Nto-act mouse brains compared to their wildtype littermates. ***B, C,*** Upper agrin variants ***(B)*** as well as middle agrin variants ***(C)*** were more efficiently cleaved in all analysed fractions of transgenic animals. For both the upper and middle agrin variants cleavage was strongest in the synaptosomal fraction. ***D, E,*** The levels of both the 90-kDa ***(D)*** and the 22-kDa ***(E)*** fragment were increased in all analysed fractions compared to wildtype levels. This increase was strongest in the synaptosomal fraction. Signal intensities of samples from Nto-act mice were normalised to corresponding signals of the wt littermate control samples (wt values set to 100 %). Data represent mean values ± S.E.M (n = 5). * = P<0.05; ** = P<0.01; *** = P<0.001.

approximately 50 % (48.2 ± 11.9 %) in the synaptosomal fraction. These results were supported by synaptosomal analyses of neurotrypsin-deficient (Ntd) mice and their wild-type littermates (P13 to P16; Fig. 25). Upper and middle full-length agrin signals were increased in all analysed fractions obtained from Ntd mice when compared to wild-type littermate controls (Fig. 25A-C, anti-C-22 antibody; Fig. 25A, D, E, anti-C-90 antibody). A pronounced increase of full-length agrin levels was also detected in the synaptosomal fraction, when analysed with both the anti-C-22 and the anti-C-90 antibodies (Fig. 25A, arrows). As a tendency, upper and middle full-length agrin levels increased strongest in synaptosomal samples from Ntd mice

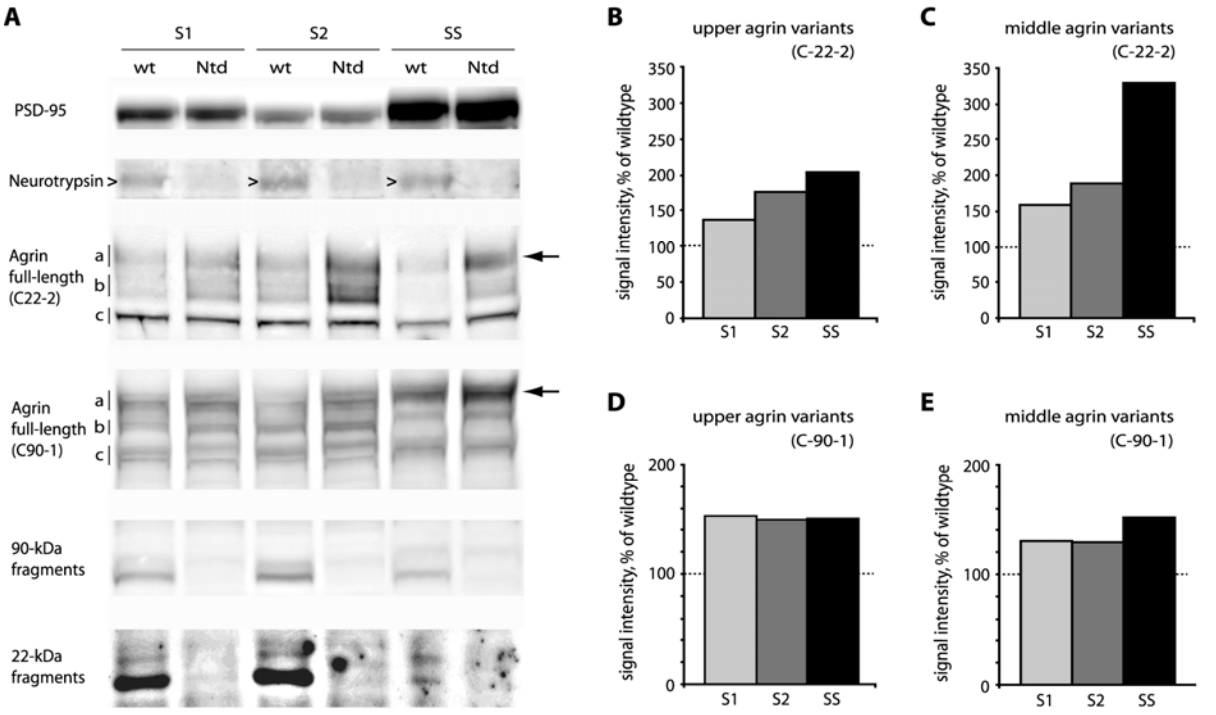

Figure 25. Neurotrypsin preferentially cleaves synaptic agrin. ***A,*** Western blot analysis of a representative synaptosomal preparation from brains of 13- to 16-days-old neurotrypsin-deficient mice (Ntd) compared to their wildtype (wt) littermate samples. Postsynaptic-density protein 95 (PSD-95) was strongly enriched in the synaptosomal fraction (SS) and served as a control for the quality of the preparation. Endogenous neurotrypsin (arrowhead) was found in the synaptosomal (SS) fraction as well as in the other fractions of the preparation (soluble fraction 1 of brain homogenate (S1), soluble fraction 2 (S2)) of wildtype animals only. The signals for upper full-length agrin were increased in the absence of neurotrypsin, especially in synaptosomes (arrow; upper (a), middle (b) and lower (c) full-length agrin variants). Molecular mass references are indicated in kDa. ***B-E,*** Quantitative Western blot analyses of synaptosomal preparations from postnatal day 13 to 16 Ntd mouse brains compared to their wildtype littermates. Signals for upper agrin variants ***(B,*** C-22-2 antibody; ***D,*** C-90-1 antibody) as well as for middle agrin variants ***(C,*** C-22-2 antibody; ***E,*** C-90-1 antibody) were stronger in all analysed fractions of Ntd animals, compared to wildtype levels. These findings indicate, in accordance to the data presented in Fig. 24, that neurotrypsin-dependent cleavage of agrin also takes place at the synapse. The finding of preferred cleavage of synaptic agrin was supported by results obtained with the C-22 antibody. Here, the increase of signals for both the upper and middle agrin variants was strongest in the synaptosomal fraction of Ntd animals. When detection of full-length agrin was performed with the C-90 antibody, this tendency was only observed for middle agrin variants. However, due to the low number of experiments performed, the data presented states only tendencies. Signal intensities of samples from Ntd mice were normalised to corresponding signals of the wt littermate control samples (wt values set to 100 %). Data represent mean values of one (C-90-1 antibody) or two independent experiments (C-22-2 antibody).

(Fig. 25B-E). However, due to the little number of possible experiments with tissue from Ntd animals, statistical analyses could not be performed and it was therefore impossible to verify these tendencies. Signal intensities of the lower group of agrin variants were not altered between wild-type and transgenic samples or between wild-type and Ntd samples (data not shown). In accordance with the results from the analysis in P9 mouse brains (section 3.1.3; Fig. 21, 22), lower full-length agrin is not a substrate of neurotrypsin in any of the analysed fractions.

In parallel with the predominant cleavage of agrin in synaptosomes, I found that the increase of agrin fragments due to neurotrypsin-overexpression was strongest in the synaptosomal fraction for both fragments. The increase of the 90-kDa agrin fragment due to neurotrypsin overexpression was over 25-fold (2787.8 ± 791.4 % (mean ± S.E.M.) of wild type; Fig. 24D) in the synaptosomal fraction, but only 5 to 6-fold in brain homogenate and the soluble fraction (594.5 ±89.2 % and 543.9 ±53.0 %, respectively; Fig. 24D). A similar but less pronounced synaptosomal enrichment was found for the 22-kDa fragment. The 22-kDa fragment was enriched two-fold (197.4 ± 25.1 %; Fig. 24E) in the synaptosomal fraction of Nto-act mice and appeared in the homogenate and the soluble fraction at about 130 percent of wild-type levels (132.6 ± 12.0 % and 127.6 ± 6.9 %, respectively; Fig. 24E).

Taken together, I found that the upper group represents the main form of full-length agrin in synaptosomes and that this group of variants was predominantly cleaved by neurotrypsin. A similar enrichment in synaptosomes was not found for the middle group of agrin variants, but their cleavage was also localised predominantly in synaptosomes. These data therefore indicated that neurotrypsin-dependent cleavage of agrin is concentrated at synapses.

3.2 *In vitro* analysis of the neurotrypsin-agrin interaction in dissociated hippocampal neuron cultures and in cos7 cells.

3.2.1 Neurotrypsin and agrin are endogenously expressed by cultured dissociated hippocampal neurons as well as by cultured astrocytes.

Neurotrypsin cleaves synaptic agrin *in vivo* (section 3.1) but the functional implications of this interaction are largely unknown. To reduce system complexity, the interaction of neurotrypsin and agrin was further analysed *in vitro*. The well characterised dissociated hippocampal neuron cultures (Banker, 1980; Goslin, 1998; Kaech and Banker, 2006) has proven a useful and suitable *in vitro* system for studying neuronal characteristics of neurotrypsin. Initial live-cell imaging experiments with these cultures revealed synaptic targeting of ectopically expressed neurotrypsin and its activity-dependent release from presynaptic terminals (Frischknecht et al., 2008). Further analyses with cultured hippocampal neurons were supposed to be performed to elucidate the neuronal effects of the neurotrypsin-dependent cleavage of agrin to support the *in vivo* findings.

To determine the endogenous expression levels for neurotrypsin as well as agrin transcripts, reverse transcriptase polymerase chain reaction (RT-PCR) was performed from dissociated hippocampal neuron cultures grown in high density as well as from cultured cortical glial cells. To confirm the integrity of the isolated mRNA in each preparation, primers specific for glyceraldehyde-3-phosphate-dehydrogenase (GAPDH) were used as a positive control. Neurotrypsin-transcripts were detected in 6 days and 13 days old dissociated hippocampal neuron cultures (DIV6 and DIV13, respectively; Fig. 26A). However, minor

glial cell contaminations may also be present in these cultures and therefore I performed RT-PCR also from cultured cortical glial cells. Neurotrypsin transcript expression was indeed detected in cultured glia, even if *in vivo* expression of neurotrypsin is believed to be restricted to neurons (Wolfer et al., 2001). Hence, this RT-PCR result for neurotrypsin transcript expression in cultured glia indicates that the general protein expression patterns may diverge *in vitro* and *in vivo*. Similar, however, less surprising results were obtained when the endogenous expression of agrin variants was assessed. Transcripts of transmembrane agrin (SN, Fig. 26B_1) and secreted agrin (LN, Fig. 26B_2) variants were detected in dissociated hippocampal neuron cultures at both analysed time points (DIV6 and DIV13, respectively; Fig. 8B) as well as in cultured cortical glia. These results suggested that the *in vitro* expression of both agrin variants is similar to their reported *in vivo* expression pattern (Kroger and Schroder, 2002). Thus, both neurotrypsin as well as agrin transcript expression was detected in hippocampal neuron cultures. However, these data rendered it impossible to definitely determine if neurotrypsin and agrin variants are expressed by cultured neurons or if their detection in neuronal cultures was due to minor glial contaminations.

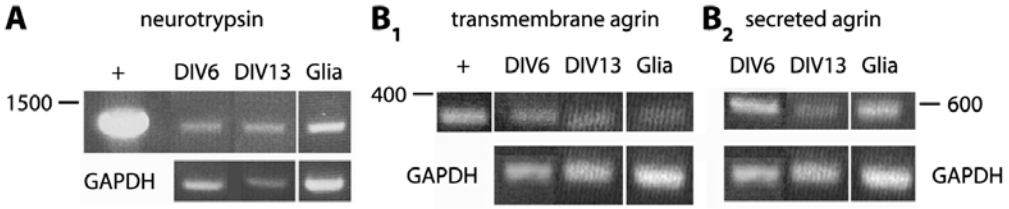

Figure 26. Neurotrypsin and agrin transcripts are expressed in hippocampal neuron cultures as well as cortical glial cell cultures. Reverse transcriptase polymerase chain reaction (RT-PCR) performed from total RNA isolated from high density dissociated mouse hippocampal neuronal cultures or from mouse cortical glial cultures. ***A,*** Neurotrypsin-specific mRNA was amplified using specific primers hybridising in transcript regions encoded by different exons. As a positive control (+), a plasmid containing the cDNA for mouse neurotrypsin was used as template DNA. Expression of neurotrypsin transcripts was confirmed in neurons that were grown for 6 or 13 days *in vitro* (DIV6 and DIV13, respectively) as well as in cultured glial cells. ***B,*** Transmembrane agrin or secreted agrin transcripts were amplified by using a common 3' primer that hybridises in the first, for all agrin-isoforms common, exon and a specific 5' primer that hybridises in the specific 5' regions of the respective transcript-variants. Expression of both variants was confirmed in DIV6 and DIV13 neurons as well as in cultured glial cells. In parallel to the neurotrypsin and agrin-specific PCR reactions, the integrity of the isolated mRNA was analysed with GAPDH-primers (GAPDH).

The endogenous expression of neurotrypsin and agrin in cultured hippocampal neurons was further analysed by immunocytochemistry using neurotrypsin and agrin specific antibodies. Hippocampal neurons were grown on poly-L-lysine coated glass coverslips and co-cultured above a separated layer of cortical glia-feeder cells used to support neuronal growth and survival. This co-culture system enabled the growth of neurons in low densities (Goslin, 1998) to allow the detailed analyses of expressed proteins, in particular their subcellular localisations in single cells. DIV8 (Fig. 27A-F) or DIV15 (Fig. 27G-L) dissociated hippocampal neuron cultures were fixed and agrin was detected with the anti-C-90-agrin

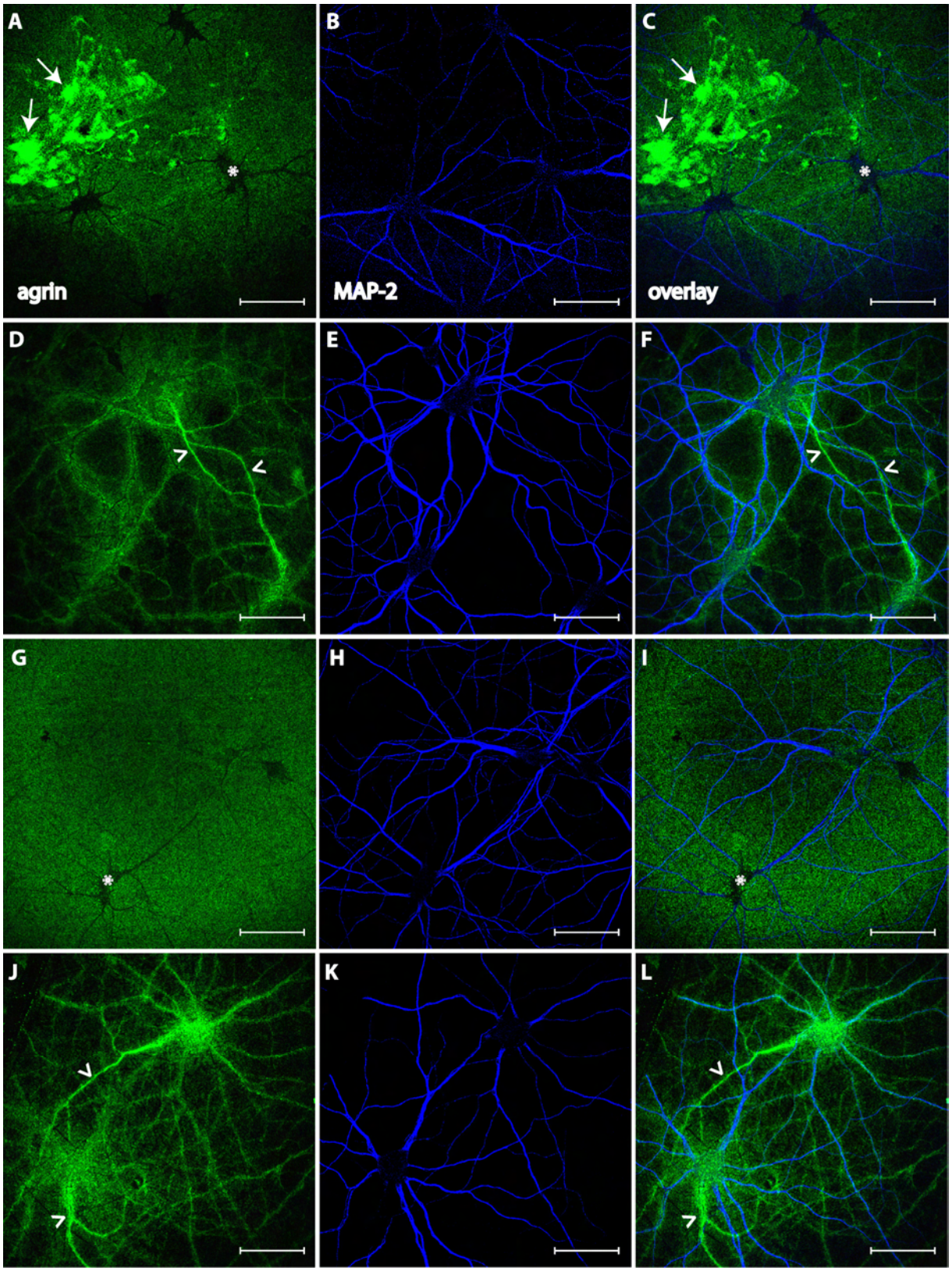

Figure 27. Agrin protein is expressed by neurons as well as glial cells. Confocal microscopy analyses of dissociated hippocampal neurons cultured for either 8 or 15 days *in vitro* (DIV8, ***A-F***; DIV15, ***G-L***, respectively). Neuronal cultures were generated from wildtype NMRI animals and cultured on glia-feeder cells generated either from agrin-deficient animals (***D-F***; ***J-L***) or from corresponding wildtype littermates (***A-C***; ***G-I***). ***A, D, G, J,*** Agrin protein ex-pression was visualised with the affinity purified anti-C-90 agrin antibody (C-90-1). ***B, E, H, K,*** Microtubuli associated protein 2 (MAP-2) was used as a marker to visualise dendritic processes of

cultured neurons. ***C, F, I, L,*** Agrin and MAP-2 specific signals were merged to better identify subcellular localisations of agrin (overlay). Independent of the age of the cultures, agrin signals were dense and evenly distributed over coverslips cultured above wildtype glia-feeder cells (DIV8, ***A-C***; DIV15, ***G-I***). Agrin signals were especially strong within and around glial cells (***A, C*** arrows), occasionally growing in between cultured neurons on the coverslips. In contrast, neuronal cell bodies were devoid of agrin signals (asterisks). However, agrin signals detected on coverslips cultured above agrin-deficient glia-feeder cells (DIV8, ***D-F***; DIV15, ***J-L***) were mainly localised to neuronal cell-bodies and neurites growing on the coverslips. Especially pronounced signals were observed along axons (arrowheads), identified as neurites devoid of MAP-2 signals. These findings strongly suggested that glia-feeder cells secrete high amounts of agrin variants that are deposited on the neuron-containing coverslips localised above the glia-feeder cell layer. By culturing neurons on agrin-deficient glia-feeder cells, thus abolishing the main source for glia-derived agrin variants, the neuronal expression pattern of agrin can be monitored. These experiments indicated that neuronal agrin is localised to all neurites but especially enriched in axons. Scale bars: 50 µm.

←

antibody using confocal microscopy. To differentiate between axonal and dendritic processes and therefore to determine the subcellular localisation of agrin-specific signals, cells were co-stained with an antibody against the dendritic marker microtubule-associated protein 2 (MAP-2). When neurons were co-cultured with wild-type glia-feeder cells, agrin-specific signals were almost uniformly distributed over the whole coverslip at both analysed time-points (DIV8, Fig. 27A-C); DIV15, Fig. 27G-I). Signals were merely absent within cell-bodies and neurites of neurons. In glial cells, occasionally growing in between the cultured neurons, however, strong agrin-specific signals were detected (Fig. 27A, C, arrows). Interestingly, coated coverslips incubated without neurons on glia-feeder cells also showed uniformly distributed agrin-specific signals (data not shown). Glial cells express a variety of agrin variants as confirmed by RT-PCR (see above). Therefore, glia-feeder cells may secrete agrin variants that are deposited on the coverslips accommodating the neurons. To solely detect neuronal agrin and, therefore, to exclude the detection of glia-feeder cell-derived secreted agrin variants, neurons were cultured on glia-feeder cells obtained from agrin-deficient mice (DIV8, Fig. 27D-F; DIV15, Fig. 27J-L). Indeed, cultures devoid of glia-feeder derived agrin variants showed a redistribution of agrin signals. Here, neuron-derived agrin was detected within and around neuronal cell-bodies and neurites of both DIV8 and DIV15 neurons. Co-staining with MAP-2 revealed that agrin signals were mainly detected in a punctuate pattern within and around dendrites and very strong concentrated within axons (arrowheads). These results confirmed that agrin is expressed by neurons as well as by glial cells. Furthermore, neuron-derived agrin localised to dendrites and axons, in accordance with previously published data (Neuhuber and Daniels, 2003), whereas secreted variants of glia-feeder origin were broadly deposited on the coverslip.

In contrast, neurotrypsin protein was not detected in dissociated hippocampal neuron cultures with any of the neurotrypsin-specific polyclonal antibodies generated in our lab. Only unspecific signals were detected with these antibodies, judged by the appearance of identical signals obtained from experiments performed with corresponding preimmune sera (data not

shown). We were so far not able to produce a highly specific antibody against neurotrypsin and low level expression of endogenous neurotrypsin may have been missed with the currently available low affinity antibodies.

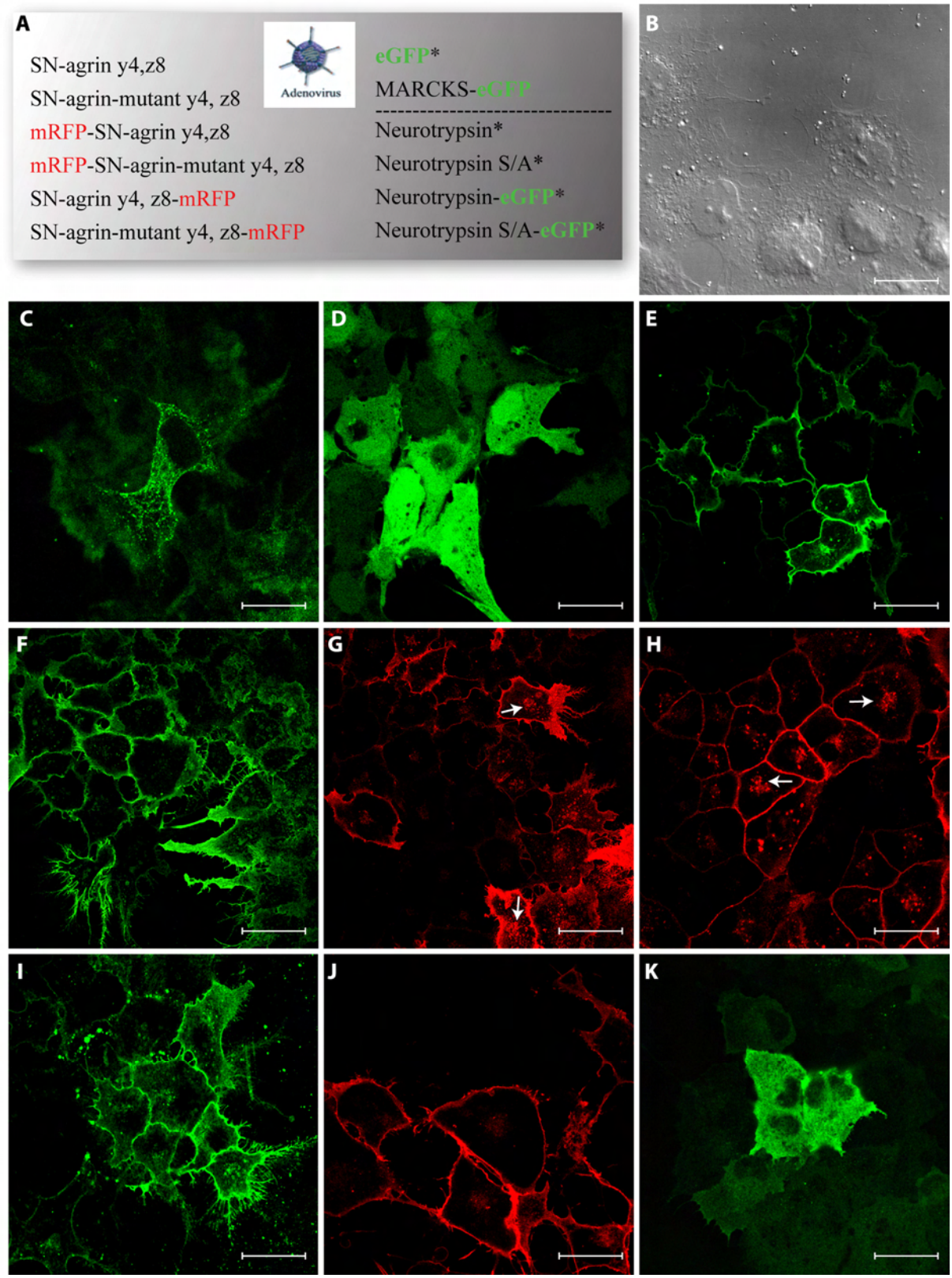

Figure 28. Efficient and successful adenovirus-mediated ectopic expression of agrin and eGFP variants in cos7 cells. Confocal microscopy analyses of cos7 cells infected with recombinant adenoviruses expressing the

respective constructs indicated in panel ***A***. ***B,*** Differential interference contrast image of a representative sample of cos7 cells growing on coverslips. Ectopically expressed proteins were identified either by antibody staining (agrin detection in ***F, I, K,*** anti-C-90 antibody) or by detection of signals emitted by the corresponding fluorescent protein of the respective fusion proteins (mRFP-signals, ***G, H, J***; eGFP-signals, ***C, D, E***). ***C,*** Neurotrypsin, C-terminally tagged with eGFP (neurotrypsin-eGFP), was mainly detected in a dotted pattern within the cell. These signals most likely resemble, as anticipated, mainly transport-vesicles filled with neurotrypsin-eGFP fusion proteins. ***D,*** Adenovirus-mediated expression of eGFP resulted in a uniformly distribution of eGFP in the cytoplasm and sometimes the nucleus of infected cells. ***E,*** Adenovirus-expressed myristoylated alanine-rich C-kinase substrate (MARCKS)-eGFP fusion proteins were successfully and efficiently targeted to cellular membranous compartments, including the plasma membrane. ***F,*** The expression pattern of wildtype transmembrane agrin-x12, y4, z8 (SN-agrin), with strong localisation mainly at the plasma membrane, confirms the successful and efficient adenovirus-mediated expression of SN-agrin. This was also confirmed for the SN-agrin fusion proteins, carrying mRFP either at agrin's C-terminus (SN-agrin-mRFP, ***G***) or at its N-terminus (mRFP-SN-agrin, ***H***). The same was true for the mutant versions of SN-agrin, not cleavable by neurotrypsin: SN-agrin-mutant (***I***), SN-agrin-mutant-mRFP (***J***) and mRFP-SN-agrin-mutant (not shown). All mRFP-agrin fusion proteins were prominently detected at the plasma membrane but also some intracellular signals (arrows) were detectable. However, both N-terminally mRFP-tagged agrin fusion protein variants were mistargeted to mainly intracellular sites of some but not all infected cells (as an example: mRFP-SN-agrin-mutant, ***K***). Scale bars: 25 μm (***B***); 30 μm (***J***); 40 μm (***C, D***); 47 μm (***E-I, K***).

←

3.2.2 Recombinant adenoviruses efficiently express functional transmembrane agrin variants in cos7 cells.

Neurotrypsin and agrin variants are endogenously expressed in dissociated hippocampal neuron cultures but due to presumably low level expression of neurotrypsin and the expression of a variety of agrin variants by glia as well as neurons, it was impossible to perform detailed analyses of the neurotrypsin-agrin interaction with the endogenously expressed proteins.

To enable the efficient expression and detection of neurotrypsin as well as defined agrin variants in cultured neurons, we chose to perform adenovirus-mediated ectopic expression of neurotrypsin and transmembrane agrin variants. Adenovirus-mediated neuronal expression of neurotrypsin variants, including neurotrypsin fused at its C-terminus to enhanced green fluorescent protein (eGFP), were already successfully established in our lab. Studies with ectopically expressed neurotrypsin fusion proteins indicated that neurotrypsin-(eGFP) variants are correctly targeted to axons and presynaptic terminals in dissociated hippocampal neuron cultures (Frischknecht et al., 2008). This was in accordance with the presynaptic localisation of endogenous neurotrypsin *in vivo* (Molinari et al., 2002; Stephan et al., 2008). In parallel to the generation of neurotrypsin expressing virus variants, a control adenovirus, expressing eGFP alone, was constructed in our lab. To determine the functional interaction of neurotrypsin and agrin, I generated recombinant adenoviruses, expressing variants of the transmembrane agrin-x12, y4, z8 isoform (SN-agrin). This isoform is strongly expressed in (hippocampal) neurons both *in vivo* and *in vitro* (O'Connor et al., 1995; Lesuisse

et al., 2000) and has been used in most of the analyses concerning agrin functions in CNS neurons (Hilgenberg et al., 1999; Bose et al., 2000; Gingras et al., 2002; Hilgenberg et al., 2002; Hoover et al., 2003). In addition, due to its expression at the plasma membrane, the transmembrane isoform of agrin may be easier to track when compared to secreted variants. Besides a wild-type agrin variant, I generated a SN-agrin expression construct that is not cleaved by neurotrypsin due to mutations of the respective amino acids in the P1 positions of the cleavage sites targeted by neurotrypsin (SN-agrin-mutant). In addition, expression constructs of SN-agrin and SN-agrin-mutant, either N-terminally or C-terminally tagged with monomeric red fluorescent protein (mRFP), were generated. Due to the physical properties of eGFP and mRFP, their fluorescent signals are easily separable using appropriate equipment, therefore allowing the simultaneous detection of co-expressed neurotrypsin-eGFP and mRFP-tagged SN-agrin variants even in live neurons. Concerning the analysis of neurotrypsin-dependent cleavage of agrin, the mRFP-agrin and agrin-mRFP constructs were believed to enable the tracking of agrin parts after neurotrypsin-dependent cleavage. SN-agrin was shown to generate filopodia-like processes on dendrites as well as axons of cultured neurons (Annies et al., 2006; McCroskery et al., 2006) and recent findings suggest that also the C-terminus of agrin is involved in structural changes of the dendritic surface (unpublished observations). In prospect of also analysing the impact of neurotrypsin activity on these functions of agrin, I generated another adenovirus, expressing a myristoylated alanine-rich C-kinase substrate (MARCKS)-eGFP fusion protein. This variant targets eGFP to all membranous compartments of the cell, including the plasma membrane (De Paola et al., 2003), and is therefore suitable to visualise morphological cell-surface alterations, including those mediated by agrin.

Initial expression analyses of constructed virus variants in infected cos7 cells confirmed the efficient and functional expression of almost all constructs. Adenovirus-mediated expression of neurotrypsin was detected in a punctuate pattern throughout the cytoplasm, expectedly representing mainly transport vesicles filled with the extracellular protease (Fig. 28C). The infection of cos7 cells with an adenovirus-eGFP construct led to the strong expression of eGFP within the cytoplasm and the nucleus (Fig. 28D). In contrast, cells infected with MARCKS-eGFP adenoviruses (Fig. 28E) revealed strong punctuated intracellular eGFP signals, presumably resembling a range of different intracellular membranous compartments, and strong continuous signals at the plasma membrane. Also the SN-agrin (Fig. 28F), SN-agrin-mutant (Fig. 28I), SN-agrin-mRFP (Fig. 28G) and SN-agrin-mutant-mRFP (Fig. 28J) variants were successfully expressed at the plasma membrane and detectable by either anti-C-90-agrin immunostaining or mRFP fluorescence of the respective fusion proteins. However, both N-terminally tagged SN-agrin or SN-agrin-mutant variants were only in some infected cells efficiently targeted to the plasma membrane (e.g., mRFP-SN-agrin in Fig. 28H). In contrast, many infected cells revealed strong intracellular expression of these constructs, in addition to its plasma membrane localisation. An example of cos7 cells expressing mistargeted mRFP-SN-agrin-mutant fusion proteins is shown in Figure 28K. Similar mistargeting was also observed with constructs alternatively carrying an

unrelated enhanced cyan fluorescent protein (eCFP) at the N-terminus of SN-agrin (data not shown). These results indicated that N-terminal fusion to SN-agrin in general may interfere with its proper targeting within the cell. However, it is unclear why mistargeting seemed to be cell-dependent as normal expression of these N-terminal fusion proteins was detectable in some infected cells. Though, even when correct and efficient targeting of agrin-mRFP and mRFP-agrin fusion constructs was observed by their predominant expression at the plasma-membrane, additional strong punctuate intracellular signals were detected in most of the infected cells (Fig. 28G, H, arrows). In contrast, only weak intracellular signals were detected in wild-type SN-agrin expressing cells. The additional intracellular signals appearing in cells expressing agrin-mRFP and mRFP-agrin variants were generally much stronger visualised by mRFP fluorescence, compared to anti-C-90-agrin antibody mediated fusion protein detection. Other immunofluorescence experiments performed in our lab indicated that the anti-C-90 antibody recognises intracellular agrin far weaker than its extracellular localised epitopes. Thus, it might be that the mRFP signal of the respective fusion proteins allows a far better detection of intracellular agrin than signals obtained by anti-agrin immunofluorescence, enabling a more sensitive detection of immature agrin variants in golgi- or transport-vesicle-like structures. However, the appearance of additional intracellular signals might alternatively indicate mistargeting of, e.g., incorrect folded and therefore potentially toxic fusion proteins. To exclude that the appearance of these additional intracellular signals were caused by mistargeting of mRFP-tagged agrin variants to lysosomes, a co-localisation study with a lysosomal marker (anti-lysosomal-associated membrane protein 1 (Lamp-1) antibody) was performed. Yet, only a minor fraction of SN-agrin-mRFP (Fig. 29A) or mRFP-SN-agrin (Fig. 29B) signals, detected by mRFP fluorescence, co-localised with Lamp-1 positive structures. Another explanation for the appearance of additional mRFP-positive intracellular structures may be the detection of endocytosed C-terminal agrin-mRFP parts released from the N-terminal moiety of agrin or N-terminal mRFP-SN-agrin parts released from the C-terminal part of agrin.

Agrin is efficiently cleaved by neurotrypsin (Reif et al., 2007) and Western blot analyses of infected cos7 cells were performed to further determine the functionality of the generated viruses. As a control, supernatant samples of transfected cos7 cells expressing SN-agrin alone or co-expressing SN-agrin and mouse neurotrypsin (mNT; Fig. 29C, D) were analysed. The anti-C-90-agrin antibody detected in the supernatant of agrin and neurotrypsin co-expressing cells the characteristic C-terminal agrin cleavage fragments, generated by neurotrypsin, with a molecular mass of around 130-kDa and 90-kDa (Fig. 29C). Only minor amounts of the 130-kDa fragment (arrowhead), resembling C-terminal agrin solely cleaved at the α-site, were detected. In contrast, the 90-kDa fragment appeared much stronger, confirming that neurotrypsin-dependent cleavage of agrin occurs predominantly at both α- and the β-cleavage sites (Reif et al., 2007). Interestingly, a band at around 130 kDa was visible also in single transfected cells expressing SN-agrin alone, indicating endogenous low level agrin cleavage (Fig. 29C, arrowhead). It is possible that cos7 cells endogenously express

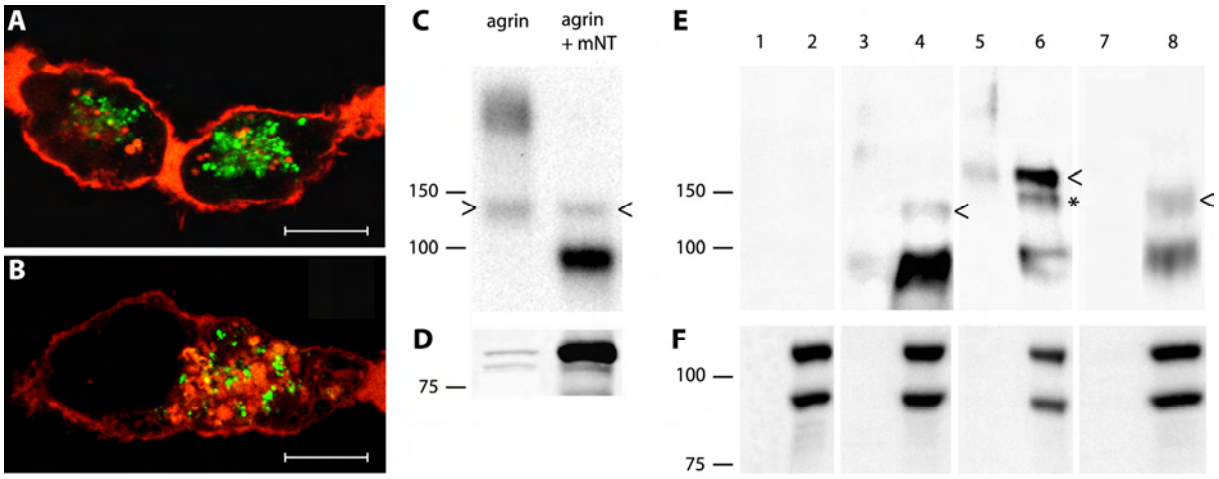

Figure 29. Adenovirus-agrin variants as well as adenovirus-neurotrypsin variants were functionally expressed in cos7 cells. ***A, B,*** Confocal microscopy analyses of cos7 cells infected with transmembrane agrin-x12, y4, z8 (SN-agrin) variants carrying mRFP either at agrin's C-terminus (SN-agrin-mRFP, ***A***) or its N-terminus (mRFP-SN-agrin, ***B***). mRFP-agrin fusion proteins were visualised by mRFP fluorescence. To determine correct targeting of the mRFP-agrin fusion proteins the cell, the intracellular localisation of fusion proteins was analysed. Mistargeting of ectopically expressed proteins to lysosomes may indicate toxic or at least aberrant protein properties. Therefore, lysosomes were co-visualised with an antibody against the lysosomal marker lysosomal-associated membrane protein 1 (Lamp-1). However, in addition to strong signals detected at the plasma membrane of cells, mRFP-positive intracellular signals (red) are not co-localising with LAMP-1 positive organells (green). This suggests the proper integrity and functional targeting of the mRFP-agrin fusion proteins within the cell. Scale bars: 10 µm (***A***); 7 µm (***B***) ***C, D,*** Western blot analysis of samples from cos7 cells transfected with SN-agrin alone or co-transfected with SN-agrin and mouse neurotrypsin (mNT). Molecular mass references are indicated in kDa. ***C,*** Agrin signals were detected with the anti-C-90 agrin antibody in supernatant samples. In contrast to cells expressing agrin alone (agrin), the co-expression of agrin and neurotrypsin (agrin+mNT) resulted in efficient processing of agrin by neurotrypsin, generating the C-90 and C-22 agrin fragments. The additional fragment detected at around 130 kDa (arrowhead) represents C-terminal agrin only cleaved at the α-site (also termed 110-kDa agrin fragment corresponding to its estimated net molecular mass (Reif et al., 2007)). This fragment also appeared in the single transfection sample (arrowhead) and may here be generated by another endogenously expressed protease. ***D,*** Full-length neurotrypsin protein expression was detected in the corresponding lysates of cos7 cells, transfected with mouse neurotrypsin, as a single band at around 85 kDa. This neurotrypsin-specific band appeared above an unspecific double band also present in the negative control (agrin transfection only). ***E, F,*** Western blot analysis of samples from cos7 cells infected with adenovirus-SN-agrin variants alone or co-infected with adenovirus-SN-agrin variants and adenovirus-neurotrypsin-eGFP. ***E,*** Agrin signals detected with the anti-C-90 agrin antibody in supernatant samples. All three analysed constructs (lanes 3, 4 – wildtype SN-agrin; lanes 5, 6 – SN-agrin-mRFP; lanes 7, 8 – mRFP-SN-agrin) were efficiently processed by co-expressed neurotrypsin-eGFP. This was indicated by the appearance of agrin cleavage products (compare to ***C***) only in samples of co-infected cells (lanes 4, 6, 8) but not in single infected cells (lanes 3, 5, 7). Mind the band-shift of the partially processed C-terminal agrin fragment at around 130 kDa (cleaved by neurotrypsin only at the α-site; arrowhead) due to mRFP fusion at the C-terminus of this agrin construct (SN-agrin-mRFP, lane 6) to around 160 kDa. However, the faint band (asterisk) below the prominent 160 kDa band might represent the partially cleaved C-terminal agrin fragment that has lost the mRFP due to proteolytic activity. As there are no antibodies against mRFP available it was impossible to determine if mRFP is partially cleaved off agrin's C-terminus. ***F,*** Neurotrypsin-eGFP was detected in cell-lysates of corresponding infected cell-samples (lane 2, cells infected with adenovirus-neurotrypsin-eGFP alone; lanes 4, 6, 8 – co-infection with adenovirus-agrin variants) as two bands at around 120 and 90 kDa. Both bands appeared to be

neurotrypsin-specific as no signals were detected in the sample of uninfected control cells (lane 1). The 120-kDa band most likely represents full-length neurotrypsin-eGFP detection, whereas the identity of the 90-kDa band is unclear.

←

low levels of neurotrypsin, even if only ectopically expressed mouse neurotrypsin with a Mr of around 85 kDa was detected in cell lysates with the anti-neurotrypsin antibody employed in this study (Fig. 29D). The two faint bands detected at around 80 to 85 kDa in the sample of single transfected, SN-agrin expressing cells, most-likely represent unspecific signals. Cos7 cells, derived from the African green monkey (*Chlorocebus aethiops*), are believed to express neurotrypsin containing an additional scavenger receptor cysteine-rich domain (SRCR domain), therefore altering its molecular mass to approximately 100 kDa (Xu and Su, 2005). However, the 90-kDa agrin cleavage product was not observed in cells expressing SN-agrin alone, indicating that the band appearing at around 130 kDa was most-likely generated by another protease. The Western blot analysis of supernatant samples of infected cos7 cells confirmed the successful adenovirus-mediated expression of wild-type SN-agrin, SN-agrin-mRFP, mRFP-SN-agrin and neurotrypsin (detected in cell lysates) variants as well as their functional interaction (Fig. 29E, F). Substantial amounts of agrin-cleavage fragments were only found in samples from cells co-expressing an agrin variant and neurotrypsin-eGFP (lanes 4, 6, 8 of Fig. 29E (anti-C-90-agrin detection) and Fig. 29F (anti-neurotrypsin(-eGFP) detection)). Both adenovirus-expressed SN-agrin (Fig. 29E, lanes 3, 4) and mRFP-SN-agrin (Fig. 29E, lanes 7, 8) were identically processed by neurotrypsin-eGFP (Fig. 29E, lanes 4, 8, respectively), generating the previously described 130-kDa (arrowhead) and 90-kDa agrin fragments (see above). The SN-agrin-mRFP variant (Fig. 29E, lanes 5, 6) was similarly and also efficiently processed by neurotrypsin (Fig. 29E, lane 6). Due to C-terminal fusion with mRFP, the original 130-kDa agrin fragment was detected at around 160 kDa (arrowhead). However, a weaker signal also appeared at around 130 kDa (asterisk), potentially indicating partially cleaved C-terminal agrin that has lost the mRFP due to proteolytic activity. As there are no antibodies against mRFP available it was impossible to determine if mRFP is partially cleaved off agrin's C-terminus. Like detected in control samples of SN-agrin expressing cells (Fig. 29C), if at all, only minor amounts of virus-expressed SN-agrin variants were processed in singly infected cells at the α-site only (SN-agrin, Fig. 29E, lane 3; SN-agrin-mRFP, Fig. 29E, lane 5; mRFP-SN-agrin, Fig. 29E, lane 7).

3.2.3 Adenovirus-mediated ectopic expression targets transmembrane agrin to dendrites as well as axons in cultured dissociated hippocampal neurons.

The generated adenovirus expression constructs were functionally expressed in cos7 cells and efficiently processed by neurotrypsin-eGFP, confirming their potential for further analyses of the functional neurotrypsin-agrin interaction in cultured hippocampal neurons. I therefore infected cultured dissociated hippocampal neurons at DIV11 with adenoviruses

expressing either SN-agrin, SN-agrin-mRFP, mRFP-SN-agrin or MARCKS-eGFP. The cells were fixed 3 days post-infection and the expression

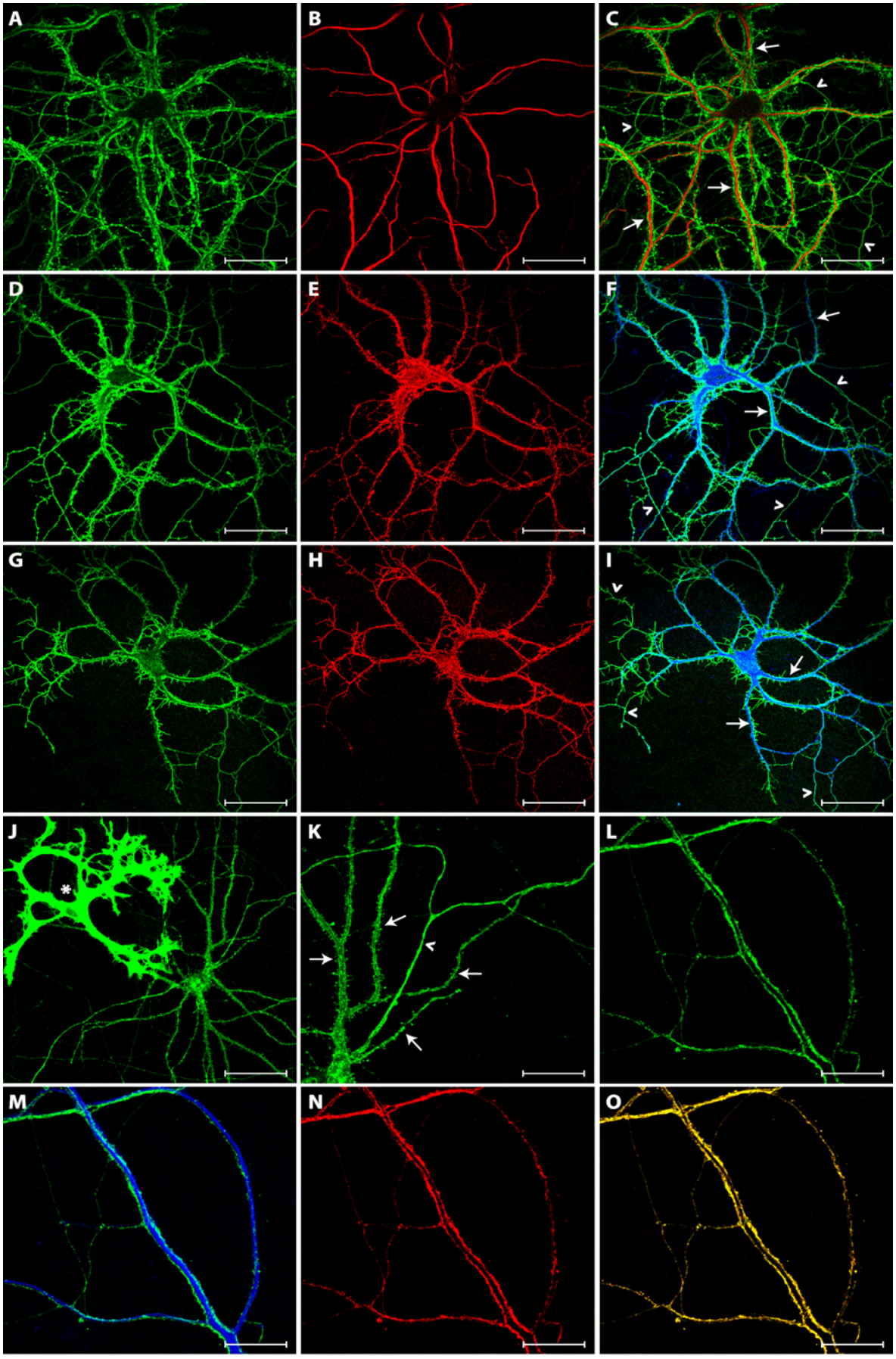

Figure 30. Transmembrane agrin is targeted to the membrane of dendrites as well as axons of cultured hippocampal neurons. Confocal microscopy analyses of hippocampal neurons cultured for 14 days (DIV14), infected with recombinant adenovirus at DIV11. Ectopically expressed proteins were identified by either antibody staining (agrin detection in ***A, D, G,*** anti-C-90 agrin antibody) or by detection of signals emitted by the corresponding fluorescent protein of the respective fusion proteins (mRFP-signals, ***E, H, N***; eGFP-signals, ***J, K, L***). Co-staining of neurons with an antibody against the dendritic marker microtubuli associated protein 2 (MAP-2) allowed the differentiation between dendrites and axons (***B, F, I, M***). ***A-C,*** Adenovirus-mediated expression of transmembrane agrin-x12, y4, z8 (SN-agrin) targeted SN-agrin to neurites of infected neurons. The merging of agrin (***A,*** anti-C-90 agrin antibody) and MAP-2 (***B***) specific signals (***C***; agrin, green; MAP-2, red) revealed that SN-agrin localised to dendrites (arrows) as well as to axons (arrowheads). Most agrin-positive axons depicted were processes from neurons whose cell bodies lay outside the depicted area. Also SN-agrin-mRFP (***D-F***) and mRFP-SN-agrin (***G-I***) were targeted to dendrites and axons of infected cells (***D, G,*** anti-C-90 agrin immunofluorescence; ***E, H,*** mRFP signals; ***F, I,*** anti-C-90 agrin (green) and anti-MAP-2 (blue) signals merged). ***J, K,*** Adenovirus-mediated expression of the myristoylated alanine-rich C-kinase substrate (MARCKS)-eGFP fusion protein in cultured neurons and astroglia (asterisk, ***J***). MARCKS-eGFP was targeted to cellular membranes of infected cells, including the plasma membrane of all neurites. Due to their different morphological properties, the axon (arrowhead) and dendrites (arrows) can easily be differentiated (***K,*** magnified section of ***J***). ***L-O***, Co-infection of a cultured neuron with adenovirus-MARCKS-eGFP and Adenovirus-SN-agrin-mRFP revealed that SN-agrin was targeted to the plasma membrane. MARCKS-eGFP was localised to the membrane of a dendrite, confirmed by merging MARCKS-eGFP (green; ***L, M***) and MAP-2 (blue, ***M***) signals. The cytoplasmatic MAP-2 signal filled the dendrite whereas the membrane-targeted eGFP was localised to the rim of the structure. The mRFP signal of the SN-agrin-mRFP fusion protein also localised to the rim of this dendrite (***N***), and exactly co-localised with MARCKS-eGFP (***O***; mRFP, red; eGFP, green; co-localisation, yellow), indicating that the SN-agrin constructs were successfully targeted to the plasma membranes of neurons. Scale bars: 45 μm (***A-F***); 50 μm (***G-J***); 20 μm (***K***); 10 μm (***L-O***).

←

patterns of the respective ectopically expressed proteins were analysed by confocal microscopy (Fig. 30). SN-agrin variant expression was detected by either anti-C-90-agrin antibody staining (SN-agrin, Fig. 30A; SN-agrin-mRFP, Fig. 30D; mRFP-SN-agrin, Fig. 30G) or by mRFP fluorescence of the corresponding mRFP-tagged SN-agrin fusion proteins (SN-agrin-mRFP, Fig. 30E; mRFP-SN-agrin, Fig. 30H). Antibody-derived signals as well as mRFP-fluorescence signals of the respective agrin variants revealed almost identical results. Like in cos7 cells, however, intracellular signals in the neuronal cell-body were stronger detected by mRFP fluorescence, compared to anti-C-90-agrin antibody signals. Nevertheless, all agrin variants were identically targeted to the neuronal periphery. To differentiate between axonal and dendritic processes and therefore to determine the subcellular localisation of agrin-specific signals, cells were co-stained with an antibody against the dendritic marker microtubule-associated protein 2 (MAP-2). Merging anti-C-90-agrin signals with MAP-2 signals verified that ectopically expressed SN-agrin (Fig. 30C), SN-agrin-mRFP (Fig. 30F) and mRFP-SN-agrin (Fig. 30I) identically localised to dendrites (arrows) as well as axons (arrowheads). The same was true for the different SN-agrin-mutant variants, uncleavable by neurotrypsin (data not shown). This targeting of ectopically expressed SN-agrin to axonal as well as dendritic compartments resembles the previously determined expression pattern of

endogenous agrin in cultured neurons (section 3.2.1). It was therefore concluded that the adenovirus-agrin variants were efficiently expressed and correctly targeted within neurons. Infection of cultured neurons with MARCKS-eGFP-expressing adenoviruses resulted in strong eGFP fluorescence in a punctuate pattern within the cell-body and in continuous signals along the neuronal surfaces, extending into the neuronal periphery (Fig. 30J, K). Glia cells are generally more efficiently infected by adenoviruses, resulting in much higher adenovirus-mediated expression levels in glia when compared to neurons. Indeed, astrocytes, occasionally growing in between the cultured neurons, were expressing high levels of MARCKS-eGFP (Fig. 30J, asterisk). However, MARCKS-eGFP was efficiently targeted to the axonal (Fig. 30K, arrowheads) as well as dendritic (Fig. 30K, arrows) membranes of neurons, even labelling thin dendritic protrusions like dendritic spines. To confirm that the SN-agrin constructs were also efficiently targeted to the plasma membrane of neurites, cultured hippocampal neurons were co-infected with MARCKS-eGFP- and SN-agrin-mRFP-expressing viruses. A dendritic segment of a co-infected cell is depicted in Figures 30L-O. Strong eGFP-fluorescence was detected at the rim of a dendrite (Fig. 30L), positively identified by MAP-2 signals filling the dendritic cytoplasm (Fig. 30M). The mRFP fluorescence of the SN-agrin-mRFP fusion protein also localised to the rim of this dendritic segment (Fig. 30N) and exactly co-localised with the MARCKS-eGFP signal (Fig. 30O), confirming correct and efficient plasma-membrane targeting of the SN-agrin variants also in cultured neurons.

3.2.4 Neurotrypsin cleaves agrin in dissociated hippocampal neuron cultures.

SN-agrin variants were successfully and efficiently expressed at the plasma membrane of axons and dendrites of cultured hippocampal neurons, utilising adenovirus mediated expression. In addition, adenovirus-mediated neurotrypsin expression in cultured neurons was previously described to target neurotrypsin predominantly to the axonal compartment (Frischknecht et al., 2008). Indeed, adenovirus-mediated expression of neurotrypsin-eGFP (Fig. 31A-C) or a catalytically inactive variant of neurotrypsin-eGFP (NT-inact-eGFP; Fig. 31D-F) were identically detected in a punctuate pattern in the neuronal cell body as well as in proximal dendrites and entire axons (arrowheads) of DIV14 neurons, when analysed by confocal microscopy. Confirming the reported preferential targeting of neurotrypsin to axons, the density of signals was much higher in axons and continuous transport of a high number of neurotrypsin-eGFP or NT-inact-eGFP positive transport vesicles was mainly detected in the entire axon of infected live neurons (data not shown but see (Frischknecht et al., 2008)). Identical signals were obtained when neurotrypsin-eGFP was detected either by eGFP fluorescence (Fig. 31A) or with an antibody against neurotrypsin (Fig. 31B), therefore confirming the integrity of the neurotrypsin expression constructs.

To investigate the interaction of ectopically expressed neurotrypsin and agrin variants, cultured dissociated hippocampal neurons were co-infected with SN-agrin-mRFP and neurotrypsin-eGFP or with SN-agrin-mRFP and NT-inact-eGFP at DIV11, fixed at DIV14

and analysed by confocal microscopy. When neurotrypsin-eGFP was co-expressed with SN-agrin-mRFP (Fig. 31G-I), neurotrypsin expression was detected in an identical pattern when compared to single expression experiments (Fig. 31G). However, SN-agrin-mRFP detection, performed by mRFP fluorescence, was clearly altered due to neurotrypsin co-expression (Fig. 31H). SN-agrin-mRFP signals were mainly detected in the neuronal cell-body but the neuronal processes were largely devoid of mRFP signals, indicating efficient neurotrypsin-dependent cleavage of agrin. In contrast, co-expression of SN-agrin-mRFP and NT-inact-eGFP (Fig. 31J-O) neither altered the targeting of NT-inact-eGFP (Fig. 31J, M) nor the original localisation of SN-agrin-mRFP (Fig. 31K, N). Besides its predominant localisation at the plasma membrane, SN-agrin-mRFP was also detected in a punctuate pattern within neurites, presumably reflecting transport vesicles (Fig. 31N, arrowheads). NT-inact-eGFP signals detected in the same neurite and supposedly also indicating transport vesicles (Fig. 31M, arrowheads), were only occasionally co-localising with intracellular SN-agrin-mRFP signals (Fig. 31O, arrows), suggesting that neurotrypsin and SN-agrin were mainly transported in different transport vesicles.

These results are in line with the previously presented data and indicate that agrin is a substrate of neurotrypsin in neurons, also when ectopically expressed in dissociated hippocampal neuron cultures. Neurotrypsin is predominantly but not exclusively expressed in the axonal compartment, whereas SN-agrin is targeted to axons as well as dendrites of cultured neurons. Co-expression experiments of SN-agrin with catalytically inactive neurotrypsin indicate independent trafficking of both proteins within the neuron and therefore supporting the hypothesis of extracellular interaction of neurotrypsin and agrin (Stephan et al., 2008). However, further and more detailed analyses are necessary to elucidate the exact mechanism of their interaction. Unfortunately, problems with both the stability of produced virus variants and high-titer virus production made it impossible for me to proceed with these analyses.

3.2.5 Transmembrane agrin is involved in the generation of additional filopodia-like protrusions on dendrites as well as axons of cultured dissociated hippocampal neurons.

Transmembrane agrin (SN-agrin) was described to cause the increased appearance of dendritic as well as axonal filopodia on cultured neurons (Annies et al., 2006; McCroskery et al., 2006). Dendritic filopodia have been characterised as precursors of dendritic spines and their induction could indicate an early stage of synapse formation (Jontes and Smith, 2000; Matus, 2005; Knott et al., 2006; Toni et al., 2007). Assuming that SN-agrin is indeed involved in filopodia-dependent generation of new synapses, neurotrypsin-dependent cleavage of agrin may interfere with agrin's function and might therefore implicate the neurotrypsin-agrin interaction in adaptive reorganisations of the synaptic circuitry.

To confirm the published effects of SN-agrin, adenovirus-mediated ectopic expression of SN-agrin in dissociated hippocampal neurons cultures was visualised by immuno-cytochemistry and analysed by confocal microscopy (Fig. 32). Cell surfaces were visualised

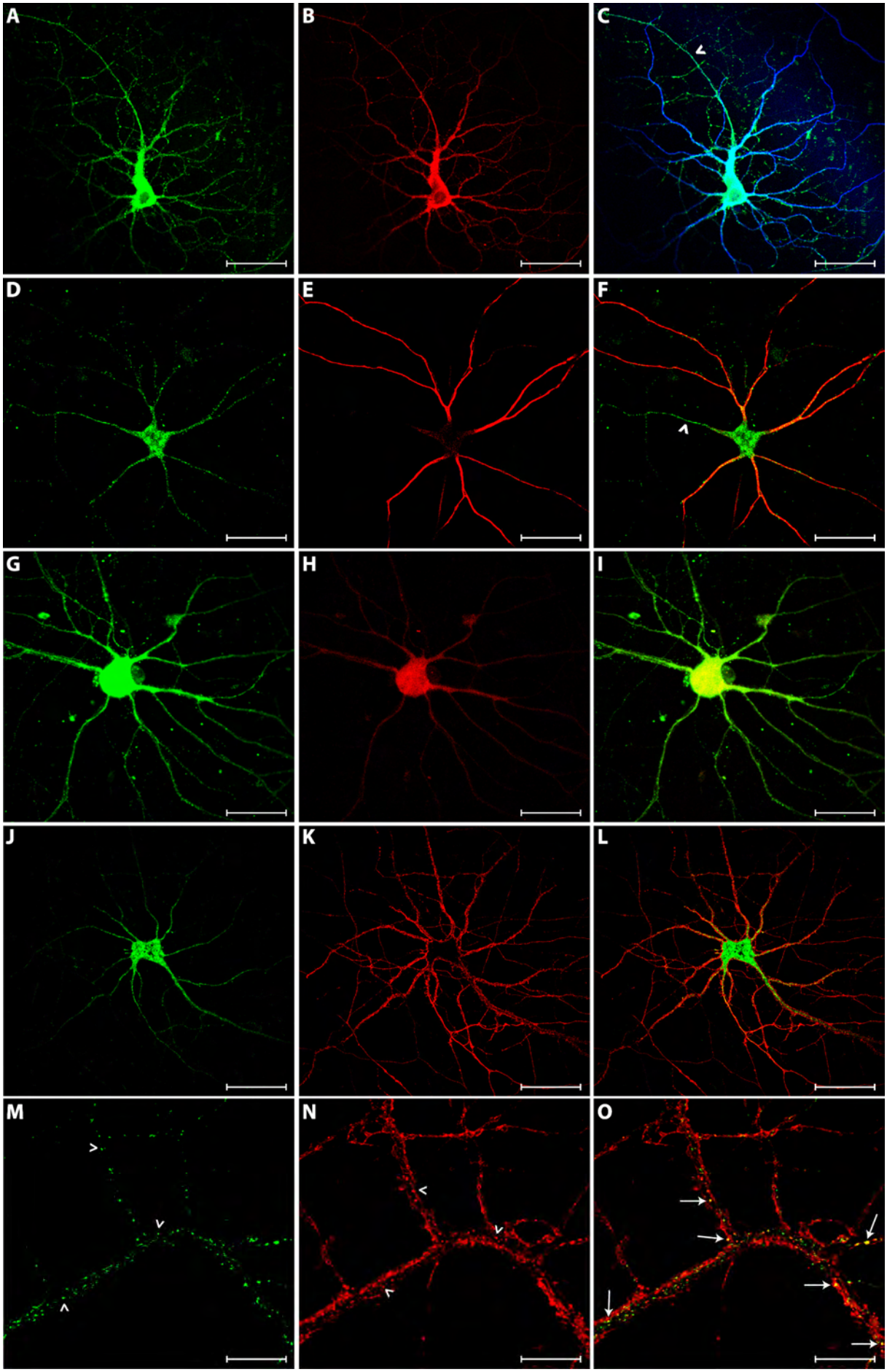
A
B
C
D
E
F
G
H
I
J
K
L
M
N
O

Figure 31. Neurotrypsin cleaves agrin in cultured neurons. Confocal microscopy analyses of adenovirus-mediated ectopic expression of agrin and neurotrypsin variants in hippocampal neurons cultured for 14 days (DIV14), infected with recombinant adenovirus at DIV11. Ectopically expressed proteins were identified either by antibody staining (neurotrypsin detection with an antibody against the proline-rich basic domain, ***B***) or by detection of signals emitted by the corresponding fluorescent protein of the respective fusion proteins (mRFP-signals, ***H, K, N***; eGFP-signals, ***A, D, G, J, M***). Co-staining of neurons with an antibody against the dendritic marker microtubuli associated protein 2 (MAP-2) allowed the differentiation between dendrites and axons (***C, E***). ***A-C,*** Adenovirus-mediated expression of neurotrypsin-eGFP, either detected by eGFP fluorescence (***A***) or anti-neurotrypsin antibody staining (***B***), was detected in a punctuate pattern in the neuronal cell-body and within neurites. Co-staining with MAP-2 revealed that neurotrypsin was mainly localised to axons (arrowhead) and proximal dendrites (***C***, eGFP, green; MAP-2, blue). ***D-F,*** Adenovirus-mediated expression of a catalytically inactive neurotrypsin-eGFP fusion protein (NT-inact-eGFP), detected by eGFP fluorescence (***D***). Comparison with MAP-2 staining (***E***) and merging of eGFP and MAP-2 specific signals confirmed that also NT-inact-eGFP was mainly localised to axons (arrowhead) and proximal dendrites (***F***, eGFP, green; MAP-2, red). ***G-I,*** Adenovirus-mediated co-expression of neurotrypsin-eGFP and transmembrane agrin-x12, y4, z8-mRFP (SN-agrin-mRFP) in cultured hippocampal neurons. Ectopically expressed neurotrypsin-eGFP (***G,*** eGFP fluorescence) was localised to the cell body as well as neurites, whereas SN-agrin-mRFP signals (***H,*** mRFP fluorescence) were mainly detectable within the cell-body of the same co-infected neuron (***I,*** merged signals; mRFP, red; eGFP, green). This distribution of agrin signals was unlike its localisation in single expression analyses (Fig. 30) and indicated that neurotrypsin cleaves agrin also in cultured neurons, leading to the removal of agrin from neuronal surfaces. ***J-O,*** Adenovirus-mediated co-expression of NT-inact-eGFP (***J, M,*** eGFP fluorescence) and SN-agrin-mRFP (***K, N,*** mRFP fluorescence) in cultured hippocampal neurons (***L, O,*** merged signals; mRFP, red; eGFP, green). In contrast to the co-expression of active neurotrypsin-eGFP and SN-agrin-mRFP, co-expression of NT-inact-eGFP and SN-agrin-mRFP did not result in the redistribution of agrin signals. In the neuronal periphery, NT-inact-eGFP signals were detected in a dotted pattern, most-likely indicating transport vesicles (***M,*** arrowheads point at some of the detectable vesicles (eGFP fluorescence)). SN-agrin-mRFP was detected at the plasma membrane as well as in a punctuate pattern within the neurite (***N,*** mRFP fluorescence), potentially representing vesicular structures (arrowheads point at some of the detectable vesicles). The overlay of NT-inact-eGFP and SN-agrin-mRFP signals revealed that only a few vesicular structures contained both NT-inact-eGFP and SN-agrin-mRFP (arrows, ***O,*** mRFP, red; eGFP, green; co-localisation, yellow). Most of the visualised, potentially vesicular structures were only labelled for one of the analysed proteins, indicating that neurotrypsin and agrin are mainly trafficked in independent transport compartments. Scale bars: 50 μm (***A-F, J-L***); 40 μm (***G-I***); 10 μm (***M-O***).

←

with agrin signals covering the plasma membrane of all neurites, detected with the anti-C-90-agrin antibody. Indeed, the overexpression of SN-agrin caused the increased appearance of filopodia-like protrusions on cultured dissociated hippocampal neurons. Neurons infected for either 4 days and analysed at DIV8 (Fig. 32A, B) or 3 days and analysed at DIV14 (Fig. 32C-H) showed a high number of dendritic (arrows) as well as axonal filopodia. (arrowheads). In immature DIV8 neurons, long filopodia-like protrusions were found mainly at distal parts of the outgrowing dendrites (Fig. 32A, arrows) as well as on distal axons (not shown). In contrast, in mature DIV14 neurons, filopodia were distributed all over dendritic processes and were mainly detected along proximal segments of dendrites (Fig. 32C). Filopodia-like protrusions along proximal segments of dendrites were also detectable on differential interference contrast images of both uninfected DIV14 neurons (Fig. 32E, arrows) and

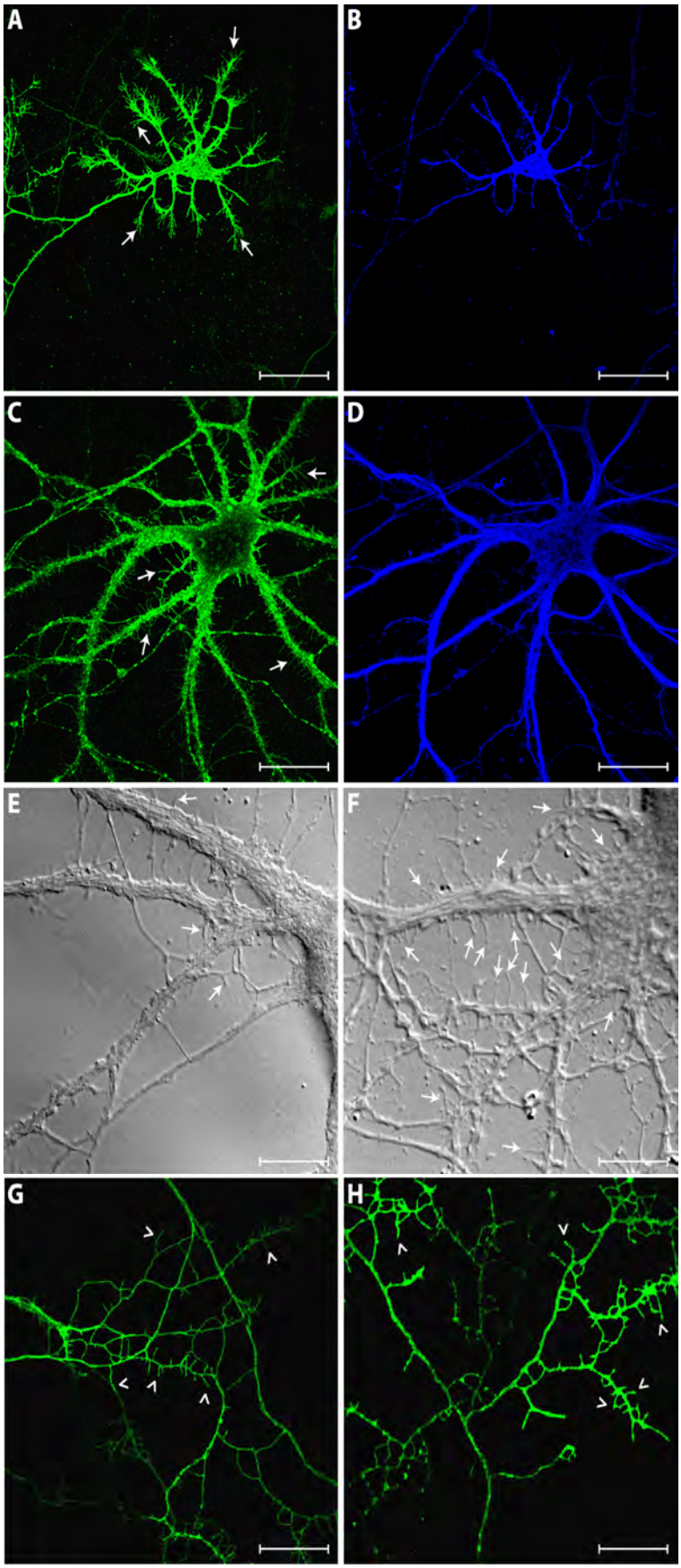

Figure 32. The overexpression of transmembrane agrin causes the increased appearance of filopodia-like protrusions on dendrites and axons of cultured hippocampal neurons. Confocal microscopy analyses of dissociated hippocampal neurons cultured for 8 or 14 days (DIV8, DIV14, respectively), infected with a recombinant adenovirus-transmembrane agrin-x12, y4, z8 (SN-agrin) variant. Agrin signals were detected with the anti-C-90 agrin antibody (***A, C, G, H***). Co-staining of neurons with an antibody against the dendritic marker microtubuli associated protein 2 (MAP-2) allowed the differentiation between dendrites and axons (***B, D***). ***A, B,*** Immature DIV8 neurons, infected with adenovirus-SN-agrin-mRFP for 4 days, developed a multitude of filopodia-like processes (***A,*** arrows) mainly along the distal parts of their MAP-2 positive dendrites (***B***). ***C-H,*** Mature DIV14 neurons, infected with adenovirus-SN-agrin-mRFP for 3 days, developed a multitude of filopodia-like processes (***C,*** arrows) mainly along the MAP-2 positive dendrites (***D***). This increase of filopodia-like protrusions (arrows) upon SN-agrin overexpression was also detected on differential interference contrast images of proximal dendrites (***F***), when compared to an uninfected control cell (***E***). In addition to the in-creased appearance of filopodia-like protrusions on dendrites, the overexpression of SN-agrin also caused the appearance of filopodia-like protrusions on distal parts of axons (***G, H,*** arrows). Scale bars: 50 μm (***A, B***); 40 μm (***C, D***); 10 μm (***E, F***), 15 μm (***G, H***).

SN-agrin overexpressing neurons (Fig. 32F, arrows). However, a clear increase of filopodia number was visible on dendrites of neurons overexpressing SN-agrin. In addition to the SN-agrin dependent increase of dendritic filopodia, the appearance of filopodia on distal segments of axons was also detectable (DIV14, Fig. 32G, H, arrowheads).

Thus, expression of SN-agrin caused the additional generation of filopodia-like protrusions at the neuronal surface of both immature and mature cultured neurons. Yet, with regards to dendritic filopodia, immature neurons mainly generated filopodia in distal regions of dendrites whereas mature neurons mainly developed filopodia in proximal dendritic regions. Therefore, one could expect that SN-agrin-mediated generation of filopodia-like protrusions may contribute to different functional processes, depending on the maturation state of the cultured neuron. Filopodia-like protrusions in immature neurons may be involved in processes of peripheral neurite formation. In contrast, filopodia in mature neurons may represent precursors of dendritic spines and, therefore, contribute to synapse generation, a process potentially targeted by neurotrypsin activity given its role in the establishment and maintenance of cognitive brain functions (Molinari et al., 2002).

3.2.6 Neurotrypsin inhibits transmembrane agrin's potential to generate filopodia-like protrusions in cultured cos7 cells.

Transmembrane agrin (SN-agrin) causes the increased appearance of filopodia-like protrusions on dendrites as well as axons of cultured dissociated hippocampal neurons. It was therefore tempting to speculate that neurotrypsin-dependent cleavage of agrin might modify this function of SN-agrin. Unfortunately, due to problems with virus stability and high-titer virus production I was not able to further analyse the effects of neurotrypsin-dependent cleavage on agrin's functions in cultured neurons. However, SN-agrin expressing cos7 cells also develop excessive filopodia-like protrusions on their cell-surface (see below) and neurotrypsin was shown to efficiently cleave agrin in cos7 cells (Fig. 29C). I therefore studied if neurotrypsin-dependent cleavage of agrin caused modifications of SN-agrin-dependent generation of filopodia-like protrusions on cos7 cells.

To determine if agrin's induction of filopodia-like protrusions at the cos7 cell surface is based on similar properties as described for its function in neurons (McCroskery et al., 2006), cos7 cells were transfected with either SN-agrin, secreted agrin (LN-agrin) or neurotrypsin expression constructs. Cells were fixed and stained 24 hour post-transfection and analysed by confocal microscopy (Fig. 33). To visualise filopodia-like protrusions, cells were stained with fluorescently-labeled Phalloidin that specifically binds to filamentous actin structures within the cell, including motile surface elements like filopodia. Alternatively, cells were transfected with the membrane-targeted eGFP variant MARCKS-eGFP to visualise the cellular surface. Thin and long filopodia-like protrusions (arrowheads) appeared only infrequently on untransfected cos7 cells (Fig. 33A) or MARCKS-eGFP expressing cells (Fig. 33B) and the surface of most cells appeared rather smooth. However, densely packed und rather uniformly distributed short protrusions were detected at the surface of only some

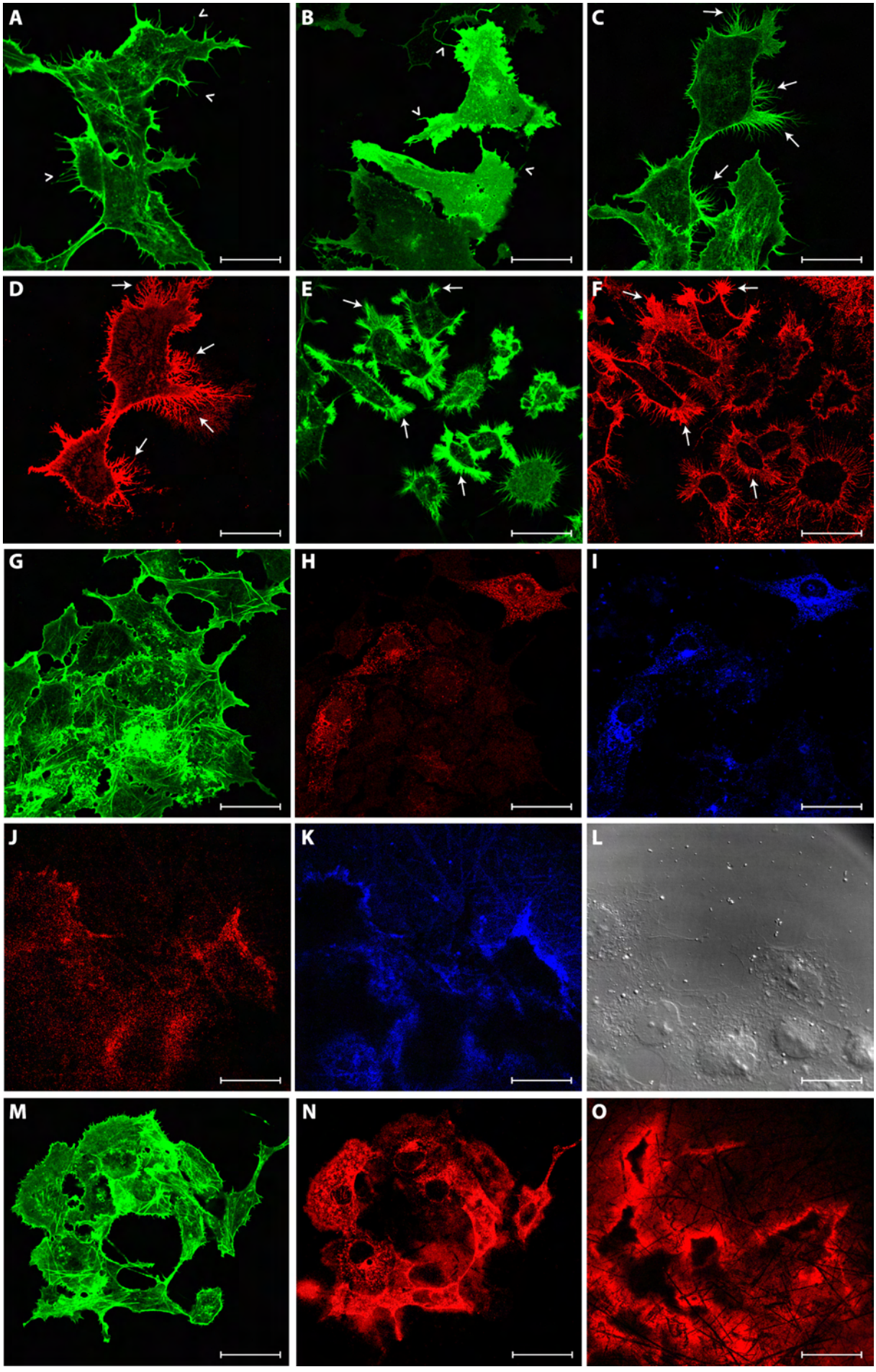
A
B
C
D
E
F
G
H
I
J
K
L
M
N
O

Figure 33. Transmembrane agrin but not secreted agrin generates additional filopodia-like structures on cos7 cell surfaces. Confocal microscopy analyses of transiently transfected cos7 cells. To visualise motile cell-surface protrusions, like filopodia, the actin cytoskeleton was labelled with fluorescence-tagged Phalloidin (***A, C, E, G, M***). Alternatively, cells were transfected with a construct targeting eGFP to cellular membranes, including the plasma membrane (***B***). This myristoylated alanine-rich C-kinase substrate (MARCKS)-eGFP fusion construct was therefore also suitable to visualise cell surface protrusions. Untransfected cos7 cells (***A***) or cells transfected with MARCKS-eGFP (***B***) occasionally developed motile and thin filopodia-like protrusions at the cellular surface (arrowheads). ***C-F,*** Transfection of cos7 with transmembrane agrin-x12, y4, z8 (SN-agrin) causes the excessive appearance of filopodia-like protrusions at the cell-surface (arrows). These protrusions may alternatively represent branched-retraction fibres (BRF, see main text) and were visualised by staining ectopically expressed agrin with the anti-C-90 agrin antibody (***D, F***). These protrusions were positive for Phalloidin signals, supporting the notion that they were indeed filopodia-like structures or BRF (***C, E***). ***G-I,*** In contrast to the effects of SN-agrin, secreted agrin-x12, y4, z8 (LN-agrin) did not cause filopodia-like protrusions or BRF. Cells transfected with LN-agrin had a smooth surface, in average exactly resembling control conditions (***G,*** Phalloidin). LN-agrin was detected in a punctuate pattern throughout the permeabilised cell with two different agrin-specific antibodies (***H,*** anti-N-terminal agrin domain (NtA) antibody; ***I,*** anti-C-90 agrin antibody), most likely indicating endoplasmatic reticulum, golgi and secretory vesicle structures. ***J-L,*** LN-agrin was indeed secreted and deposited around the cell, as visualised with not permeabilised cells, by either anti-NtA-dependent (***J***) or anti-C-90 agrin-dependent (***K***) fluorescence. To identify the cellular borders, the corresponding differential interference contrast image is shown in panel ***L***. ***M-O,*** The cell surface of cos7 cells transfected with neurotrypsin was indistinguishable from control cells (***M,*** Phalloidin). Ectopically expressed neurotrypsin was detected in a vesicular pattern within permeabilised cells (***N***) and deposited around cells, when not permeabilised cells were analysed (***O***). Scale bars: 25 μm (***A-D, J-L***); 50 μm (***G-I***); 55 μm (***E, F***), 47 μm (***M-O***).

←

untransfected or MARCKS-eGFP expressing cells (data not shown). Only around 19 % of control cells showed an extraordinary amount of filopodia at their surface (Table 2). In strong contrast, 86.8 % of cos7 cells expressing SN-agrin developed extensive filopodia-like protrusions at their surface (Table 2; Fig. 33C-F, arrows), visualised by both Phalloidin-staining (Fig. 33C, E) and anti-C-90-agrin immunoreactivity (Fig. 33D, F). These protrusions were irregularly distributed over the whole cellular surface and appeared sometimes in bundles or as long and branched structures. Alternatively to the definition as filopodia, these sometimes very long and branched structures might resemble branched retraction fibres (BRF) that emerge from extensive cell movements (internal communication with A. Matus, FMI Basel, Switzerland; see also (Taylor and Robbins, 1963)). It is therefore unclear if the morphological changes on cos7 cells generated by SN-agrin are comparable to effects triggered by SN-agrin in neurons. Analyses of cos7 cells expressing LN-agrin confirmed that this effect was SN-agrin specific. The surface of LN-agrin expressing cells was mostly smooth and indistinguishable from untransfected cells, as confirmed by Phalloidin signals (Fig. 33G). LN-agrin signals were detected by both the anti-NtA-agrin antibody (Fig. 33H) and the anti-C-90-agrin antibody (Fig. 33I) within the permeabilised cell in a punctuate pattern, presumably reflecting transport vesicles. The functional expression of LN-agrin was supported by its efficient secretion and deposition around the cell, visualised in nonpermeabilised cells again by both anti-NtA-agrin (Fig. 33J) and anti-C-90-agrin

immunoreactivity (Fig. 33K). Also the surface of neurotrypsin-overexpressing cos7 cells was indistinguishable from control cells (Fig. 33M; 15.9 % of the neurotrypsin-expressing cells with many filopodia versus 18.9 % of control cells, Table 2). Like LN-agrin, neurotrypsin was detected in a punctuate pattern, potentially resembling mostly secretory vesicles (Fig. 33N), and was efficiently secreted and deposited around transfected cells (Fig. 33O). These results confirmed that exclusively the transmembrane variant of agrin causes alterations of the cos7 cell surface, generating the excessive appearance of filopodia-like protrusions or BRF.

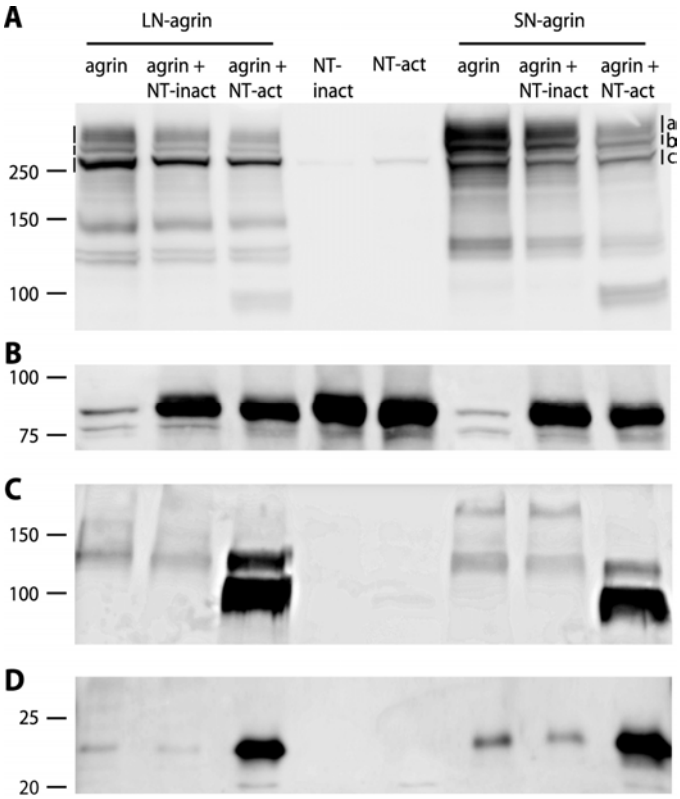

Figure 34. Transmembrane and secreted agrin variants are both efficiently cleaved by neurotrypsin in cos7 cells. Western blot analysis of transfected cos7 cells to determine neurotrypsin-dependent (NT-act) cleavage of both transmembrane agrin-x12, y4, z8 (SN-agrin) and secreted agrin-x12, y4, z8 (LN-agrin). As a control, co-expression of agrin variants with a catalytically inactive variant of neurotrypsin (NT-inact) was performed. Two different cell pools were independently transfected with either a neurotrypsin or an agrin variant and mixed 24 hours post-transfection. Therefore, mainly extracellular cleavage of both SN-agrin and LN-agrin was assessed. Molecular mass references are indicated in kDa. ***A,*** Full-length agrin detection with the anti-C-90 agrin antibody in cos7 cell-lysate samples. Both full-length variants of LN-agrin and SN-agrin were detected as three distinct groups of bands above 250 kDa, indicating differentially glycanated forms of full-length agrin, termed upper (a), middle (b) and lower (c) variants of agrin. In parallel to full-length agrin detection, some additional but less intense bands appeared in all analysed cell lysate samples, possibly representing partially cleaved agrin variants. ***B,*** Both mouse NT-act as well as mouse NT-inact were detected in cell-lysate samples as a single band at around 85 kDa on top of a potentially unspecific double-band that was also present in control samples transfected with agrin alone. ***C,*** Detection of the 90-kDa agrin fragment with the anti-C-90 agrin antibody in supernatant samples. Both LN-agrin and SN-agrin were similarly and efficiently cleaved by neurotrypsin. The 90-kDa fragment only appeared in samples of cells co-transfected with agrin and NT-act. In addition, the 110-kDa agrin fragment, in cos7 supernatants detected at around 130 kDa and representing C-terminal agrin exclusively cleaved at the α-site, appeared stronger in agrin and NT-act co-expression samples. ***D,*** Detection of the 22-kDa agrin fragment with the anti-C-22 agrin antibody in supernatant samples. Completing the results depicted in panel ***C***, neurotrypsin also efficiently generated the 22-kDa fragments from both LN-agrin and SN-agrin isoforms.

The filopodia-generating activity in cultured neurons was localised to the N-terminal half of SN-agrin, approximately N-terminal to the neurotrypsin α-cleavage site within agrin (McCroskery et al., 2006). A similar functional dependency was observed in cos7 cells as only SN-agrin but not LN-agrin was able to generate excessive filopodia-like protrusions or BRF. The LN-agrin and SN-agrin variants used in this study only differed in their very N-

terminal domain, arguing for either a direct effect of the transmembrane domain or, more likely, for an effect depending on SN-agrin's targeting to the plasma membrane. However, it is possible that neurotrypsin-dependent cleavage of agrin and a resulting relocation of C-terminal agrin fragments to functional interaction sites, e.g., at the cell surface, may activate an additional function to generate filopodia-like protrusions. Therefore, the inactive LN-agrin variant represented a useful control to analyse potential effects of the C-terminal agrin fragments released by neurotrypsin-dependent cleavage and to determine the active region within agrin that causes the generation of filopodia on cos7 cells.

Only SN-agrin was so far confirmed to be a substrate of neurotrypsin in eukaryotic cells and a direct interaction between LN-agrin and neurotrypsin, however expected, was not yet analysed. To test if LN-agrin is also a substrate of neurotrypsin, either LN-agrin or SN-agrin variants were co-expressed with neurotrypsin in cos7 cells and potential cleavage was analysed by Western blotting (Fig. 34). Neurotrypsin-dependent cleavage of agrin is supposed to occur mainly extracellularly. However, high levels of overexpression of proteins in the same cell may alter their physiological properties and may therefore lead to an unphysiological interaction of neurotrypsin and agrin. Thus, experimental conditions were chosen to mainly promote detection of physiological relevant extracellular cleavage of agrin. This was attempted by expression of neurotrypsin and agrin from different cell pools. Cos7 cells were single transfected with either agrin or neurotrypsin variants. These different cell pools were mixed 24 hour post-transfection and further co-cultured for additional 24 hours. However, potentially unphysiological interactions between neurotrypsin and agrin variants could theoretically still have occurred due to cell-lysis in culture or during the sample preparation procedure. In singly transfected cos7 cells, expressing either agrin variant alone, full-length agrin variants of both LN-agrin and SN-agrin were detected as three distinct groups of bands (Fig. 34A), similar to their detection *in vivo* (section 3.1). Yet, in LN-agrin-expressing cell lysate samples, bottom full-length agrin was the strongest variant detected, whereas in lysates of SN-agrin expressing cells all three distinct groups of full-length agrin variants were equally as strong. This discrepancy is likely explained by the different characteristics of the respective agrin variants. SN-agrin is mainly expressed at the cellular membrane and therefore detected in cell lysates, while fully mature and heavily glycanated variants of LN-agrin are presumably efficiently secreted and thus only detected weakly in cell lysates. Anyhow, SN-agrin as well as LN-agrin were identically cleaved by neurotrypsin. Upon co-expression with active neurotrypsin (NT-act), the signal intensities of mainly upper and middle full-length agrin variants of both SN-agrin and LN-agrin decreased (Fig. 34A). In addition, all three C-terminal cleavage fragments were generated by neurotrypsin from both variants. The 130-kDa fragment, resembling C-terminal agrin solely cleaved at the α-site, increased only slightly when compared to samples expressing agrin alone but both the 90-kDa and the 22-kDa agrin were efficiently generated by the activity of ectopically expressed neurotrypsin. Interestingly, very low amounts of the 22-kDa fragments also appeared in cells expressing either LN-agrin or SN-agrin alone. This again indicated (see section 3.2.2),

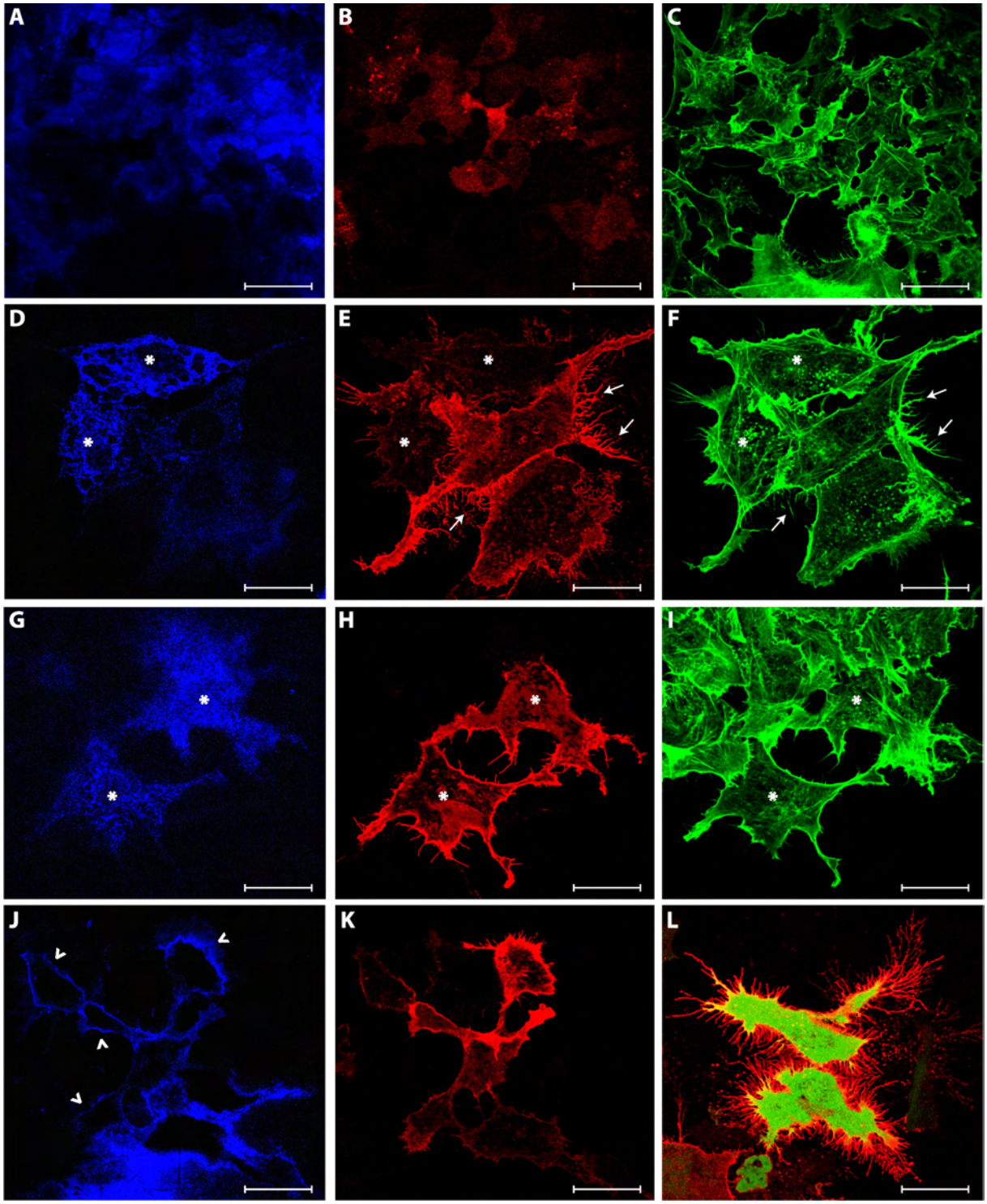

Figure 35. Neurotrypsin inhibits the function of transmembrane agrin to generate filopodia-like structures on cos7 cell surfaces. Confocal microscopy analyses of transiently transfected cos7 cells. To visualise motile cell-surface protrusions, the actin cytoskeleton was labelled with fluorescence-tagged Phalloidin (***C, F, I***). ***A-C,*** The co-transfection of neurotrypsin (***A,*** anti-neurotrypsin antibody) and secreted agrin-x12, y4, z8 (LN-agrin, ***B,*** anti-C-90 agrin antibody) had no effect on the generation of filopodia-like structures or branched retraction fibres (BRF) at the cos7 cell surface. Phalloidin signals in co-expressing cells were indistinguishable from signals obtained in control cells, indicating that the released C-terminal agrin fragments do not cause filopodia-like protrusions or BRF on cos7 cells. ***D-F,*** Co-transfection of cos7 cells with neurotrypsin (***D,*** anti-neurotrypsin antibody) and transmembrane agrin-x12, y4, z8 (SN-agrin, ***E,*** anti-C-90 agrin antibody) expression constructs. C-terminal agrin was efficiently removed by neurotrypsin from cell-surfaces of co-expressing cells (asterisks).

Interestingly, co-expression of neurotrypsin and SN-agrin also resulted in the inhibition of SN-agrin's potential to generate filopodia-like structures or BRF at the cos7 cell surface. Phalloidin signals in co-expressing cells (asterisks) were indistinguishable from signals obtained with control cells, indicating that neurotrypsin blocks agrin's function to generate filopodia-like structures or BRF (***F***). However, filopodia-like protrusion or BRF were still present on some cells only singly transfected with SN-agrin (arrows). ***G-K,*** Co-transfection of cos7 cells with catalytically inactive neurotrypsin (NT-inact) and SN-agrin expression constructs. Permeabilised (***G-I***) as well as not permeabilised cells (***J, K***) co-expressing NT-inact (***G, J,*** anti-neurotrypsin antibody) and SN-agrin (***H, K,*** anti-C-90 agrin antibody) were analysed. Phalloidin signals of permeabilised, co-expressing cells were indistinguishable from signals obtained with control cells (***I***), indicating that also NT-inact blocks agrin's function to generate filopodia-like structures or BRF. Therefore, the inhibition potential of neurotrypsin did not depend on the catalytical activity of neurotrypsin and, thus, not on agrin cleavage. Neurotrypsin is recruited to cell membranes when co-expressed with agrin (***J***, not permeabilised cells, arrowheads) and might therefore inhibit SN-agrin's function by direct protein-protein interactions with agrin. ***L,*** Cos7 cells co-expressing SN-agrin and eGFP develop an extensive amount of filopodia-like protrusions or BRF, similar to cells expressing SN-agrin alone. This indicates that solely co-transfection of cells does not interfere with SN-agrin's function. Scale bars: 50 μm (***A-C, J, K***); 20 μm (***D-F***); 25 μm (***G-I, L***).

←

in addition to the generation of the 130-kDa fragment in cells expressing agrin alone, that cos7 cells either express low levels of endogenous neurotrypsin or other proteases with low activity on C-terminal agrin cleavage.

To analyse if neurotrypsin-dependent cleavage alters agrin's function to cause filopodia-like structures or BRF, cos7 cells were co-transfected with SN-agrin and neurotrypsin or with SN-agrin and a catalytically inactive variant of neurotrypsin (NT-inact). To determine if released C-terminal agrin fragments have a potentially positive effect on the generation of filopodia-like protrusions on cos7 cells (see above), LN-agrin was co-expressed with neurotrypsin. The transfected cells were fixed 24 hours post-transfection and stained with anti-neurotrypsin and anti-C-90-agrin antibodies to visualise ectopic protein expression. Subsequently, processed cells were stained with fluorescently labelled Phalloidin to visualise filopodia-like structures and were finally analysed by confocal microscopy (Fig. 35). Cos7 cells co-expressing LN-agrin and neurotrypsin did not show any alterations in their respective protein expression patterns, compared to LN-agrin or neurotrypsin single transfections (Fig. 35A-C). Furthermore, no alterations of the cell-surface morphology were observed as Phalloidin-signals of co-expressing cells (Fig. 35C) were indistinguishable to control cells (Fig. 35A, B). Thus, neurotrypsin-dependent cleavage of agrin did not cause a positive effect on the increase of filopodia number on cos7 cells. These results indicated that the effect of agrin observed in cos7 cells strictly relied on transmembrane agrin activity, presumably localised within the N-terminal segment prior to the α-cleavage site of agrin, similar to its published effects in cultured neurons (Annies et al., 2006; McCroskery et al., 2006). Interestingly, the co-expression of SN-agrin and neurotrypsin resulted in the inhibition of SN-agrin's function to generate filopodia-like structures or BRF (Fig. 35D-F). Cos7 cells co-expressing high levels of both SN-agrin and neurotrypsin (asterisks) showed reduced cell-surface signals of agrin due to the release of the C-terminal fragments from the

transmembrane-bound N-terminus of agrin (Fig. 35E). In addition, only 33.3 % of co-expressing cells developed extensive filopodia-like or BRF structures, in strong contrast to 86.8 % of cells expressing SN-agrin alone (Table 2; Fig. 35E, F). This inhibition of agrin's function was specifically limited to co-expressing cells, as single transfected cells on the same coverslip, expressing agrin alone, still developed extensive filopodia-like structures (Fig. 35E, F, arrows). Thus, many co-expressing cells revealed a cell-surface that was almost indistinguishable from control cells (Fig. 35F), indicating the ability of neurotrypsin to block SN-agrin's function to generate filopodia-like protrusions or BRF in cos7 cells. However, even catalytically inactive neurotrypsin (NT-inact) was able to block SN-agrin's function (Fig. 35G-I). Again, the cell surface of cells co-expressing SN-agrin and NT-inact (asterisks) was rather smooth with no or only few filopodia-like protrusions (Fig. 35I), comparable to SN-agrin and active neurotrypsin co-expressing cells as well as to control samples. To exclude the possibility that the general co-transfection of cells caused alterations in cellular functions, possibly as a result of exceeding levels of ectopically expressed proteins, thereby leading to the inhibition of SN-agrin's function, I co-transfected cos7 cells with SN-agrin and an unrelated eGFP expression construct. However, 70.4 % of co-transfected cells expressing high levels of both SN-agrin and eGFP were filopodia positive (Table 2; Fig. 35L), therefore confirming the specific inhibition of SN-agrin's function by neurotrypsin in cos7 cells.

Table 2: Neurotrypsin inhibits SN-agrin's function to generate filopodia-like structures at the cos7 cell surface.

cos7 cells transfected with:	*filopodia-positive cells*	*filopodia-negative cells*	*percentage filopodia-positive cells*
control (untransfected)	20	86	**18.9**
neurotrypsin	17	90	**15.9**
SN-agrin	99	15	**86.8**
SN-agrin + neurotrypsin	15	45	**33.3**
SN-agrin + eGFP	27	8	**70.4**

Quantification of filopodia-positive cells. Transfected cos7 cells were fixed and stained with specific antibodies to visualise neurotrypsin and agrin expression. Additional staining with fluorescently labelled Phalloidin enabled the visualisation of the cell-surface morphology, including filopodia-like structures. Cells were subsequently analysed by confocal microscopy to roughly estimate the quantity of filopodia positive and negative cells for each set of transfections (Fig. 33, 35). The appearance of an excess of filopodia-like structures at multiple sites of the cellular surface identified cos7 cells as filopodia-positive. In contrast, filopodia-negative cells had a similar appearance as the average control cell with little or no filopodia (Fig. 33A, B).

Taken together, these experiments indicated that the ability of agrin to generate filopodia-like protrusions or BRF on cos7 cells is strictly dependent on the transmembrane isoform of agrin, in accordance with published effects in cultured neurons ((McCroskery et

al., 2006)). Furthermore, neurotrypsin inhibits SN-agrin's function, however, independent of its catalytic activity. The mechanism of SN-agrin to cause filopodia in cultured neurons was shown to involve clustering of SN-agrin molecules (Annies et al., 2006) and the overexpression of this variant may have led to automatic clustering of SN-agrin proteins accumulating in high densities at the cellular surface. Neurotrypsin binds to extracellular epitopes of SN-agrin variants and is recruited to cell-membranes (Fig. 35J, arrowheads). It is therefore likely that the inhibiting activity of neurotrypsin was caused by its potential to form protein-protein interactions with agrin. Thus, binding of neurotrypsin to agrin may have blocked the clustering of SN-agrin variants, necessary for filopodia-generation.

4. Discussion

The neuronal serine protease neurotrypsin cleaves agrin *in vitro* (Reif et al., 2007) and cleavage was also observed at the NMJ *in vivo* (Bolliger, M. *et al.,* unpublished observations). To analyse if agrin is a substrate of neurotrypsin in the CNS, I performed a detailed biochemical analysis with mouse brain tissue and analysed potential functional effects of the neurotrypsin-agrin interaction *in vitro*.

I found that neurotrypsin cleaves the extracellular proteoglycan agrin predominantly at or in the vicinity of synapses in the murine brain, resulting in increased concentrations of agrin fragments and decreased full-length agrin at synapses. To further elucidate the potential effects of the neurotrypsin-agrin interaction, I generated, and successfully tested, recombinant adenoviruses that efficiently expressed variants of transmembrane agrin in cultured neurons. These adenoviruses complete a series of previously produced neurotrypsin-expressing viruses (Frischknecht et al., 2008) and therefore enable future detailed analyses of the neurotrypsin-agrin interaction *in vitro*. Adenovirus-mediated overexpression of transmembrane agrin resulted in the increased appearance of dendritic as well as axonal filopodia on cultured dissociated hippocampal neurons, thereby confirming recently published observations (Annies et al., 2006; McCroskery et al., 2006). Furthermore, transmembrane agrin-overexpression also caused a similar effect in cos7 cells and here, co-expression analyses revealed that neurotrypsin indeed inhibits the function of agrin to induce filopodia-like structures, although in a catalytically independent manner.

4.1 Characterisation of agrin protein expression in the murine brain.

Agrin is a complex heparan sulphate proteoglycan and alternative splicing leads to tissue-dependent expression of a variety of different isoforms with distinct functional properties (Bezakova and Ruegg, 2003). Transcript expression analyses in the brain revealed that several cell types, including endothelial and glial cells, express a variety of agrin isoforms while neurons supposedly express these and an additional subset of alternatively spliced variants (Kroger and Schroder, 2002). Agrin protein is found in the CNS on neuronal cell surfaces at various locations, including synapses (Halfter et al., 1997; Koulen et al., 1999; Kroger and Schroder, 2002; Neuhuber and Daniels, 2003; Ksiazek et al., 2007; Stephan et al., 2008), as well as in glial cells and in the basal lamina lining blood vessels (Barber and Lieth, 1997; Halfter et al., 1997; Ksiazek et al., 2007; Stephan et al., 2008). However, due to limitations in the availability of isoform-specific antibodies, differentiation between alternative agrin variants has not been achieved.

Using a variant of SDS-PAGE based on a Bis-Tris buffer adjusted to neutral pH, I was able to resolve brain-derived full-length agrin as three distinct groups of variants with different levels of glycanation, termed upper, middle and lower full-length agrin. The occurrence of differential glycanated variants may indicate differences in the molecules

maturation states whereby lower full-length agrin might represent the most immature agrin variant in an early posttranslational stage. Alternatively, agrin variants expressed by different cell types or with different subcellular localisations might vary in their glycanation pattern, thereby expressing differing functional properties (Brickman et al., 1998; Lindahl et al., 1998).

To investigate whether a particular isoform of agrin was predominant at CNS synapses, I isolated synaptosomes by subcellular fractionation and analysed them with SDS-PAGE. I found that the upper group of agrin variants was the major form in synaptosomes, exceeding the lower variants five-fold, while its excess in the other cellular fractions was less than two-fold. This finding indeed suggests a correlation between the molecule's glycanation state and its subcellular localisation. Glycanation of extracellular matrix molecules, like agrin, serves many diverse functions in the CNS, particularly but not exclusively at the synapse (Yamaguchi, 2002; Dityatev and Schachner, 2003; Kim et al., 2003; Kleene and Schachner, 2004; Dityatev and Schachner, 2006; Van Vactor et al., 2006). Glycans have been shown to bind a variety of different molecules, like chemokines or cell adhesion factors (Kleene and Schachner, 2004; Van Vactor et al., 2006), and the heparan sulphate glycan chains of agrin in particular were shown to bind basic fibroblast growth factor 2 (FGF-2) and thrombospondins (Cotman et al., 1999). Heavy glycanation of synaptic agrin and therefore synaptic accumulation, e.g., of bound thrombospondins or other so far unknown factors would enable their spatially concentrated presentation to their respective receptors.

4.2 Neurotrypsin-dependent cleavage of agrin is concentrated at synapses *in vivo*.

Agrin is the only known and potentially unique substrate of neurotrypsin, considering neurotrypsin's strict substrate requirements (Reif et al., 2007). In line with this argumentation, the temporal as well as spatial expression pattern of agrin and neurotrypsin in the CNS are closely related (Stephan et al., 2008; and unpublished observations).

Neurotrypsin was shown to specifically cleave agrin *in vitro*, releasing two C-terminal fragments from the N-terminal moiety of agrin. I confirmed that agrin is also a substrate of neurotrypsin in the CNS and showed that the C-terminal 90-kDa and the 22-kDa agrin fragments were exclusively generated by neurotrypsin in the murine brain.

Comparison of the three groups of agrin variants with regards to their *in vivo* cleavage revealed that neurotrypsin-dependent cleavage of agrin affected only the glycanated agrin, i.e., the upper and middle variants. Importantly, synaptic upper agrin variants were clearly the preferred proteolytic target of neurotrypsin when compared with agrin found in other subcellular fractions. Synaptosomes from neurotrypsin-overexpressing mice exhibited a significantly stronger reduction of full-length agrin and showed the strongest increase for both agrin fragments. The synaptosomal preparation protocol utilises tissue homogenisation to finally yield synaptosomes, biochemically enriched synaptic structures, containing mainly resealed presynaptic membranes associated with post- and perisynaptic structures, e.g., astroglial membranes enclosing the synapses *in vivo*. The soluble fraction of the preparation,

however, contains a heterogenous pool of both soluble proteins and small membranous particles and fragments, including synaptic vesicles and other synaptic material. Therefore, contamination with targeted synaptic agrin material could explain the detection of neurotrypsin-dependent cleavage of agrin in the soluble fraction. Hence, neurotrypsin may exlusively target synaptic agrin, although extrasynaptic cleavage of agrin cannot be excluded.

The locally concentrated increase of the 90-kDa and 22-kDa agrin fragments at the expense of full-length agrin that was found upon increasing neurotrypsin supports the notion of a precursor-product relationship between full-length agrin and its neurotrypsin-dependent fragments and thus characterises neurotrypsin-dependent cleavage of agrin as a locally concentrated event at or in the vicinity of the synapse.

The notion of a locally concentrated cleavage of agrin at synapses and thus a synaptic source of agrin fragments is corroborated by the stronger increase of the 90-kDa fragment as compared with the 22-kDa fragment in synaptosomes from neurotrypsin-overexpressing mice. Agrin binds with high affinity to α-dystroglycan through a binding site located between the two neurotrypsin-dependent cleavage sites (Gesemann et al., 1996; Gesemann et al., 1998). Therefore, the 90-kDa fragment may be efficiently retained at the site of its production. The 22-kDa fragment, in contrast, appears to be more diffusible. Its appearance in the cerebrospinal fluid (CSF; unpublished observations) indicates that it is either produced in excess over its potential receptors or that its receptor interactions are more volatile than those of the 90-kDa fragment. Because at least stoichiometric amounts are expected for the 22-kDa fragment based on the pattern of proteolytic cleavages that are required for generating the 90-kDa and 22-kDa fragments, its minor increase observed in synaptosomes upon increasing neurotrypsin indicates a synaptic source that has been cleared by a diffusional flux passing via the non-synaptic tissue to the CSF. In accordance with this conclusion, the increase of the 22-kDa fragment observed under transgenic overexpression of neurotrypsin reaches considerably lower levels in all non-synaptosomal fractions as well as in brain homogenates, when compared to the synaptosomal fraction.

Spatially concentrated cleavage of agrin by neurotrypsin at synapses is in accordance with our immuno-electron microscopic localisation of neurotrypsin to presynaptic terminals (Molinari et al., 2002; Stephan et al., 2008) and our recent live imaging studies with cultured hippocampal neurons show that neurotrypsin is transported to synapses and released from presynaptic terminals in an activity-dependent manner (Frischknecht et al., 2008). In addition, neurotrypsin was found to linger at its synaptic release sites for several minutes before disappearing. The molecular mechanism of transient retention of neurotrypsin at the synapse remains to be determined. Interactions with cell surface or ECM components are possible. Basic segments resembling the one found at the N-terminus of neurotrypsin could exert a retaining function via interaction with glycosaminoglycans, possibly those of agrin, and other negatively charged surface components. This was already shown for other positively charged secreted molecules (see also section 4.2.1), including chemokines, cell adhesion molecules or

axon guidance factors, like netrin (Kappler et al., 2000). Restricted mobility by cell-surface and ECM association via its C-terminal basic segment is crucial for netrin's role as a chemotropic agent in axonal guidance (Baker et al., 2006). For neurotrypsin, the transient local lingering at its synaptic site of externalisation may be essential for the spatially concentrated proteolytic action at or near the synapse. In addition, the transient nature of the extracellular presence of neurotrypsin after synaptic externalisation might indicate a temporal restriction of neurotrypsin's synaptic actions.

4.3. Neurotrypsin-dependent cleavage of agrin at the synapse: loss-of-function or gain-of-function?

Nerve-derived agrin plays a crucial and well characterised role at the NMJ (Ruegg and Bixby, 1998). However, studies about the functions of agrin in the CNS are only just emerging and little is known about agrin's interplay with its potential interaction partners, also expressed at CNS synapses (Figure 36). A peptide containing the LG-3 domain of agrin, closely resembling the 22-kDa agrin fragment, was shown to bind to and signal through a synaptic receptor (Hoover et al., 2003) that was identified as the α3-subunit of the Na^+/K^+-ATPase (Hilgenberg et al., 2006). Its inhibitory activity on the Na^+/K^+-ATPase was demonstrated to result in membrane depolarisation and increased action potential firing. A role of agrin in the formation or maintenance of excitatory synapses through a mechanism activated via the MAP kinase signalling pathway has been suggested from the observation that agrin-deficient mice, rescued from perinatal death by transgenic expression of agrin in motoneurons, exhibited a reduced number of synapses in the cerebral cortex (Ksiazek et al., 2007). The agrin receptor in this process has not been identified. However, the authors demonstrated a striking coincidence of agrin-dependent synapse loss and the expression of MuSK in a subpopulation of excitatory synapses and suggested MuSK, which previously was thought not to be expressed in the CNS, as a possible agrin receptor in the CNS. As MuSK activation at the NMJ was unequivocally shown to depend on the C-terminal LG-3 domain of agrin (Gesemann et al., 1995), this domain could also play a role in the activation of MuSK in the CNS.

The region covered by the 90-kDa fragment was shown to interact with heparin (i.e., heparan sulphate proteoglycans), α-dystroglycan and different integrins (Burgess et al., 2002). The diverse synaptic functions reported for these molecules (Cavaldesi et al., 1999; Yamaguchi, 2002; Clegg et al., 2003; Montanaro and Carbonetto, 2003; Kleene and Schachner, 2004; Arcangeli and Becchetti, 2006; Shi and Ethell, 2006) may be modified by binding of agrin or the 90-kDa fragment alone.

Antibody-induced clustering of endogenous agrin as well as the overexpression of transmembrane agrin were recently reported to induce dendritic filopodia in cultured neurons ((Annies et al., 2006; McCroskery et al., 2006); this study, section 3.2.5). Dendritic filopodia are discussed to represent precursors of dendritic spines (Ziv and Smith, 1996; Jontes and Smith, 2000; Portera-Cailliau et al., 2003; Toni et al., 2007), postsynaptic specialisations

mainly associated with excitatory synapses (Ethell and Pasquale, 2005; Lippman and Dunaevsky, 2005; Matus, 2005). Therefore, potential neurotrypsin-dependent modifications of agrin's function may lead to alterations in the synaptic circuitry. Interestingly, recent publications have further strengthened the evidence that the dynamic plasticity of dendritic spines is related to learning and memory processes (Holtmaat et al., 2005; Segal, 2005; Holtmaat et al., 2006; Knott et al., 2006) and aberrations in dendritic structure and dendritic spine morphology have been correlated with MR disorders (Newey et al., 2005). Furthermore, newly generated spines are mainly formed in close proximity to existing synapses (Toni et al., 2007). The addition of C-terminal agrin as well as the overexpression of transmembrane agrin caused the development of filopodia-like protrusions on cultured myotubes (Uhm et al., 2001), supporting the hypothesis that neurotrypsin activity may have a direct effect on agrin's function. In contrast, the N-terminal region of agrin, corresponding to the N-terminal part up to the first neurotrypsin cleavage site, was shown to be sufficient for filopodia induction in cultured neurons (McCroskery et al., 2006). For this scenario, neurotrypsin-dependent cleavage might destabilise agrin's N-terminal region, leading to a rapid degradation or internalisation, thus negatively affecting its role in filopodia generation.

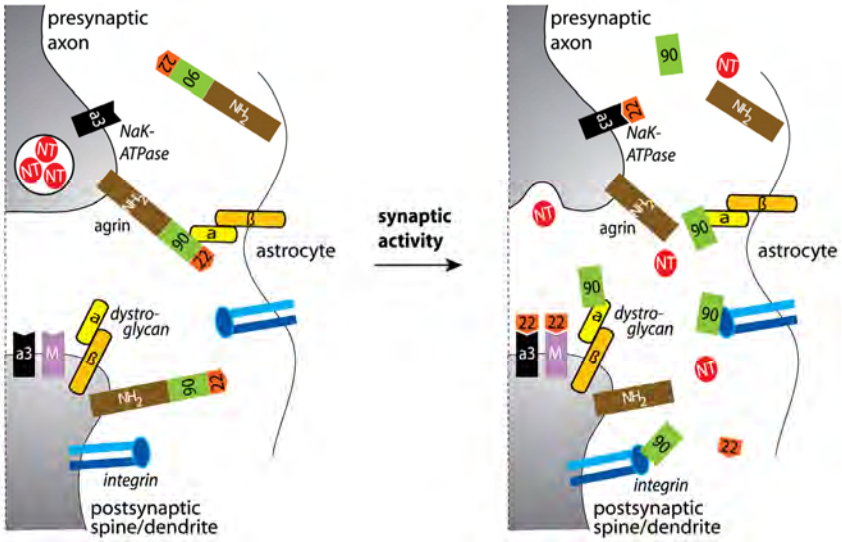

Figure 36. Model of the neurotrypsin-dependent cleavage of synaptic agrin. In the CNS, neurotrypsin (NT) is mainly localised to intracellular vesicles in presynaptic terminals. In contrast, synaptic agrin is mainly localised to extracellular perisynaptic sites. Upon synaptic activity, neurotrypsin is secreted from presynaptic terminals and cleaves synaptic agrin at two sites, generating the 90-kDa and the 22-kDa fragments. Cleavage of agrin may either disrupt its interaction with synaptic partners or enable the released C-terminal fragments to bind to their respective receptors. The region of agrin corresponding to the 90-kDa fragment was shown to interact specifically with α-dystroglycan, integrins and heparin (i.e., heparan sulphate proteoglycans, not depicted, but see Fig. 19A, (Burgess et al., 2002)) that are expressed by neurons or astroglia enclosing the synapse (Smalheiser and Collins, 2000; Winder, 2001; Zaccaria et al., 2001; Yamaguchi, 2002; Clegg et al., 2003). Similarly, the 22-kDa agrin fragment was shown to bind to synaptic receptors. Recent evidence suggests that a C-terminal agrin fragment, closely resembling the 22-kDa fragment generated by neurotrypsin, specifically interacts with the α3-Na^+/K^+-ATPase (α3) at synapses, modifying its functional properties (see Discussion). This isoform of Na^+/K^+-ATPase was shown to localise to presynaptic sites as well as to the postsynaptic plasma membrane (Kim et al., 2007; Taguchi et al., 2007). Another well characterised receptor for the 22-kDa agrin fragment is the receptor tyrosine kinase MuSK (M). MuSK was recently shown to be expressed in the CNS and localised to CNS synapses (Ksiazek et al., 2007), however, its specific subcellular localisation is not known. According to its exclusive location in the postsynaptic membrane of the NMJ, we assigned MuSK to the postsynaptic membrane of CNS synapses.

To obtain first insights into the potential effects of neurotrypsin activity on agrin's function to generate filopodia-like protrusions, I studied their interaction in transiently transfected cos7 cells. Here, similar to published effects in cultured neurons (McCroskery et al., 2006), I observed that transmembrane agrin but not secreted agrin was able to generate filopodia-like structures on cos7 cells. This effect appeared exclusively dependent on the N-terminal half of agrin, as an excess of C-terminal agrin fragments in the culture medium of cells, co- expressing neurotrypsin and secreted agrin, did not yield any impact on the cell morphology. Yet both catalytically active and inactive variants of neurotrypsin inhibited transmembrane agrin's function on cos7 cells, arguing for an effect independent of agrin cleavage. The clustering of transmembrane agrin molecules was suggested to be necessary for the development of agrin's function (Annies et al., 2006). Uncontrolled ectopic expression of agrin in cultured cells has probably triggered automatic clustering of agrin, simply by overloading the cell-surface with continuously delivered agrin molecules. I have shown that neurotrypsin binds to agrin at the cell surface and it is therefore likely that neurotrypsin acted as a spacer between agrin molecules, thus preventing clustering of agrin molecules and inhibiting its function. Observations with cos7 cells, representing a non-polarised cell-type employed for an initial and quick readout of the neurotrypsin-agrin interaction, may however not directly relate to neuronal functions. Especially the neurotrypsin-agrin interaction, believed to occur at or near the synapse, will eventually have to be analysed directly in neurons.

The temporal as well as spatial expression pattern of agrin and neurotrypsin in the CNS are closely related with peak expression during early postnatal development, a period known for extensive synapse generation and major remodelling of synaptic circuits by elimination of excessive or unfavourable connections (Hua and Smith, 2004). Furthermore, both neurotrypsin and agrin are also, but less abundantly, expressed in the adult mouse brain where distinct plasticity-related changes of the synaptic circuitry continue to occur (Chklovskii et al., 2004; Knott et al., 2006). Their distinct developmental regulated expression and the reported involvement of neurotrypsin and agrin in synaptic functions suggest that they play potential roles in synapse generation, synapse refinement and/or synapse elimination.

Neurotrypsin-dependent cleavage of agrin at the synapse may alter agrin's synaptic functions, either by abolishing functions of full-length agrin residing at synapses or by activating regions of agrin from synapse-resident agrin. Thus, the release of active fragments could promote interactions with their respective receptors that were inaccessible for full-length agrin. Further work will be required to elucidate the role of neurotrypsin-dependent cleavage on agrin's synaptic functions and to determine whether cleavage by neurotrypsin induces, modifies, or terminates the activity of agrin at the synapse.

4.4 Virus-mediated expression of neurotrypsin and agrin variants to further analyse parameters of their interaction in dissociated neuronal cultures.

Dissociated hippocampal neuron cultures have proven to be a suitable *in vitro* system to analyse neuronal properties of neurotrypsin. Studies with ectopically expressed

neurotrypsin variants allowed the determination of its activity-dependent synaptic capture and synaptic externalisation (Frischknecht et al., 2008), a finding that is in accordance with its presynaptic localisation *in vivo* (Molinari et al., 2002; Stephan et al., 2008). Efficient ectopic expression of neurotrypsin in cultured neurons was achieved by adenovirus-mediated expression and I therefore generated additional agrin-expressing adenoviruses to complete the tools for further analyses of the neurotrypsin-agrin interaction. Ectopically expressed transmembrane agrin variants were efficiently targeted to axons as well as dendrites, similar to endogenously expressed agrin variants in neuronal cultures ((Escher et al., 1996; Neuhuber and Daniels, 2003); section 3.2.1). Furthermore, the ubiquitous distribution along neuronal surfaces in culture is in line with agrin's expression pattern *in vivo* (Halfter et al., 1997; Koulen et al., 1999; Ksiazek et al., 2007; Stephan et al., 2008), confirming that also the agrin variants are functionally ectopically expressed in cultured hippocampal neurons. It may therefore be concluded that this *in vitro* system meets the basic requirements for further functional studies of the neurotrypsin-agrin interaction. Preliminary experiments with cultured neurons co-expressing neurotrypsin and transmembrane agrin variants revealed that neurotrypsin cleaves agrin in cultured nerve cells. However, neurotrypsin expression led to the complete removal of agrin signals from cellular surfaces, contradicting the assumption of locally restricted synaptic cleavage which resulted from *in vivo* observations. This ubiquitous removal of agrin, however, may have been a result of the high expression levels of neurotrypsin detected in the analysed cells. Expression of the extracellular protease neurotrypsin in cos7 cells resulted in its effective secretion and deposition around cells. High neuronal expression of neurotrypsin may therefore have resulted in excessive extracellular deposition of neurotrypsin and, finally, in extrasynaptic digestion of agrin in neurons. In addition, intracellular interaction in early transport compartments, potentially caused by high expression levels and therefore overloading of the transport machinery, may also have led to ubiquitous agrin cleavage. Again, preliminary results obtained with cultured neurons expressing moderate levels of catalytically inactive neurotrypsin and transmembrane agrin suggested that neurotrypsin and transmembrane agrin are mainly transported in alternate transport compartments and argued for their mainly extracellular interaction. A precondition for detailed future analyses will therefore be to achieve moderate expression levels for both neurotrypsin and agrin proteins. Alternatively, synaptic interaction may also be studied at contact sites of individual neurons expressing agrin or neurotrypsin alone. In addition, studying the neurotrypsin-agrin system in live neurons will be an additional means to decipher details of their interaction.

The co-expression of mRFP-tagged transmembrane agrin and eGFP-tagged neurotrypsin will allow their simultaneous detection in living neurons, thereby enabling the detection of dynamic parameters of their interaction. The application of either N-terminally or C-terminally mRFP-tagged agrin variants is believed to enable the tracking of both domains of agrin after neurotrypsin-dependent cleavage, potentially allowing a complete readout of neurotrypsin-dependent effects on agrin function or localisation. Finally, the supplementary

usage of uncleavable agrin variants as well as catalytically inactive variants of neurotrypsin will enable the verification of functional data.

4.5 Conclusion:

The severe mental retardation found in humans with a loss-of-function mutation in the neurotrypsin gene (Molinari et al., 2002) indicates neurotrypsin as an essential regulator of adaptive synaptic plasticity that is crucial for establishing and maintaining cognitive brain functions. I showed that neurotrypsin cleaves the proteoglycan agrin in the CNS, liberating a middle 90-kDa and a C-terminal 22-kDa fragment from the N-terminal moiety of agrin. Deciphering the regional and functional parameters of the interaction between neurotrypsin and agrin in the brain may thus lead us towards understanding neurotrypsin's essential role in cognitive functions. In this line of thoughts, we recently demonstrated that synaptic neurotrypsin is contained in intracellular stores and that both recruitment of neurotrypsin to synapses and synaptic exocytosis of neurotrypsin are enhanced by neuronal activity (Frischknecht et al., 2008). In this study we also found that externalised neurotrypsin transiently lingers at the synapse, before it disappears by diffusion or degradation. In the current study I also presented evidence that neurotrypsin-dependent cleavage of agrin is focused at or in the vicinity of synapses, where it affects mainly the most heavily glycanated variants of synaptic agrin, which predominate at the synapse. Agrin is a key regulator of the maturation and the maintenance of the neuromuscular junction and recent evidence suggests that agrin may also play an important role in the formation and the maintenance of CNS synapses. The selective activity-dependent externalisation of neurotrypsin and its local cleavage of agrin at the synapse make neurotrypsin an ideal regulator of structural and functional reorganisations of the synaptic circuitry. However, further studies will be required to determine the direct functional implications of agrin's synaptic cleavage by neurotrypsin.

References

Aimes RT, Zijlstra A, Hooper JD, Ogbourne SM, Sit ML, Fuchs S, Gotley DC, Quigley JP, Antalis TM (2003) Endothelial cell serine proteases expressed during vascular morphogenesis and angiogenesis. Thromb Haemost 89:561-572.

Akhondzadeh S (1999) Hippocampal synaptic plasticity and cognition. J Clin Pharm Ther 24:241-248.

Akli S, Caillaud C, Vigne E, Stratford-Perricaudet LD, Poenaru L, Perricaudet M, Kahn A, Peschanski MR (1993) Transfer of a foreign gene into the brain using adenovirus vectors. Nat Genet 3:224-228.

Allen NJ, Barres BA (2005) Signaling between glia and neurons: focus on synaptic plasticity. Curr Opin Neurobiol 15:542-548.

Annies M, Bittcher G, Ramseger R, Loschinger J, Woll S, Porten E, Abraham C, Ruegg MA, Kroger S (2006) Clustering transmembrane-agrin induces filopodia-like processes on axons and dendrites. Mol Cell Neurosci 31:515-524.

Arcangeli A, Becchetti A (2006) Complex functional interaction between integrin receptors and ion channels. Trends Cell Biol 16:631-639.

Bains JS, Oliet SH (2007) Glia: they make your memories stick! Trends Neurosci 30:417-424.

Baker KA, Moore SW, Jarjour AA, Kennedy TE (2006) When a diffusible axon guidance cue stops diffusing: roles for netrins in adhesion and morphogenesis. Curr Opin Neurobiol 16:529-534.

Banker GA (1980) Trophic interactions between astroglial cells and hippocampal neurons in culture. Science 209:809-810.

Barber AJ, Lieth E (1997) Agrin accumulates in the brain microvascular basal lamina during development of the blood-brain barrier. Dev Dyn 208:62-74.

Basel-Vanagaite L, Taub E, Halpern GJ, Drasinover V, Magal N, Davidov B, Zlotogora J, Shohat M (2007) Genetic screening for autosomal recessive nonsyndromic mental retardation in an isolated population in Israel. Eur J Hum Genet 15:250-253.

Benarroch EE (2007) Tissue plasminogen activator: beyond thrombolysis. Neurology 69:799-802.

Benfenati F (2007) Synaptic plasticity and the neurobiology of learning and memory. Acta Biomed 78 Suppl 1:58-66.

Berninger B, Bi GQ (2002) Synaptic modification in neural circuits: a timely action. Bioessays 24:212-222.

Bezakova G, Ruegg MA (2003) New insights into the roles of agrin. Nat Rev Mol Cell Biol 4:295-308.

Binder BR, Mihaly J, Prager GW (2007) uPAR-uPA-PAI-1 interactions and signaling: a vascular biologist's view. Thromb Haemost 97:336-342.

Blanpied TA, Ehlers MD (2004) Microanatomy of dendritic spines: emerging principles of synaptic pathology in psychiatric and neurological disease. Biol Psychiatry 55:1121-1127.

Bliss TV, Collingridge GL (1993) A synaptic model of memory: long-term potentiation in the hippocampus. Nature 361:31-39.

Boda B, Nikonenko I, Alberi S, Muller D (2006) Central Nervous System Functions of PAK Protein Family: From Spine Morphogenesis to Mental Retardation. Mol Neurobiol 34:67-80.

Boda B, Alberi S, Nikonenko I, Node-Langlois R, Jourdain P, Moosmayer M, Parisi-Jourdain L, Muller D (2004) The mental retardation protein PAK3 contributes to synapse formation and plasticity in hippocampus. J Neurosci 24:10816-10825.

Bode W, Huber R (1992) Natural protein proteinase inhibitors and their interaction with proteinases. Eur J Biochem 204:433-451.

Bose CM, Qiu D, Bergamaschi A, Gravante B, Bossi M, Villa A, Rupp F, Malgaroli A (2000) Agrin controls synaptic differentiation in hippocampal neurons. J Neurosci 20:9086-9095.

Brickman YG, Ford MD, Gallagher JT, Nurcombe V, Bartlett PF, Turnbull JE (1998) Structural modification of fibroblast growth factor-binding heparan sulfate at a determinative stage of neural development. J Biol Chem 273:4350-4359.

Burgess RW, Dickman DK, Nunez L, Glass DJ, Sanes JR (2002) Mapping sites responsible for interactions of agrin with neurons. J Neurochem 83:271-284.

Campbell RE, Tour O, Palmer AE, Steinbach PA, Baird GS, Zacharias DA, Tsien RY (2002) A monomeric red fluorescent protein. Proc Natl Acad Sci U S A 99:7877-7882.

Carlisle HJ, Kennedy MB (2005) Spine architecture and synaptic plasticity. Trends Neurosci 28:182-187.

Caroni P (1997) Overexpression of growth-associated proteins in the neurons of adult transgenic mice. J Neurosci Methods 71:3-9.

Cavaldesi M, Macchia G, Barca S, Defilippi P, Tarone G, Petrucci TC (1999) Association of the dystroglycan complex isolated from bovine brain synaptosomes with proteins involved in signal transduction. J Neurochem 72:1648-1655.

Chelly J, Mandel JL (2001) Monogenic causes of X-linked mental retardation. Nat Rev Genet 2:669-680.

Cheusova T, Khan MA, Enz R, Hashemolhosseini S (2006) Identification of developmentally regulated expression of MuSK in astrocytes of the rodent retina. J Neurochem 99:450-457.

Chklovskii DB, Mel BW, Svoboda K (2004) Cortical rewiring and information storage. Nature 431:782-788.

Clegg DO, Wingerd KL, Hikita ST, Tolhurst EC (2003) Integrins in the development, function and dysfunction of the nervous system. Front Biosci 8:d723-750.

Cohen NA, Kaufmann WE, Worley PF, Rupp F (1997) Expression of agrin in the developing and adult rat brain. Neuroscience 76:581-596.

Cooke SF, Bliss TV (2006) Plasticity in the human central nervous system. Brain 129:1659-1673.

Cotman SL, Halfter W, Cole GJ (1999) Identification of extracellular matrix ligands for the heparan sulfate proteoglycan agrin. Exp Cell Res 249:54-64.

Cubitt AB, Heim R, Adams SR, Boyd AE, Gross LA, Tsien RY (1995) Understanding, improving and using green fluorescent proteins. Trends Biochem Sci 20:448-455.

De Paola V, Arber S, Caroni P (2003) AMPA receptors regulate dynamic equilibrium of presynaptic terminals in mature hippocampal networks. Nat Neurosci 6:491-500.

De Paola V, Holtmaat A, Knott G, Song S, Wilbrecht L, Caroni P, Svoboda K (2006) Cell type-specific structural plasticity of axonal branches and boutons in the adult neocortex. Neuron 49:861-875.

DeChiara TM, Bowen DC, Valenzuela DM, Simmons MV, Poueymirou WT, Thomas S, Kinetz E, Compton DL, Rojas E, Park JS, Smith C, DiStefano PS, Glass DJ, Burden SJ, Yancopoulos GD (1996) The receptor tyrosine kinase MuSK is required for neuromuscular junction formation in vivo. Cell 85:501-512.

Denzer AJ, Gesemann M, Schumacher B, Ruegg MA (1995) An amino-terminal extension is required for the secretion of chick agrin and its binding to extracellular matrix. J Cell Biol 131:1547-1560.

Dickson BJ (2002) Molecular mechanisms of axon guidance. Science 298:1959-1964.

Dityatev A, Schachner M (2003) Extracellular matrix molecules and synaptic plasticity. Nat Rev Neurosci 4:456-468.

Dityatev A, Schachner M (2006) The extracellular matrix and synapses. Cell Tissue Res 326:647-654.

Du Y, Dreyfus CF (2002) Oligodendrocytes as providers of growth factors. J Neurosci Res 68:647-654.

Duffau H (2006) Brain plasticity: from pathophysiological mechanisms to therapeutic applications. J Clin Neurosci 13:885-897.

Escher G, Bechade C, Levi S, Triller A (1996) Axonal targeting of agrin in cultured rat dorsal horn neurons. J Cell Sci 109 (Pt 13):2959-2966.

Ethell IM, Pasquale EB (2005) Molecular mechanisms of dendritic spine development and remodeling. Prog Neurobiol 75:161-205.

Ethell IM, Ethell DW (2007) Matrix metalloproteinases in brain development and remodeling: synaptic functions and targets. J Neurosci Res 85:2813-2823.

Fernandez F, Garner CC (2007) Over-inhibition: a model for developmental intellectual disability. Trends Neurosci 30:497-503.

Ferns M, Hoch W, Campanelli JT, Rupp F, Hall ZW, Scheller RH (1992) RNA splicing regulates agrin-mediated acetylcholine receptor clustering activity on cultured myotubes. Neuron 8:1079-1086.

Ferns MJ, Campanelli JT, Hoch W, Scheller RH, Hall Z (1993) The ability of agrin to cluster AChRs depends on alternative splicing and on cell surface proteoglycans. Neuron 11:491-502.

Ferreira A (1999) Abnormal synapse formation in agrin-depleted hippocampal neurons. J Cell Sci 112 (Pt 24):4729-4738.

Frerking M, Nicoll RA (2000) Synaptic kainate receptors. Curr Opin Neurobiol 10:342-351.

Frischknecht R, Fejtova A, Viesti M, Stephan A, Sonderegger P (2008) Activity-Induced Synaptic Capture and Exocytosis of the Neuronal Serine Protease Neurotrypsin. J Neurosci 28:1568-1579.

Fritschy JM, Brunig I (2003) Formation and plasticity of GABAergic synapses: physiological mechanisms and pathophysiological implications. Pharmacol Ther 98:299-323.

Frotscher M, Zhao S, Graber W, Drakew A, Studer D (2007) New ways of looking at synapses. Histochem Cell Biol 128:91-96.

Galliciotti G, Sonderegger P (2006) Neuroserpin. Front Biosci 11:33-45.

Garcia-Osta A, Tsokas P, Pollonini G, Landau EM, Blitzer R, Alberini CM (2006) MuSK expressed in the brain mediates cholinergic responses, synaptic plasticity, and memory formation. J Neurosci 26:7919-7932.

Garner CC, Waites CL, Ziv NE (2006) Synapse development: still looking for the forest, still lost in the trees. Cell Tissue Res 326:249-262.

Garner CC, Zhai RG, Gundelfinger ED, Ziv NE (2002) Molecular mechanisms of CNS synaptogenesis. Trends Neurosci 25:243-251.

Gautam M, Noakes PG, Moscoso L, Rupp F, Scheller RH, Merlie JP, Sanes JR (1996) Defective neuromuscular synaptogenesis in agrin-deficient mutant mice. Cell 85:525-535.

Gesemann M, Denzer AJ, Ruegg MA (1995) Acetylcholine receptor-aggregating activity of agrin isoforms and mapping of the active site. J Cell Biol 128:625-636.

Gesemann M, Brancaccio A, Schumacher B, Ruegg MA (1998) Agrin is a high-affinity binding protein of dystroglycan in non-muscle tissue. J Biol Chem 273:600-605.

Gesemann M, Cavalli V, Denzer AJ, Brancaccio A, Schumacher B, Ruegg MA (1996) Alternative splicing of agrin alters its binding to heparin, dystroglycan, and the putative agrin receptor. Neuron 16:755-767.

Giger RJ, Ziegler U, Hermens WT, Kunz B, Kunz S, Sonderegger P (1997) Adenovirus-mediated gene transfer in neurons: construction and characterization of a vector for heterologous expression of the axonal cell adhesion molecule axonin-1. J Neurosci Methods 71:99-111.

Gingras J, Ferns M (2001) Expression and localization of agrin during sympathetic synapse formation in vitro. J Neurobiol 48:228-242.

Gingras J, Rassadi S, Cooper E, Ferns M (2002) Agrin plays an organizing role in the formation of sympathetic synapses. J Cell Biol 158:1109-1118.

Gingras J, Rassadi S, Cooper E, Ferns M (2007) Synaptic transmission is impaired at neuronal autonomic synapses in agrin-null mice. Dev Neurobiol 67:521-534.

Glass DJ, Apel ED, Shah S, Bowen DC, DeChiara TM, Stitt TN, Sanes JR, Yancopoulos GD (1997) Kinase domain of the muscle-specific receptor tyrosine kinase (MuSK) is sufficient for phosphorylation but not clustering of acetylcholine receptors: required role for the MuSK ectodomain? Proc Natl Acad Sci U S A 94:8848-8853.

Glass DJ, Bowen DC, Stitt TN, Radziejewski C, Bruno J, Ryan TE, Gies DR, Shah S, Mattsson K, Burden SJ, DiStefano PS, Valenzuela DM, DeChiara TM, Yancopoulos GD (1996) Agrin acts via a MuSK receptor complex. Cell 85:513-523.

Goslin K, Asmussen,H. and Banker, G. (1998) Rat Hippocampal Neurons in Low-Density Culture. In: Culturing Nerve Cells (Banker GaG, K., ed), pp 339-370. Cambridge, Massachusetts: MIT Press.

Graham FL, Smiley J, Russell WC, Nairn R (1977) Characteristics of a human cell line transformed by DNA from human adenovirus type 5. J Gen Virol 36:59-74.

Groc L, Gustafsson B, Hanse E (2006) AMPA signalling in nascent glutamatergic synapses: there and not there! Trends Neurosci 29:132-139.

Gschwend TP, Krueger SR, Kozlov SV, Wolfer DP, Sonderegger P (1997) Neurotrypsin, a novel multidomain serine protease expressed in the nervous system. Mol Cell Neurosci 9:207-219.

Halassa MM, Fellin T, Haydon PG (2007) The tripartite synapse: roles for gliotransmission in health and disease. Trends Mol Med 13:54-63.

Halfter W, Schurer B, Yip J, Yip L, Tsen G, Lee JA, Cole GJ (1997) Distribution and substrate properties of agrin, a heparan sulfate proteoglycan of developing axonal pathways. J Comp Neurol 383:1-17.

Hayashi Y, Majewska AK (2005) Dendritic spine geometry: functional implication and regulation. Neuron 46:529-532.

Hedstrom L (2002) Serine protease mechanism and specificity. Chem Rev 102:4501-4524.

Henry MD, Campbell KP (1996) Dystroglycan: an extracellular matrix receptor linked to the cytoskeleton. Curr Opin Cell Biol 8:625-631.

Heim R, Cubitt AB, Tsien RY (1995) Improved green fluorescence. Nature 373:663-664.

Hilgenberg LG, Smith MA (2004) Agrin signaling in cortical neurons is mediated by a tyrosine kinase-dependent increase in intracellular Ca2+ that engages both CaMKII and MAPK signal pathways. J Neurobiol 61:289-300.

Hilgenberg LG, Hoover CL, Smith MA (1999) Evidence of an agrin receptor in cortical neurons. J Neurosci 19:7384-7393.

Hilgenberg LG, Ho KD, Lee D, O'Dowd DK, Smith MA (2002) Agrin regulates neuronal responses to excitatory neurotransmitters in vitro and in vivo. Mol Cell Neurosci 19:97-110.

Hilgenberg LG, Su H, Gu H, O'Dowd DK, Smith MA (2006) Alpha3Na+/K+-ATPase is a neuronal receptor for agrin. Cell 125:359-369.

Hoch W, Ferns M, Campanelli JT, Hall ZW, Scheller RH (1993) Developmental regulation of highly active alternatively spliced forms of agrin. Neuron 11:479-490.

Holtmaat A, Wilbrecht L, Knott GW, Welker E, Svoboda K (2006) Experience-dependent and cell-type-specific spine growth in the neocortex. Nature 441:979-983.

Holtmaat AJ, Trachtenberg JT, Wilbrecht L, Shepherd GM, Zhang X, Knott GW, Svoboda K (2005) Transient and persistent dendritic spines in the neocortex in vivo. Neuron 45:279-291.

Hook VY (2006) Protease pathways in peptide neurotransmission and neurodegenerative diseases. Cell Mol Neurobiol 26:449-469.

Hoover CL, Hilgenberg LG, Smith MA (2003) The COOH-terminal domain of agrin signals via a synaptic receptor in central nervous system neurons. J Cell Biol 161:923-932.

Hua JY, Smith SJ (2004) Neural activity and the dynamics of central nervous system development. Nat Neurosci 7:327-332.

Iijima N, Tanaka M, Mitsui S, Yamamura Y, Yamaguchi N, Ibata Y (1999) Expression of a serine protease (motopsin PRSS12) mRNA in the mouse brain: in situ hybridization histochemical study. Brain Res Mol Brain Res 66:141-149.

Ito-Ishida A, Kakegawa W, Yuzaki M (2006) ERK1/2 but not p38 MAP kinase is essential for the long-term depression in mouse cerebellar slices. Eur J Neurosci 24:1617-1622.

Ji RR, Bose CM, Lesuisse C, Qiu D, Huang JC, Zhang Q, Rupp F (1998) Specific agrin isoforms induce cAMP response element binding protein phosphorylation in hippocampal neurons. J Neurosci 18:9695-9702.

Johnston MV (2004) Clinical disorders of brain plasticity. Brain Dev 26:73-80.

Jontes JD, Smith SJ (2000) Filopodia, spines, and the generation of synaptic diversity. Neuron 27:11-14.

Juttner R, Rathjen FG (2005) Molecular analysis of axonal target specificity and synapse formation. Cell Mol Life Sci 62:2811-2827.

Kaech S, Banker G (2006) Culturing hippocampal neurons. Nat Protoc 1:2406-2415.

Kandel E (2000) Principles of Neural Science, 4th Edition. New York: The McGraw-Hill Compamies Inc.

Kappler J, Franken S, Junghans U, Hoffmann R, Linke T, Muller HW, Koch KW (2000) Glycosaminoglycan-binding properties and secondary structure of the C-terminus of netrin-1. Biochem Biophys Res Commun 271:287-291.

Kärber G (1931) Beitrag zur kollektiven Behandlung pharmakologischer Reihenversuche. Arch Exp Path Pharmak 162:480-483.

Keller A (2002) Use-dependent inhibition of dendritic spines. Trends Neurosci 25:541-543; discussion 543-544.

Khan AR, James MN (1998) Molecular mechanisms for the conversion of zymogens to active proteolytic enzymes. Protein Sci 7:815-836.

Kim JH, Sizov I, Dobretsov M, von Gersdorff H (2007) Presynaptic Ca2+ buffers control the strength of a fast post-tetanic hyperpolarization mediated by the alpha3 Na(+)/K(+)-ATPase. Nat Neurosci 10:196-205.

Kim MJ, Cotman SL, Halfter W, Cole GJ (2003) The heparan sulfate proteoglycan agrin modulates neurite outgrowth mediated by FGF-2. J Neurobiol 55:261-277.

Kitabatake Y, Sailor KA, Ming GL, Song H (2007) Adult neurogenesis and hippocampal memory function: new cells, more plasticity, new memories? Neurosurg Clin N Am 18:105-113, x.

Kleene R, Schachner M (2004) Glycans and neural cell interactions. Nat Rev Neurosci 5:195-208.

Knott GW, Holtmaat A, Wilbrecht L, Welker E, Svoboda K (2006) Spine growth precedes synapse formation in the adult neocortex in vivo. Nat Neurosci 9:1117-1124.

Koulen P, Honig LS, Fletcher EL, Kroger S (1999) Expression, distribution and ultrastructural localization of the synapse-organizing molecule agrin in the mature avian retina. Eur J Neurosci 11:4188-4196.

Kreis P, Thevenot E, Rousseau V, Boda B, Muller D, Barnier JV (2007) The p21-activated kinase 3 implicated in mental retardation regulates spine morphogenesis through a Cdc42-dependent pathway. J Biol Chem 282:21497-21506.

Kroger S, Schroder JE (2002) Agrin in the developing CNS: new roles for a synapse organizer. News Physiol Sci 17:207-212.

Ksiazek I, Burkhardt C, Lin S, Seddik R, Maj M, Bezakova G, Jucker M, Arber S, Caroni P, Sanes JR, Bettler B, Ruegg MA (2007) Synapse loss in cortex of agrin-deficient mice after genetic rescue of perinatal death. J Neurosci 27:7183-7195.

Kummer TT, Misgeld T, Sanes JR (2006) Assembly of the postsynaptic membrane at the neuromuscular junction: paradigm lost. Curr Opin Neurobiol 16:74-82.

Laemmli UK (1970) Cleavage of structural proteins during the assembly of the head of bacteriophage T4. Nature 227:680-685.

Lagercrantz H, Ringstedt T (2001) Organization of the neuronal circuits in the central nervous system during development. Acta Paediatr 90:707-715.

Lesuisse C, Qiu D, Bose CM, Nakaso K, Rupp F (2000) Regulation of agrin expression in hippocampal neurons by cell contact and electrical activity. Brain Res Mol Brain Res 81:92-100.

Li Z, Massengill JL, O'Dowd DK, Smith MA (1997) Agrin gene expression in mouse somatosensory cortical neurons during development in vivo and in cell culture. Neuroscience 79:191-201.

Li Z, Hilgenberg LG, O'Dowd DK, Smith MA (1999) Formation of functional synaptic connections between cultured cortical neurons from agrin-deficient mice. J Neurobiol 39:547-557.

Lin W, Burgess RW, Dominguez B, Pfaff SL, Sanes JR, Lee KF (2001) Distinct roles of nerve and muscle in postsynaptic differentiation of the neuromuscular synapse. Nature 410:1057-1064.

Lindahl U, Kusche-Gullberg M, Kjellen L (1998) Regulated diversity of heparan sulfate. J Biol Chem 273:24979-24982.

Lippman J, Dunaevsky A (2005) Dendritic spine morphogenesis and plasticity. J Neurobiol 64:47-57.

Liu BP, Cafferty WB, Budel SO, Strittmatter SM (2006) Extracellular regulators of axonal growth in the adult central nervous system. Philos Trans R Soc Lond B Biol Sci 361:1593-1610.

Lujan R, Shigemoto R, Lopez-Bendito G (2005) Glutamate and GABA receptor signalling in the developing brain. Neuroscience 130:567-580.

Lukes A, Mun-Bryce S, Lukes M, Rosenberg GA (1999) Extracellular matrix degradation by metalloproteinases and central nervous system diseases. Mol Neurobiol 19:267-284.

Malenka RC, Nicoll RA (1999) Long-term potentiation--a decade of progress? Science 285:1870-1874.

Matus A (2005) Growth of dendritic spines: a continuing story. Curr Opin Neurobiol 15:67-72.

McAllister AK (2007) Dynamic aspects of CNS synapse formation. Annu Rev Neurosci 30:425-450.

McCroskery S, Chaudhry A, Lin L, Daniels MP (2006) Transmembrane agrin regulates filopodia in rat hippocampal neurons in culture. Mol Cell Neurosci 33:15-28.

Miller R (1973) Nonparametric estimates of the mean tollerance in bioassays. Biometrica 3:535-542

Ming GL, Song H (2005) Adult neurogenesis in the mammalian central nervous system. Annu Rev Neurosci 28:223-250.

Mohanty S, Spinas GA, Maedler K, Zuellig RA, Lehmann R, Donath MY, Trub T, Niessen M (2005) Overexpression of IRS2 in isolated pancreatic islets causes proliferation and protects human beta-cells from hyperglycemia-induced apoptosis. Exp Cell Res 303:68-78.

Molinari F, Rio M, Meskenaite V, Encha-Razavi F, Auge J, Bacq D, Briault S, Vekemans M, Munnich A, Attie-Bitach T, Sonderegger P, Colleaux L (2002) Truncating neurotrypsin mutation in autosomal recessive nonsyndromic mental retardation. Science 298:1779-1781.

Montanaro F, Carbonetto S (2003) Targeting dystroglycan in the brain. Neuron 37:193-196.

Nadkarni S, Jung P (2007) Modeling synaptic transmission of the tripartite synapse. Phys Biol 4:1-9.

Neuhuber B, Daniels MP (2003) Targeting of recombinant agrin to axonal growth cones. Mol Cell Neurosci 24:1180-1196.

Neumann FR, Bittcher G, Annies M, Schumacher B, Kroger S, Ruegg MA (2001) An alternative amino-terminus expressed in the central nervous system converts agrin to a type II transmembrane protein. Mol Cell Neurosci 17:208-225.

Neves G, Cooke SF, Bliss TV (2008) Synaptic plasticity, memory and the hippocampus: a neural network approach to causality. Nat Rev Neurosci 9:65-75.

Newey SE, Velamoor V, Govek EE, Van Aelst L (2005) Rho GTPases, dendritic structure, and mental retardation. J Neurobiol 64:58-74.

Ngo ST, Noakes PG, Phillips WD (2007) Neural agrin: a synaptic stabiliser. Int J Biochem Cell Biol 39:863-867.

Nicoll RA, Malenka RC (1995) Contrasting properties of two forms of long-term potentiation in the hippocampus. Nature 377:115-118.

Nimchinsky EA, Sabatini BL, Svoboda K (2002) Structure and function of dendritic spines. Annu Rev Physiol 64:313-353.

Nitkin RM, Smith MA, Magill C, Fallon JR, Yao YM, Wallace BG, McMahan UJ (1987) Identification of agrin, a synaptic organizing protein from Torpedo electric organ. J Cell Biol 105:2471-2478.

Numajiri T, Mitsui S, Hisa Y, Ishida T, Nishino K, Yamaguchi N (2006) The expression of a motoneuron-specific serine protease, motopsin (PRSS12), after facial nerve axotomy in mice. J Plast Reconstr Aesthet Surg 59:393-397.

O'Connor LT, Lauterborn JC, Smith MA, Gall CM (1995) Expression of agrin mRNA is altered following seizures in adult rat brain. Brain Res Mol Brain Res 33:277-287.

Oliet SH, Piet R, Poulain DA, Theodosis DT (2004) Glial modulation of synaptic transmission: Insights from the supraoptic nucleus of the hypothalamus. Glia 47:258-267.

Page MJ, Macgillivray RT, Di Cera E (2005) Determinants of specificity in coagulation proteases. J Thromb Haemost 3:2401-2408.

Parkhomovskiy N, Kammesheidt A, Martin PT (2000) N-acetyllactosamine and the CT carbohydrate antigen mediate agrin-dependent activation of MuSK and acetylcholine receptor clustering in skeletal muscle. Mol Cell Neurosci 15:380-397.

Pavlov I, Lauri S, Taira T, Rauvala H (2004) The role of ECM molecules in activity-dependent synaptic development and plasticity. Birth Defects Res C Embryo Today 72:12-24.

Payment P, Trudel M (1993) Isolation and identification of viruses: titration of viruses in cell culture by cytopathic effect. New York: Marcel Dekker Inc.

Phelan P, Gordon PR (1997) Isolation of synaptosomes, growth cones and their subcellular compounds, Second edition Edition: Oxford University Press.

Portera-Cailliau C, Pan DT, Yuste R (2003) Activity-regulated dynamic behavior of early dendritic protrusions: evidence for different types of dendritic filopodia. J Neurosci 23:7129-7142.

Proba K, Gschwend TP, Sonderegger P (1998) Cloning and sequencing of the cDNA encoding human neurotrypsin. Biochim Biophys Acta 1396:143-147.

Radrizzani M, Carminatti H, Pivetta OH, Idoyaga Vargas VP (1995) Developmental regulation of Thy 1.2 rate of synthesis in the mouse cerebellum. J Neurosci Res 42:220-227.

Reif R, Sales S, Hettwer S, Dreier B, Gisler C, Wolfel J, Luscher D, Zurlinden A, Stephan A, Ahmed S, Baici A, Ledermann B, Kunz B, Sonderegger P (2007) Specific cleavage of agrin by neurotrypsin, a synaptic protease linked to mental retardation. FASEB J 21:3468-3478.

Rubio ME (2000) Selective targeting of glutamate receptors in neurons. Mol Neurobiol 21:1-19.

Ruegg MA, Bixby JL (1998) Agrin orchestrates synaptic differentiation at the vertebrate neuromuscular junction. Trends Neurosci 21:22-27.

Rulicke T (2004) Pronuclear Microinjection of Mouse Zygotes. Totowa, NJ, USA: The Humana Press Inc.

Rupp F, Payan DG, Magill-Solc C, Cowan DM, Scheller RH (1991) Structure and expression of a rat agrin. Neuron 6:811-823.

Samson AL, Medcalf RL (2006) Tissue-type plasminogen activator: a multifaceted modulator of neurotransmission and synaptic plasticity. Neuron 50:673-678.

Sanes JR, Lichtman JW (1999) Development of the vertebrate neuromuscular junction. Annu Rev Neurosci 22:389-442.

Sanes JR, Lichtman JW (2001) Induction, assembly, maturation and maintenance of a postsynaptic apparatus. Nat Rev Neurosci 2:791-805.

Sauer B (1998) Inducible gene targeting in mice using the Cre/lox system. Methods 14:381-392.

Schwenk F, Baron U, Rajewsky K (1995) A cre-transgenic mouse strain for the ubiquitous deletion of loxP-flanked gene segments including deletion in germ cells. Nucleic Acids Res 23:5080-5081.

Segal M (2005) Dendritic spines and long-term plasticity. Nat Rev Neurosci 6:277-284.

Serpinskaya AS, Feng G, Sanes JR, Craig AM (1999) Synapse formation by hippocampal neurons from agrin-deficient mice. Dev Biol 205:65-78.

Shen K (2004) Molecular mechanisms of target specificity during synapse formation. Curr Opin Neurobiol 14:83-88.

Shepherd JD, Huganir RL (2007) The cell biology of synaptic plasticity: AMPA receptor trafficking. Annu Rev Cell Dev Biol 23:613-643.

Shi Y, Ethell IM (2006) Integrins control dendritic spine plasticity in hippocampal neurons through NMDA receptor and Ca2+/calmodulin-dependent protein kinase II-mediated actin reorganization. J Neurosci 26:1813-1822.

Shiosaka S (2004) Serine proteases regulating synaptic plasticity. Anat Sci Int 79:137-144.

Smalheiser NR, Collins BJ (2000) Coordinate enrichment of cranin (dystroglycan) subunits in synaptic membranes of sheep brain. Brain Res 887:469-471.

Smith MA, Hilgenberg LG (2002) Agrin in the CNS: a protein in search of a function? Neuroreport 13:1485-1495.

Spearman C (1908) The method of right and wrong cases (constant stimuli) without Gaus's formulae. Brit J Psychol 2:227-242.

Stephan A, Matoes J, Kozlov S, Cinelli P, Kistler A, Hettwer S, Rülicke T, Streit P, Kunz B, Sonderegger P (2008) Neurotrypsin cleaves agrin locally at the synapse. FASEB J, in press, Jan. 29, 2008 [Epub ahead of print].

Sternberg N, Hamilton D (1981) Bacteriophage P1 site-specific recombination. I. Recombination between loxP sites. J Mol Biol 150:467-486.

Tada T, Sheng M (2006) Molecular mechanisms of dendritic spine morphogenesis. Curr Opin Neurobiol 16:95-101.

Taguchi K, Kumanogoh H, Nakamura S, Maekawa S (2007) Ouabain-induced isoform-specific localization change of the Na+, K+-ATPase alpha subunit in the synaptic plasma membrane of rat brain. Neurosci Lett 413:42-45.

Taylor AC, Robbins E (1963) Observations on microextensions from the surface of isolated vertebrate cells. Dev Biol 7:660-673.

Thomas G (2002) Furin at the cutting edge: from protein traffic to embryogenesis and disease. Nat Rev Mol Cell Biol 3:753-766.

Tollefson AE, Scaria A, Hermiston TW, Ryerse JS, Wold LJ, Wold WS (1996) The adenovirus death protein (E3-11.6K) is required at very late stages of infection for efficient cell lysis and release of adenovirus from infected cells. J Virol 70:2296-2306.

Toni N, Teng EM, Bushong EA, Aimone JB, Zhao C, Consiglio A, van Praag H, Martone ME, Ellisman MH, Gage FH (2007) Synapse formation on neurons born in the adult hippocampus. Nat Neurosci 10:727-734.

Triller A, Choquet D (2003) Synaptic structure and diffusion dynamics of synaptic receptors. Biol Cell 95:465-476.

Tsen G, Halfter W, Kroger S, Cole GJ (1995) Agrin is a heparan sulfate proteoglycan. J Biol Chem 270:3392-3399.

Tsim KW, Ruegg MA, Escher G, Kroger S, McMahan UJ (1992) cDNA that encodes active agrin. Neuron 8:677-689.

Uhm CS, Neuhuber B, Lowe B, Crocker V, Daniels MP (2001) Synapse-forming axons and recombinant agrin induce microprocess formation on myotubes. J Neurosci 21:9678-9689.

Van Vactor D, Wall DP, Johnson KG (2006) Heparan sulfate proteoglycans and the emergence of neuronal connectivity. Curr Opin Neurobiol 16:40-51.

Washbourne P, McAllister AK (2002) Techniques for gene transfer into neurons. Curr Opin Neurobiol 12:566-573.

Wessel D, Flugge UI (1984) A method for the quantitative recovery of protein in dilute solution in the presence of detergents and lipids. Anal Biochem 138:141-143.

Wilkemeyer MF, Smith KL, Zarei MM, Benke TA, Swann JW, Angelides KJ, Eisensmith RC (1996) Adenovirus-mediated gene transfer into dissociated and explant cultures of rat hippocampal neurons. J Neurosci Res 43:161-174.

Winder SJ (2001) The complexities of dystroglycan. Trends Biochem Sci 26:118-124.

Winzen U, Cole GJ, Halfter W (2003) Agrin is a chimeric proteoglycan with the attachment sites for heparan sulfate/chondroitin sulfate located in two multiple serine-glycine clusters. J Biol Chem 278:30106-30114.

Witcher MR, Kirov SA, Harris KM (2007) Plasticity of perisynaptic astroglia during synaptogenesis in the mature rat hippocampus. Glia 55:13-23.

Wolfer DP, Lang R, Cinelli P, Madani R, Sonderegger P (2001) Multiple roles of neurotrypsin in tissue morphogenesis and nervous system development suggested by the mRNA expression pattern. Mol Cell Neurosci 18:407-433.

Xia B, Martin PT (2002) Modulation of agrin binding and activity by the CT and related carbohydrate antigens. Mol Cell Neurosci 19:539-551.

Xu HL, Su B (2005) Genetic evidence of a strong functional constraint of neurotrypsin during primate evolution. Cytogenet Genome Res 108:303-309.

Yamaguchi Y (2002) Glycobiology of the synapse: the role of glycans in the formation, maturation, and modulation of synapses. Biochim Biophys Acta 1573:369-376.

Yamamura Y, Yamashiro K, Tsuruoka N, Nakazato H, Tsujimura A, Yamaguchi N (1997) Molecular cloning of a novel brain-specific serine protease with a kringle-like structure and three scavenger receptor cysteine-rich motifs. Biochem Biophys Res Commun 239:386-392.

Yepes M, Lawrence DA (2004) Neuroserpin: a selective inhibitor of tissue-type plasminogen activator in the central nervous system. Thromb Haemost 91:457-464.

Zaccaria ML, Di Tommaso F, Brancaccio A, Paggi P, Petrucci TC (2001) Dystroglycan distribution in adult mouse brain: a light and electron microscopy study. Neuroscience 104:311-324.

Zalfa F, Achsel T, Bagni C (2006) mRNPs, polysomes or granules: FMRP in neuronal protein synthesis. Curr Opin Neurobiol 16:265-269.

Zhang Y, Pothakos K, Tsirka SA (2005) Extracellular proteases: biological and behavioral roles in the mammalian central nervous system. Curr Top Dev Biol 66:161-188.

Ziv NE, Smith SJ (1996) Evidence for a role of dendritic filopodia in synaptogenesis and spine formation. Neuron 17:91-102.

Zuo Y, Yang G, Kwon E, Gan WB (2005a) Long-term sensory deprivation prevents dendritic spine loss in primary somatosensory cortex. Nature 436:261-265.

Zuo Y, Lin A, Chang P, Gan WB (2005b) Development of long-term dendritic spine stability in diverse regions of cerebral cortex. Neuron 46:181-189.

Acknowledgements

I would like to thank Prof. Dr. Peter Sonderegger for giving me the opportunity to do my PhD in his lab, for his supervision and for his continuous and great support of my work and scientific education! I would also like to thank my PhD committee members Prof. Dr. Peter Streit and PD Dr. Jack Rohrer for taking their time to answer all my questions and for their continuous and kind support. I am very grateful to Prof. Dr. Jean-Marc Fritschy who agreed to additionally join my PhD committee for the examination of my thesis and the oral presentation, as well as for finding the time to discuss and suggest possibilities for my scientific future. I would like to thank all past and present members of the Sonderegger lab for their help, advice and for creating a really friendly and relaxed atmosphere, with special thanks to Andreas Kistler, José María Mateos, Beat Kunz, Daniel Blaser, Andreas Zurlinden, Renato Frischknecht, Stefan Hettwer, Raymond Reif, Pascal Walther and Alexander Ludwig. My parents deserve special thanks for their continuous support of my education and their unreserved believe in the successful progression of my scientific career. This also holds true for all my friends, thanks to all of you but especially to Ilona, who, besides being a true and special friend, helped me in lots of different ways during the course of my PhD.

Curriculum Vitae

Name	STEPHAN
Vorname	Alexander
Geburtsdatum	07.10.1975
Geburtsort	Hamburg, Deutschland
Nationalität	Deutsch

Ausbildung

1986-1995	Gymnasium Heidberg, Hamburg, Deutschland; Abschluss: Abitur
1995-1997	Ausbildung mit Abschluss zum Bankkaufmann, Hamburger Sparkasse, Hamburg, Deutschland
1997-2003	Studium der Biologie, Universität Hamburg, Deutschland Diplomfächer: Zoologie, Biochemie, Molekularbiologie Diplomarbeit in der Arbeitsgruppe von Prof. Dr. Thomas Jentsch, Zentrum für Molekulare Neurobiologie Hamburg (ZMNH), Deutschland. Thema: *Untersuchungen zur physiologischen Funktion des Chloridkanals ClC-7 in Fibroblasten adulter Mäuse (mus musculus).*
07.03.2003	Abschluss als Diplom Biologe
2003-2008	Doktorand in der Arbeitsgruppe von Prof. Dr. Peter Sonderegger, Biochemisches Institut der Universität Zürich, Schweiz. Thema: *Analyse der funktionellen Interaktion von Neurotrypsin und Agrin im Zentralen Nervensystem der Maus (mus musculus).*

Publikationen

Olcese, J. et al, 2002, *Nocturnal accumulation of cyclic 3´,5´-guanosine monophosphate (cGMP) in the chick pineal organ is dependent on activation of guanylyl cyclase-B*, J. Neuroendocrinol., 14(1), 14-18.

Reif, R. et al, 2007, *Highly specific cleavage of agrin by neurotrypsin, a synaptic protease linked to mental retardation*, FASEB J., 21(13), 3468-78.

Frischknecht, R. et al, 2008, *Activity-induced synaptic capture and exocytosis of the neuronal serine protease neurotrypsin*, J. Neurosci., 28(7), 1568-79.

Stephan, A. et al, 2008, *Neurotrypsin cleaves agrin locally at the synapse*, FASEB J., in press, Jan. 29, 2008 [Epub ahead of print].